

<http://researchspace.auckland.ac.nz>

***ResearchSpace@Auckland***

### **Copyright Statement**

The digital copy of this thesis is protected by the Copyright Act 1994 (New Zealand).

This thesis may be consulted by you, provided you comply with the provisions of the Act and the following conditions of use:

- Any use you make of these documents or images must be for research or private study purposes only, and you may not make them available to any other person.
- Authors control the copyright of their thesis. You will recognise the author's right to be identified as the author of this thesis, and due acknowledgement will be made to the author where appropriate.
- You will obtain the author's permission before publishing any material from their thesis.

To request permissions please use the Feedback form on our webpage.

<http://researchspace.auckland.ac.nz/feedback>

### **General copyright and disclaimer**

In addition to the above conditions, authors give their consent for the digital copy of their work to be used subject to the conditions specified on the [Library Thesis Consent Form](#) and [Deposit Licence](#).

# **Microencapsulation of Phase Change Materials (PCMs) for Thermal Energy Storage Application**

**Refat Al Shannaq**



**A thesis submitted in fulfilment of the requirements for the degree of Doctor of  
Philosophy in Chemical & Materials Engineering, The University of Auckland,**

**2015**

# **Abstract**

In an attempt to reduce the amount of energy consumption of heating and cooling in buildings, considerable efforts have been made to use phase change materials within the building envelope. Phase change materials (PCMs) are organic or inorganic compounds, which melt and solidify with a melting range suitable for the specific application. They have the ability to absorb and release large amount of heat during phase transition. A challenge with PCMs undergoing phase change at ambient temperature, such as those used in buildings, is in containing them in an appropriate matrix. This is because organic PCMs have a tendency to leak or exude to the surface of the matrices in which they are contained, during the phase change process. This leads to the surface of building walls or ceiling, containing them becoming oily and stained, and to the thermal storage properties of the PCM gradually diminishing. Encapsulation of phase change materials (PCMs) in micro size can be assisted to overcome these problems.

This thesis describes the preparation of PCMs microcapsules using cross linking poly methyl methacrylate (PMMA) as a shell by means of suspension polymerization method. The emulsion stability using mixed surfactant was studied. The use of mixed surfactants improved the suspension stability of the emulsion, produced a monodisperse droplets size distribution with no significant shifting of droplets size over time and reduced the buckles and microcapsule size significantly. Adding pentaerythritol tetraacrylate (cross-linking agent) improved the surface morphology and produced microcapsules with a much higher PCM content. Furthermore, the effect of adding different types and concentrations of nucleating agents to the PCM prior to encapsulation on the PCMs behaviour was investigated. Adding small amount of nucleating agent such as Rubitherm®RT58 and 1-octadecanol to PCM prior encapsulation eliminated PCMs supercooling completely.

Microencapsulation PCMs by suspension polymerization usually requires a long time to achieve a high monomer conversion. Efforts have been made to shorten the reaction period of polymerization by using photo-induced suspension polymerization at room temperature. This thesis presents a novel process of microencapsulating PCMs using a falling thin film closed loop UV reactor. The results show that PCM microcapsules properties depend mainly on the method used for preparing emulsion. Smooth, compact and dry spherical microcapsules with reasonable heat storage capacity were prepared when a mixture of monomers was added to

the PCM emulsion. Furthermore, particles are agglomerated to lumps and no microcapsules obtained when only MMA was used. However, the morphology of the PCMs microcapsules improved dramatically when cross linking agent (PETRA) was used. No serious change in the surface morphology of RT21 microcapsules was observed when the irradiated time was reduced from 2 hours to 1 hour. In fact the heat storage capacity of the RT21 microcapsules increased from 80.5 to 90.3 J/g when the irradiated time decreased from 2 hours to 1 hour. This could be due to the less conversion of the monomers, thus produced a thinner shell capsules and hence higher heat storage capacity.

In practical applications, especially in building, the shell of PCMs microcapsules must have enough robustness to avoid shell rupturing during the mixing process with building materials. PCMs microcapsules are also used in slurry to improve thermal performance of heat exchangers and these microcapsules need to sustain the high shear caused by pumping the suspension. In an attempt to improve the shell mechanical strength of the PCMs microcapsules, double shell PCMs microcapsules with polymer and metal coatings were fabricated. The PCMs microcapsules were coated with metal in two simple steps (1) surface functionalization of PCMs microcapsules (polymer single shell) using polydopamine (PDA) and (2) electroless plating of silver (Ag) metal. SEM images show that the PDA was successfully attached to the PCMs microcapsules shown by the dark distinctive layer and small fragments of PDA on the surface of RT21 microcapsules. The inner polymer shell of the PCMs microcapsules was completely covered with Ag (outer metal shell). The polymer rupturing load was increased from 0.45 to 6.6 mN, which was confirmed by optical microscope images before and after nanocompression of single microcapsules.

Finally a simple, quick and effective process of encapsulating PCMs was invented. The encapsulated PCMs produced by the process of the invention have been found to be of high quality. The encapsulated products have a smooth and compact surface, a relatively high PCM content and thermally stable. In addition, the process of the invention gives a relatively high materials recovery rate, e.g. up to 90%, or higher.

# **Acknowledgements**

First of all, I would like to express my special thanks to my main supervisor Prof. Mohammed Farid for his financial support and valuable guidance. Further, I am grateful to my co-supervisor Dr. Michelle Dickinson for her helping in proofread of some chapters in the thesis.

Also, I would like to acknowledge the New Zealand Foundation for Research, Science and Technology for the financial support, that's offered to me through MBIE project entitled "production of phase change materials from waste plastics with innovative encapsulation technologies to manufacture high value products for niche thermal applications" as well as Qatar Foundation for the financial support given to me through the project No: NPRP 5-093-2-034 entitled "Developing innovative phase change materials based on raw materials available in Qatar".

Many thanks to Prof. Shaheen Al-Muhtaseb, professor in Department of Chemical Engineering at Qatar University and Dr. Jamal Kurdi, associate professor in school of Engineering Technology at College of the North Atlantic-Qatar for their useful advice and helping while I am in Qatar University doing PhD related research.

My sincere thanks to the technical staff working at Auckland University, who have helped me in technicians issues during my PhD journey: Mr. Ray Hoffmann, Mr Peter Buchanan and Mrs Laura Liang. Finally, my warm thanks to the technical staff working at Qatar University for their helping in constructed and assembled a UV thin film reactor, especially Mr. Saeed Gad and Dr. Ahmed El-Khatat.

# Table of Contents

Abstract .....	i
Acknowledgements .....	iii
Table of Contents .....	iv
List of Figures .....	viii
List of Tables .....	xi
<b>Chapter One: Introduction</b>	
1.1 Project Motivation .....	1
1.2 Study objectives .....	4
1.3 Structure of the thesis.....	5
<b>Chapter Two: General Background on Phase Change Materials (PCMs)</b>	
2. Thermal energy storage.....	7
2.1 Classification of solid-liquid phase change materials.....	8
2.1.1 Organic PCMs (paraffin and non-paraffin compounds).....	9
2.1.1.1 Paraffin .....	9
2.1.1.2 Non-paraffin .....	10
2.1.2 Inorganic PCMs.....	11
2.1.3 Eutectic mixtures .....	12
2.2 Criteria of PCMs selections .....	13
2.3 Application of PCMs in Building .....	14
<b>Chapter Three: Background on Microencapsulation of Phase Change Materials (PCMs) for Thermal Energy Storage Systems</b>	
Abstract .....	17
3.1 Introduction.....	17
3.2 Morphology of the capsules.....	17
3.3 Microencapsulation of phase change materials (MEPCMs).....	18
3.3.1 Interfacial polymerization (polycondensation).....	19
3.3.2 In-situ polymerization .....	23
3.3.3 Suspension polymerization.....	28
3.3.4 Coacervation-phase separation method .....	33
3.3.5 Spray-drying and other methods of PCMs microencapsulation .....	34
3.4 Conclusion .....	36
<b>Chapter Four: Emulsion Stability and Cross-Linking of PMMA Microcapsules Containing Phase Change Materials</b>	
Abstract .....	38

4.1 Introduction.....	39
4.2 Experimental .....	40
4.2.1 Materials .....	40
4.2.2 Synthesis of PCMs Microcapsules .....	41
4.2.2.1 Emulsification.....	41
4.2.2.2 Polymerization.....	41
4.2.3 Characterization of Microcapsules .....	41
4.2.3.1 Scanning Electron Microscope (SEM) .....	41
4.2.3.2 Differential Scanning Calorimetry (DSC) .....	42
4.2.3.3 Particle Size and Particle Size Distribution (PSD).....	43
4.2.3.4 Thermal Gravimetric Analyser (TGA) .....	43
4.2.3.5 Mass loss .....	43
4.3 Results and Discussion .....	43
4.3.1 Effect of surfactants on the emulsion stability, morphology and thermal properties of PCM microcapsules .....	43
4.3.2 Effect of cross linking agent on the morphology of microcapsules .....	47
4.3.3 Effect of cross linking agent on the thermal properties of microcapsules.....	48
4.3.4 Effect of core/shell mass ratio on the morphology of microcapsules.....	49
4.3.5 Effect of core/shell mass ratio on mass loss through microcapsules.....	50
4.3.6 Effect of core/shell mass ratio on the thermal stability of microcapsules .....	53

## **Chapter Five: Supercooling Elimination of Phase Change Materials (PCMs) Microcapsules**

Abstract.....	54
5.2 Introduction.....	55
5.2 Experimental .....	58
5.2.1 Materials .....	58
5.2.2 Synthesis of PCMs Microcapsules .....	58
5.2.2.1 Emulsification.....	58
5.2.2.2 Polymerization.....	59
5.2.3 Characterization of Microcapsules .....	59
5.3 Results and Discussion .....	60

## **Chapter Six: The Use of Thin Film Closed Loop UV Reactor for Microencapsulation of Phase Change Materials (PCMs)**

Abstract.....	71
6.1 Introduction.....	72
6.1.1 Photoinitiator .....	72

6.1.2 Monomers.....	75
6.1.3 Effect of oxygen on photopolymerization .....	76
6.1.4 Microencapsulation of PCMs using UV curing .....	76
6.2 Experimental .....	78
6.2.1 Materials .....	78
6.2.2 Preparation of emulsion.....	78
6.2.2.1 Method ‘1’ .....	78
6.2.2.2 Method ‘2’ .....	79
6.2.3 Photopolymerization.....	79
6.3 PCM microcapsules characterizations .....	82
6.3.1 Scanning Electron Microscope (SEM) .....	82
6.3.2 Differential Scanning Calorimetry (DSC).....	82
6.4 Results and Discussion .....	82
6.4.1 Effect of emulsion preparation method on microencapsulation of RT21 .....	82
6.4.2 Effect of adding cross linking agent with different numbers of cross-linkable functional moieties on the properties of RT21 microcapsules .....	85
6.4.3 Effect of PETRA concentrations on the RT21 microcapsules properties .....	87
6.4.4 Effect of cross-linking agents mixture concentrations and emulsion circulating time on the RT21 microcapsules properties .....	89
<b>Chapter Seven: Fabrication and Characterization of PCMs Microcapsules Coated with Silver</b>	
Abstract.....	92
7.1 Introduction.....	93
7.2 Experimental .....	95
7.2.1 Materials .....	95
7.2.2 Synthesis of metal coated PCMs microcapsules .....	95
7.2.2.1 Surface functionalization of PCMs microcapsules.....	96
7.2.2.2 Electroless plating .....	97
7.2.3 PCMs/Ag microcapsules characterizations .....	98
7.2.3.1 Scanning electron microscope (SEM) and energy dispersive X-ray spectroscopy (EDX) integrated system .....	98
7.2.3.2 Differential scanning calorimeter (DSC).....	98
7.2.3.3 MTS XP Nanoindenter .....	98
7.3 Results and discussion .....	99
<b>Chapter Eight: Microencapsulation of Fatty Acids, Fatty Acid Esters, Fatty Alcohols and Paraffin</b>	
8.1 Field of the invention .....	109

8.2 Background of the invention.....	109
8.3 Summary of the invention.....	111
8.4 Description of the invention.....	115
8.4.1 General description of process of the invention .....	115
8.4.2 Components of the reaction mixture .....	116
8.4.2.1 PCMs .....	116
8.4.2.2 Acrylate monomer .....	117
8.4.2.3 Cross-linking agent.....	117
8.4.2.4 Polymerisation initiator .....	117
8.4.2.5 Other additives.....	118
8.4.3 Process conditions .....	118
8.5 WHAT WE CLAIM IS:.....	119
8.6 Experimental .....	122
8.6.1 Batch Reactions .....	122
8.6.2 Product testing .....	123
8.6.2.1 Differential Scanning Calorimeter (DSC) .....	123
8.6.2.2 Scanning Electron Microscopy (SEM).....	123
8.6.2.3 Thermal Cycling .....	123
8.7 Results and Discussion .....	123
8.8 Appendix (DSC curves of some selected samples) .....	129
<b>Chapter Nine: Conclusions and Recommendations</b>	
9.1 Author's contributions/achievements .....	132
9.2 Conclusions.....	132
9.2.1 Conclusion from Chapter Four .....	132
9.2.2 Conclusion from Chapter Five .....	132
9.2.3 Conclusion from Chapter Six .....	133
9.2.4 Conclusion from Chapter Seven.....	133
9.2.5 Conclusion from Chapter Eight.....	133
9.3 Recommendations for future work .....	134
References.....	135

# List of Figures

<b>Figure 1.1</b> Electricity generations by fuel type in New Zealand in 2012 .....	<b>1</b>
<b>Figure 1.2</b> Crude oil prices 1861-20114 US dollars per barrel.....	<b>2</b>
<b>Figure 1.3</b> Electricity consumption by sector in New Zealand for 2012 .....	<b>2</b>
<b>Figure 1.4</b> Proportion of New Zealand household energy consumption. ....	<b>3</b>
<b>Figure 1.5</b> New Zealand electricity use per household over time (1946-2005).....	<b>3</b>
<b>Figure 2.1</b> Classification of energy storage materials.....	<b>7</b>
<b>Figure 2.2</b> Classification of PCMs.....	<b>8</b>
<b>Figure 2.3</b> Classification of materials that can be used as PCM, melting enthalpy and melting temperature .....	<b>13</b>
<b>Figure 3.1</b> Scheme diagrams of several different types of morphology of microcapsules .....	<b>18</b>
<b>Figure 3.2</b> Schematic formation of the MEPCM by interfacial polymerization.....	<b>19</b>
<b>Figure 3.3</b> Wall formation reaction of polyurea microcapsules: (a) reaction between TDI and DETA, (b) reaction between TDI and hydrolysed TDI and (c) reaction between TDI and NP-10.....	<b>20</b>
<b>Figure 3.4</b> SEM images of the microcapsules synthesized using different amine monomers: (a) EDA, (b) DETA, (c) Jeffamine, and (d) Cracked microcapsule Particle. ....	<b>22</b>
<b>Figure 3.5</b> (a) Schematic diagram of the fabrication of monodisperse PCM polyurea microcapsules in a tubular microfluidic device and (b) photograph of O/W PCM droplets produced at the tubular junction. ....	<b>22</b>
<b>Figure 3.6</b> Schematic formation of the n-octadecane microcapsules by in-situ polymerization .....	<b>24</b>
<b>Figure 3.7</b> DSC cooling curves of PCM microcapsules synthesized with various stirring rates .....	<b>25</b>
<b>Figure 3.8</b> SEM photos of (a) conventional PCM microcapsules and (b) silver-nanoparticles PCM microcapsules .....	<b>26</b>
<b>Figure 3.9</b> (a) TGA curves of silver nanoparticles-PCM microcapsules and conventional PCM microcapsules and (b) weight loss trends of silver nanoparticles-PCM microcapsules and conventional PCM microcapsules at 130 °C.....	<b>27</b>
<b>Figure 3.10</b> Schematic diagram showing mechanism of capsule formation using suspension polymerisation.....	<b>29</b>
<b>Figure 3.11</b> SEM images of (a) cross-section of PolySt/ paraffin microcapsules, (b) cross-section of poly (St-MMA) /paraffin microcapsules, (c) general view of PMMA microcapsules, (d) cross-section of inner structure of PMMA/paraffin microcapsules and (e) cross-section of Poly (MMA-co-MA-co-MAA)/paraffin microcapsules .....	<b>32</b>
<b>Figure 3.12</b> Schematic diagram of typical encapsulation process based on complex coacervation.....	<b>33</b>
<b>Figure 3.13</b> Schematic representation of the spray drying equipment used for fabricated PCM microcapsules.....	<b>35</b>

<b>Figure 3.14</b> SEM images of RT27 microcapsules produced using two different methods and shell materials after 3000 thermal cycles: (a) suspension polymerization method (polystyrene shell) and (b) spray drying method (LDPE–EVA shell).....	<b>36</b>
<b>Figure 4.1</b> Schematic diagram of LR-2.ST laboratory polymerization reactor .....	<b>42</b>
<b>Figure 4.2</b> Digital camera photographs of the PCM emulsion stability in the case of mixed surfactants system at (a) 0 day and (b) after one day.....	<b>45</b>
<b>Figure 4.3</b> Digital camera photographs of the PCM emulsion stability in the case of single surfactant system at (a) 0 day and (b) after one day .....	<b>45</b>
<b>Figure 4.4</b> Droplet size distributions of the PCM emulsion .....	<b>46</b>
<b>Figure 4.5</b> SEM surface morphology micrographs of the PCM microcapsules: (a) Single surfactant and (b) Mixed surfactants.....	<b>47</b>
<b>Figure 4.6</b> SEM surface morphology micrographs of PCM microcapsules: (a) Uncross-linked microcapsules (b) Cross-linked microcapsules with PETRA .....	<b>47</b>
<b>Figure 4.7</b> DSC curves of (a) Bulk RT21 and (b) Cross linked PMMA/RT21 microcapsules (Red curve) and uncross-linked PMMA/RT21 microcapsules (Blue curve).....	<b>48</b>
<b>Figure 4.8</b> SEM surface morphology micrographs of PCM microcapsules with different mass ratio of PCM to monomer: (a) 1:1, (b) 1.5:1, (c) 2:1 and (d) 3: 1 .....	<b>50</b>
<b>Figure 4.9</b> Percentage mass losses of (a) bulk RT21and (b) RT21 microcapsules with different core/shell mass ratio.....	<b>52</b>
<b>Figure 4.10</b> TGA curves of Bulk RT21 and RT21microcapsules with different core/shell mass ratio .....	<b>53</b>
<b>Figure 5.1</b> Set temperatures of water bath .....	<b>59</b>
<b>Figure 5.2</b> Accelerated thermal cycling set-up .....	<b>60</b>
<b>Figure 5.3</b> DSC curves of bulk RT21 (solid black line) and RT21MCs (dash black line) .....	<b>61</b>
<b>Figure 5.4</b> DSC curves of the bulk RT21 (black solid line), RT21MC-15wt. % RT58 (red dash line) and RT21MC-15wt. % 1- octadecanol (blue dot line) .....	<b>62</b>
<b>Figure 5.5</b> SEM photos of (a) RT21MC and (b) RT21MC-15wt. % RT58.....	<b>63</b>
<b>Figure 5.6</b> Percentage mass losses of RT21MC, RT21MC-15wt. % RT58 and RT21MC-15wt. % 1- octadecanol.....	<b>63</b>
<b>Figure 5.7</b> DSC curves of PCM microcapsules containing a) 5 wt. % RT58 and b) 15 wt. % RT58 .....	<b>65</b>
<b>Figure 5.8</b> SEM photos of a) RT21MC-5 wt. % RT58 and b) RT21MC-15wt. % RT58.....	<b>66</b>
<b>Figure 5.9</b> Percentage mass losses of RT21MC-5wt. % RT58 and RT21MC-15wt. % RT58 .....	<b>66</b>
<b>Figure 5.10</b> DSC curves of PCM microcapsules before and after thermal cycling .....	<b>67</b>
<b>Figure 5.11</b> SEM photos of RT21 microcapsules with 5 wt.% RT58: (a) 0 cycle (b) 2000 cycles.....	<b>68</b>
<b>Figure 5.12</b> Heat storage and realese performance of RT21 microcapsules before and after thermal cycling.....	<b>69</b>
<b>Figure 5.13</b> Heat realease curve of RT21 and RT21 microcapsules.....	<b>70</b>

<b>Figure 6.1</b> Categories of photopolymerizations reactions .....	<b>73</b>
<b>Figure 6.2</b> UV absorption spectra of MMA and PMMA in mini-emulsion polymerization during polymerization.....	<b>73</b>
<b>Figure 6.3</b> Molecular structures of monoacrylate or monomethacrylate monomer and its corresponding polymer repeat unit .....	<b>75</b>
<b>Figure 6.4</b> Molecular structures of monomers with varying numbers of acrylate reactive groups.....	<b>76</b>
<b>Figure 6.5</b> Overall sketch diagram of the falling thin film closed loop UV reactor. ....	<b>80</b>
<b>Figure 6.6</b> Camera photos of (a) MH module, 250W mercury lamp, (b) Ballast and (c) igniter.....	<b>81</b>
<b>Figure 6.7</b> A thin film PCMs emulsion flow. ....	<b>81</b>
<b>Figure 6.8</b> SEM images and digital camera photographs of RT21 microcapsules prepared using the two different methods of emulsion preparation: (a) Method '1' and (b) Method '2' .....	<b>83</b>
<b>Figure 6.9</b> DSC curves of RT21 microcapsules prepared using the two different methods of emulsion.....	<b>84</b>
<b>Figure 6.10</b> DSC curve and SEM photo of the produced microspheres .....	<b>85</b>
<b>Figure 6.11</b> SEM photos of RT21 microcapsules produced using (a) EGDM and (b) PETRA .....	<b>86</b>
<b>Figure 6.12</b> DSC curves of RT21 microcapsules produced using (a) EGDM and (b) PETRA .....	<b>86</b>
<b>Figure 6.13</b> SEM photos of RT21 microcapsules with versus PETRA concentrations: (a) 0 wt. %, (b) 15 wt. %, (c) 30 wt. % and (d) 50 wt. % .....	<b>87</b>
<b>Figure 6.14</b> DSC heating curves of RT21 microcapsules with versus PETRA concentrations: (a) 0 wt. %, (b) 15 wt. %, (c) 30 wt. % and (d) 50 wt. % .....	<b>88</b>
<b>Figure 6.15</b> SEM photos of RT21 microcapsules prepared with different mixture concentrations of cross-linking agents and emulsion circulating time: (a) mixture A (two hours irradiated time) (b) mixture B (two hours irradiated time) and (c) mixture B (one hour irradiated time).....	<b>91</b>
<b>Figure 7.1</b> (a) Schematic illustration of sequence steps for preparing PCMs-Ag microcapsules and (b) possible mechanism of dopamine oxidative self-polymerization.....	<b>97</b>
<b>Figure 7.2</b> Sequence steps of nanocompression of a single microcapsule .....	<b>99</b>
<b>Figure 7.3</b> SEM photos of (a) RT21 microcapsules, (b) RT21-PDA microcapsules, (c) RT21/Ag microcapsules, (d) RT21-PDA/Ag microcapsules-magnification 8000 x, (e) RT21-PDA/Ag microcapsules-magnification 15000x and (f) RT21-PDA/Ag microcapsules-magnification 50000x. ....	<b>100</b>
<b>Figure 7.4</b> EDX patterns of (a) RT21 microcapsules and (b) RT21-PDA/Ag microcapsules .....	<b>101</b>
<b>Figure 7.5</b> DSC curves of RT21 microcapsules and RT21-PDA/Ag microcapsules.....	<b>102</b>

<b>Figure 7.6</b> SEM images of (a) 24D microcapsules, (b) 24D-PDA microcapsules, (c, d and e) 24D-PDA/Ag microcapsules with different magnifications and (f) broken 24D-PDA/Ag microcapsules with shell and Ag layer thickness of 450.6 and 175.9 nm respectively.....	<b>104</b>
<b>Figure 7.7</b> Force vs. Displacement curve for the nanoindentation of blank epoxy resin, with a 10 $\mu$ m radius Diamond conical tip.....	<b>106</b>
<b>Figure 7.8</b> Force vs. Displacement curve for the nanoindentation of blank epoxy resin, 24D and 24D/Ag microcapsules .....	<b>107</b>
<b>Figure 7.9</b> Optical microscope images of 24D microcapsule (a) before compression and (b) after compression .....	<b>108</b>
<b>Figure 7.10</b> Optical microscope images of 24-D/Ag microcapsule (a) before compression and (b) after compression .....	<b>108</b>
<b>Figure 8.1</b> Product PCMs weight content vs. sample number as reported in the Table 8.1 .	<b>125</b>
<b>Figure 8.2</b> SEM images of: (a) Cross-linked PMMA (without PCMs) and (b and c) PT24 capsules (sample 2) with different magnifications .....	<b>127</b>
<b>Figure 8.3</b> SEM images of PT24 capsules (sample 2) at different positions after 50 thermal cycles (a and b) position 1 and (c and d) position 2.....	<b>128</b>
<b>Figure 8.4</b> Thermal cycling test of sample 2.....	<b>129</b>
<b>Figure 8.5</b> DSC curve of sample 1 .....	<b>129</b>
<b>Figure 8.6</b> DSC curve of sample 2 .....	<b>130</b>
<b>Figure 8.7</b> DSC curve of sample 8 .....	<b>130</b>
<b>Figure 8.8</b> DSC curve of sample 9 .....	<b>131</b>

## List of Tables

<b>Table 2.1</b> Comparison of various heat storage media (stored energy = 10 <sup>6</sup> KJ, $\Delta T$ = 15 °K)..	<b>8</b>
<b>Table 2.2</b> Some selected paraffin's along-with their melting point and latent heat of fusion ..	<b>9</b>
<b>Table 2.3</b> some selected non-paraffin's PCMs.....	<b>10</b>
<b>Table 2.4</b> listed of some inorganic substances with optional use as PCMs .....	<b>11</b>
<b>Table 2.5</b> Organic and inorganic eutectics with optional use as PCM.....	<b>12</b>
<b>Table 2.6</b> Comparison of organic and inorganic materials for thermal energy storage .....	<b>12</b>
<b>Table 2.7</b> Criteria of PCMs selections .....	<b>13</b>
<b>Table 2.8</b> Thermal properties of potential PCMs for building application .....	<b>15</b>
<b>Table 2.9</b> Thermal properties of potential commercially PCMs for building application .....	<b>16</b>
<b>Table 3.1</b> Methods used for microencapsulation .....	<b>19</b>
<b>Table 3.2</b> Examples of maximum allowed residue limits of formaldehyde in textiles and similar products.....	<b>28</b>
<b>Table 4.1</b> Concentrations of materials used in the preparation of PCM microcapsules (PCMMCs).....	<b>44</b>

<b>Table 4.2</b> Chemical recipe ingredients used for preparation of PCM microcapsules (PCMMCs) with different mass ratio of PCM to monomers.....	<b>49</b>
<b>Table 4.3</b> Comparison between selected PCM microcapsules from the literature and RT21 microcapsules obtained in this work.....	<b>51</b>
<b>Table 5.1</b> Chemical recipe ingredients of RT21 microcapsules containing a nucleating agent .....	<b>58</b>
<b>Table 5.2</b> Thermal properties of RT21 microcapsules .....	<b>64</b>
<b>Table 5.3</b> Thermal properties of the RT21 microcapsules before and after thermal cycling ..	<b>68</b>
<b>Table 6.1</b> Commercial photoinitiators used in this study.....	<b>74</b>
<b>Table 6.2</b> Total values at maximum in 300 mm distance [w/m <sup>2</sup> ] of the mercury UV lamp ...	<b>81</b>
<b>Table 6.3</b> Thermal properties of RT21 microcapsules prepared using the two different methods of emulsion preparation.....	<b>84</b>
<b>Table 6.4</b> Thermal properties of RT21 microcapsules with versus PETRA concentrations... 89	
<b>Table 6.5</b> Thermal properties of RT21 microcapsules prepared with different mixture concentrations of cross-linking agents and emulsion circulating time .....	<b>90</b>
<b>Table 7.1</b> Thermal and physical properties of PCMs microcapsules .....	<b>103</b>
<b>Table 8.1</b> Summarised results of PT24 microcapsules .....	<b>126</b>

# Introduction

1

## 1.1 Project Motivation

Electricity generation is the main form of energy transformation in New Zealand and comes from a range of energy sources. Figure 1.1 illustrates the proportions of New Zealand's electricity generation by fuel type in 2012. About 77 % of electricity generation comes from renewable resources and 23 % from fossil fuel thermal plants [1].

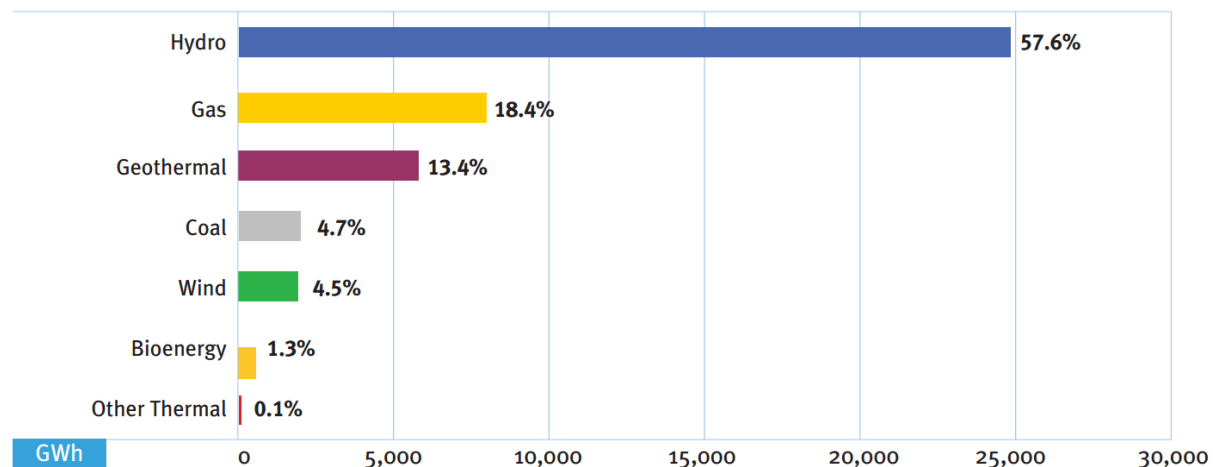


**Figure 1.1** Electricity generations by fuel type in New Zealand in 2012 [1].

Oil is the largest source of energy worldwide, and it has a strong influence on the country's economy. In New Zealand the total oil production is limited and most of oil is imported. Electricity generation from fossil fuel thermal plants (combustion of oil) plays a crucial role in New Zealand's electricity system by providing base load, backup and peak load supply. Worldwide, the demand for crude oil is increasing by approximately 2 % each year and the consumption presently around 28,000 million barrels/year. The continuous rise of oil consumption and the limited resources; increase the price of oil year after year as shown in Figure 1.2 [2]. In an attempt to reduce the dependency on fossil fuels, considerable efforts have been made to find alternative renewable sources of energy or reduce the energy consumption through design and construction of efficient energy systems.

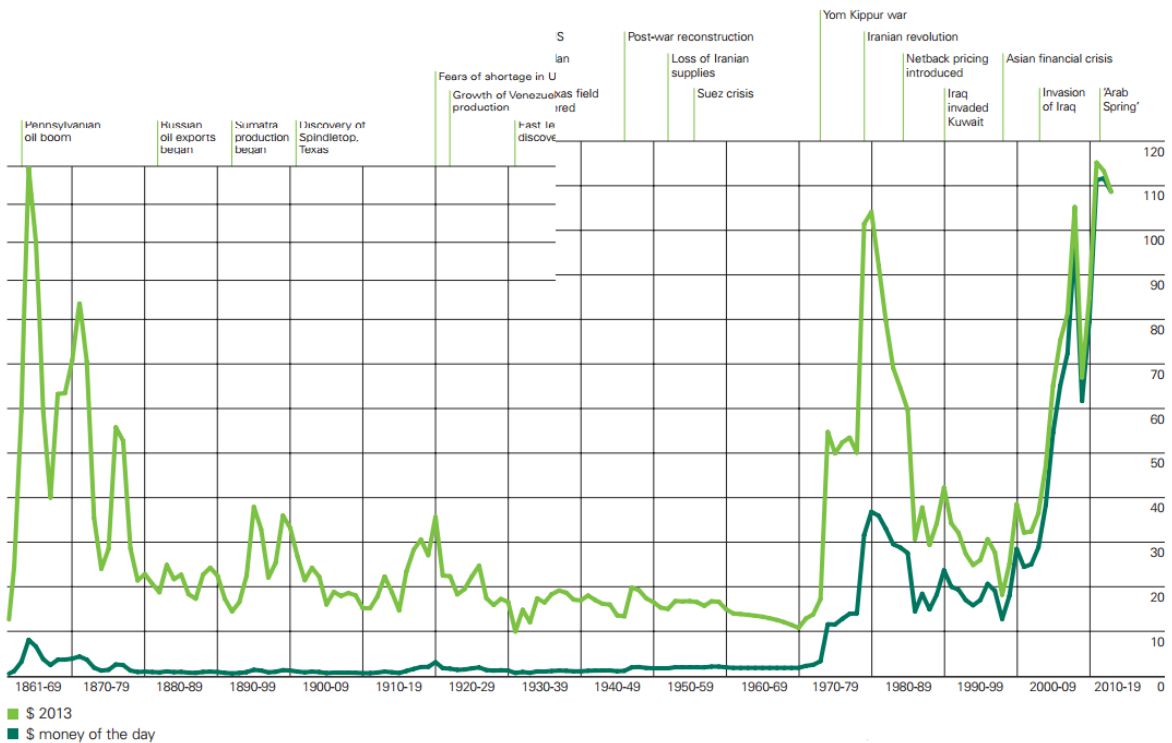


**Figure 1.2** Crude oil prices 1861-20114 US dollars per barrel [2].

The residential (households) sector accounts for around one third of total electricity consumption in New Zealand during 2012 as shown in Figure 1.3. The space heating accounts for the largest portion for electricity consumption in household over the others by 34 %. Hot water accounts the second largest portion after space heating as shown in Figure 1.4. The proportions vary by locations, hence up to 70 % of energy use in the coldest climate.

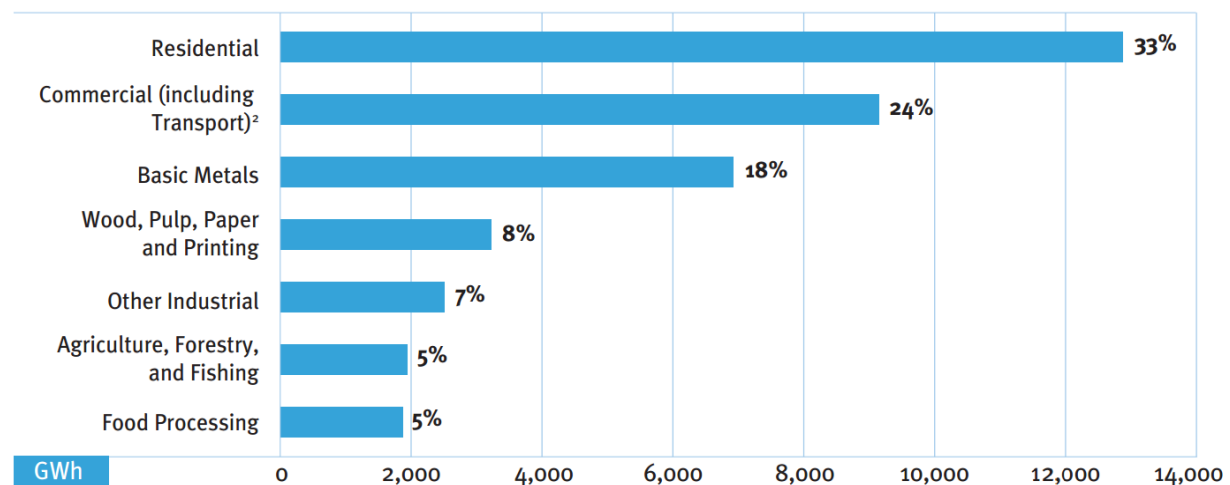


**Figure 1.3** Electricity consumption by sector in New Zealand for 2012 [1].

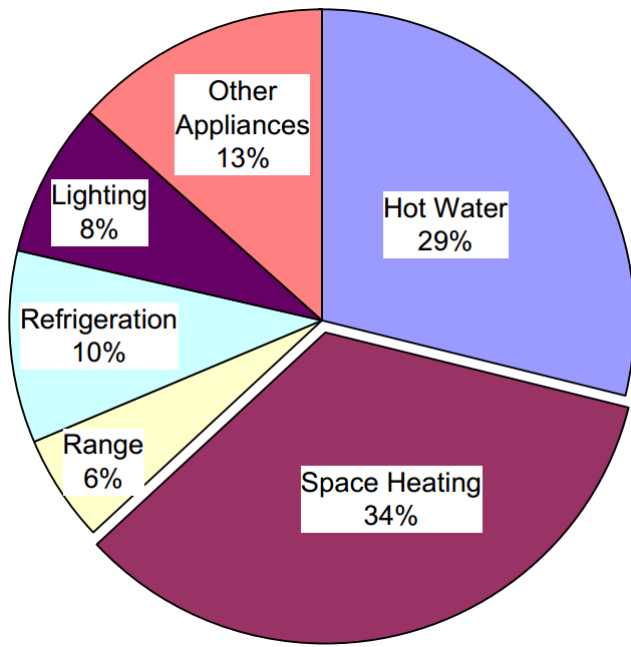


**Figure 1.4** Proportion of New Zealand household energy consumption [3].

The number of population increases over time, with a corresponding increase in the number of houses, thus increasing household energy consumption. The household energy consumption trend over the 50 years from 1955 to 2005 is increased nearly 3 times as shown in Figure 1.5. Statistics New Zealand, Household Economic Survey: Year ended 30 June 2007, up to 40% of energy is used to heat up the houses (A typical household of four people spends around NZ\$2,800 a year on energy not including transport), so it is useful to find an efficient approach to make them more energy efficient.

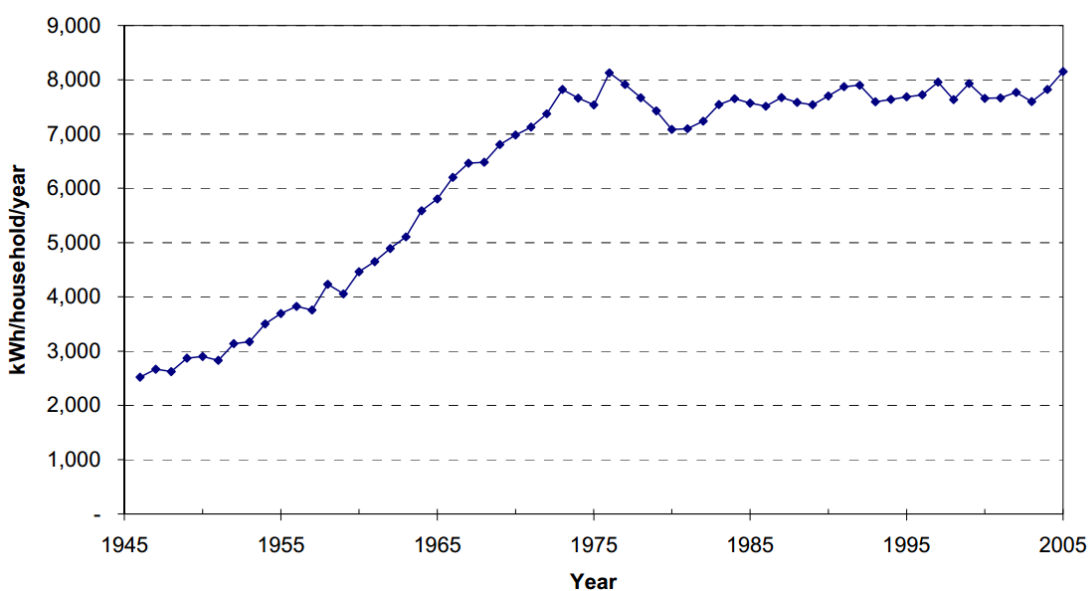


**Figure 1.5** New Zealand electricity use per household over time (1946-2005) [3].

In an attempt to enhance the thermal insulation of building, thus reduce the amount of energy consumption by heating and cooling, considerable efforts have been made to use phase change materials (PCMs) within the building envelope [4-7]. PCMs are organic or inorganic compounds, which melt and solidify with a melting range suitable for a given application. They have the ability to absorb and release large amounts of heat during their phase transition. For building application, PCMs with phase transition temperatures in the range of 18-28 °C are promising selection as it's in the range of human comfort temperature.

The use of PCMs within building materials could be helped in two ways: (1) Active solar energy stores (less energy consumption). In this way a temperature fluctuation of surrounding environment should be above and below the melting temperatures of PCMs during a day and night respectively. During a day when the sun is available the PCMs absorbs the heat and prevent indoor temperature to rise up, while in the night when the temperature drop down the energy absorbed during a day is released and rising up indoor temperature, thus no or less cooling and heating required. (2) electricity peak-load shifting (saving money) [8]. In most of countries around the world the price of electricity is changed over a day according to the demand by industry, commercial and residential activities. The use of PCMs in building could help in shifts most of the load coming from residential air conditions from peak to off-peak electricity tariffs.

A challenge with PCMs, especially with PCMs undergoing phase change at ambient temperature, such as those used in buildings, is in containing them in an appropriate matrix. This is because organic PCMS have a tendency to leak or exude to the surface of the matrices in which they are contained, during the phase change process. This leads to the surface becoming oily and stained, and to the thermal storage properties of the PCM gradually diminishing. Encapsulation of phase change materials (PCMs) in micro size can assist to overcome these problems [9-13].

## **1.2 Study objectives**

The objectives of this study were as follow:

- (1) Conduct a literature review on different types of PCMs and select a promising candidate, which fit a potential application.

- (2) Conduct a comprehensive literature review on different methods of microencapsulation, which applicable for PCMs and select the most proper one based on the experimental work that have been done in the literature.
- (3) Identify the suitable shell materials for microencapsulation of PCM in terms of physical and chemical properties, toxicity, availability and cost.
- (4) Use the selected proper microencapsulation method and shell materials to microencapsulate the PCMs using thermal process. This scope encompasses the following aspects:
  - (a) Investigate the stability of the emulsion through the use of mixed surfactants.
  - (b) Investigate the effect of adding cross linking agent on the PCM microcapsules characteristics.
  - (c) Study the effect of adding different types and concentrations of nucleating agents to the PCM prior encapsulation on the thermal properties such as crystallization temperatures and thermal energy capacity of the PCMs microcapsules.
- (5) Investigate the applicability of using thin film closed loop UV reactor for microencapsulation PCMs.
- (6) Study the feasibility of metal coating PCMs microcapsules using electroless plating method, and its effect on the PCMs microcapsules properties such as mechanical strength.
- (7) Propose a simple, efficient, cheap and quick method for microencapsulation PCMs

### **1.3 Structure of the thesis**

This thesis contains nine chapters. The classifications and thermal properties of potential PCMs for building application are presented in Chapter 2. The microencapsulation methods applicable to PCMs and current experimental work in the field of microencapsulation of PCM are covered in Chapter 3.

A prerequisite for manufacturing good characteristics PCM microcapsules is the ability to produce stable emulsion with a well-controlled droplets size. The stability of emulsion through the use of mixed surfactants and the effect of adding pentaerythritol tetraacrylate (PETRA) as cross linking agent on the PCM microcapsules characteristics are reported in Chapter 4.

PCM microcapsules with supercooling have limited widespread use as latent heat stores, thus adding different types and concentrations of nucleating agents to the PCM prior encapsulation and their effect on the thermal properties, surface morphology and shell permeability of the PCM microcapsules are presented in Chapter 5.

Thermal-initiated free-radical polymerization method is commonly used in dispersion polymerization for microencapsulating of PCM. In this method the polymerization reaction initiated at elevated temperature and usually needed long time to achieve high monomer conversion. Chapter 6 presents a novel process of microencapsulating of PCM using falling thin film closed loop UV reactor at room temperature in an attempt to shorten the reaction period.

The heat storage capacity of PCMs, its well containment inside microcapsules and the useful life of these microcapsules as well as the shell mechanical strength are considered key parameters in assessing quality of PCMs microcapsules. In practical applications, especially in building, the shell of PCM microcapsule must have enough robustness to avoid shell rupturing during the mixing process with building materials. PCM microcapsules are also used in slurry to improve thermal performance of heat exchangers and these microcapsules need to sustain the high shear caused by pumping the suspension. Chapter 7 presents novel double shell PCMs microcapsules with both polymer and metal coatings in an attempt to improve the shell mechanical strength of the PCMs microcapsules.

A new, simple, efficient and quick method for microencapsulation of PCM is proposed in Chapter 8. Finally, conclusion and recommendation for future work are presented in Chapter 9.

# General Background on Phase Change Materials (PCMs)

2

## 2. Thermal energy storage

Thermal energy can be stored either as sensible heat, thermochemical energy storage or as latent heat using a phase change material (PCM) (Figure 2.1). Thermal energy storage (TES) plays an important role in reducing the mismatch between supply and demand, improving the performance and reliability of energy systems.

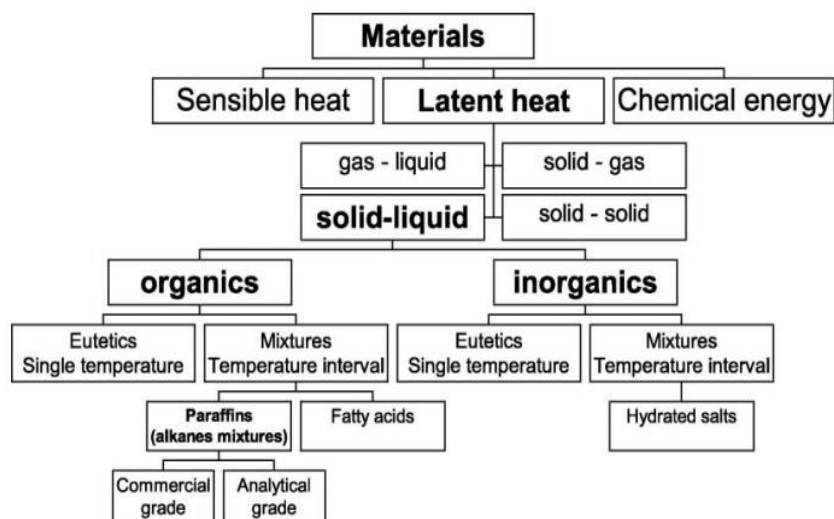


**Figure 2.1** Classification of energy storage materials [14].

Amongst the various heat storage techniques of interest, latent heat storage media can store large quantity of heat in less weight and volume of material in comparison with sensible heat storage media (Table 2.1). Moreover, it can absorb and release heat within small temperature differences.

Various physical and chemical transformations of the PCM may occur, accompanied either by absorption or releasing heat. These transformations can be classified into solid-gas, liquid-gas, solid-solid and solid-liquid phase transition. Changes of phase involving a gas, i.e. vaporisation, condensation, sublimation have a much higher latent heat than other transitions, as the molecular change in structure is much more proclaimed. However, these transitions involving a gas are usually not suitable for TES applications due to the difficulties of managing the large change in volume.

Phase change materials undergoes a solid-liquid phase change transition are most commonly utilized. These materials having a small change in volume during phase change transition compared with liquid-gas transition and have larger latent heat of storage than solid-solid transition.

**Table 2.1** Comparison of various heat storage media (stored energy =  $10^6$  KJ,  $\Delta T = 15$  °K) [15].

Heat Storage Materials				
	Sensible Heat Storage		Latent Heat Storage	
Property	Rock	Water	Organic PCM	Inorganic PCM
Latent heat of fusion (kJ/kg)	-	-	190	230
Specific heat (kJ/kg)	1.0	4.2	2.0	2.0
Density (kg/m <sup>3</sup> )	2240	1000	800	1600
Storage mass for storing $10^6$ KJ (Kg)	67,000	16,000	5,300	4,350
Storage Volume for storing $10^6$ KJ (m <sup>3</sup> )	30	16	6.6	2.7

## 2.1 Classification of solid-liquid phase change materials

The solid-liquid PCMs comprise organic PCMs, inorganic PCMs and eutectics. A comparison of these different kinds of PCMs is listed in Figure 2.2.

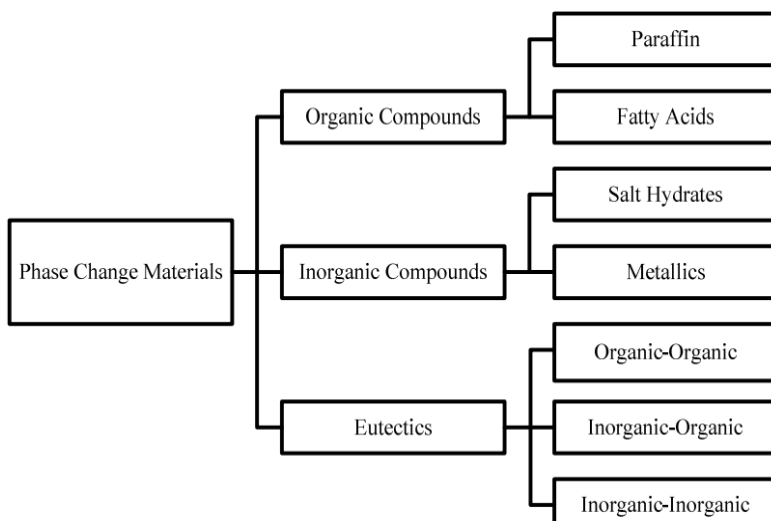


**Figure 2.2** Classification of PCMs [4].

## 2.1.1 Organic PCMs (paraffin and non-paraffin compounds).

### 2.1.1.1 Paraffin

Paraffin is a term that can be used synonymously with alkane indicating hydrocarbons with the general formula  $C_nH_{2n+2}$ . The mixture of alkanes that falls within the  $20 \leq n \leq 40$  ranges and appear as solid state at room temperature refer as paraffin wax. The availability of paraffin in large melting temperature ranges with reasonable latent heat, less volume change during phase transition ( $\sim 10\%$ ) and thermally reliable (have very long freeze-melt cycle) make it a promising candidate for thermal energy storage applications. Table 2.2 shows some selected paraffins along-with their melting point, latent heat of fusion and groups.

**Table 2.2** Some selected paraffin's along-with their melting point and latent heat of fusion [16]

Number of carbon atoms	Melting point (°C)	Latent heat of fusion (kJ/kg)
14	5.5	228
15	10	205
16	16.7	237.1
17	21.7	213
18	28	244
19	32	222
20	36.7	246
21	40.2	200
22	44	249
23	47.5	232
24	50.6	255
25	49.4	238
26	56.3	256
27	58.8	236
28	61.6	253
29	63.4	240
30	65.4	251

### 2.1.1.2 Non-paraffin

Non-paraffin PCMs which refer to fatty acids and fatty acids ester are characterized by the formula  $\text{CH}_3(\text{CH}_2)_{2n}\text{COOH}$ . It possesses some superior properties over other PCMs such as good chemical stability, non-toxicity, non-pollutant and shows long term thermal stability when heated above its melting point. The potential changes in the thermal characteristics of organic PCMs such as RT21 and esters with time when heated above their melting points were investigated [17]. It was found that the paraffin based PCM undergoes an irreversible physical change which alters its thermal characteristics. Paraffin mixtures have higher vapour pressures than most esters, which makes them more susceptible to weight loss and change in physical properties due to the evaporation of light compounds. While the more stable ester mixture experiences no change in mass and was thermally stable during the entire heating period. The major drawbacks of non-paraffin PCMs are the materials large-scale availability and cost, were they are more expensive than paraffin's. Table 2.3 shows some selected non-paraffin PCMs.

**Table 2.3** some selected non-paraffin's PCMs

PCM	Melting point	Heat of fusion	Reference
	(°C)	(kJ/kg)	
$\text{CH}_3(\text{CH}_2)_{16}\text{COO}(\text{CH}_2)_3\text{CH}_3$ Butyl stearate	18-23	140	[5]
$\text{CH}_3(\text{CH}_2)_{12}\text{COOC}_3\text{H}_7$ Propyl palmitate	16-19	186	[5]
$\text{CH}_3(\text{CH}_2)_{16}\text{COOCH}(\text{CH}_3)$ Isopropyl stearate	14-18	140-142	[18]
$\text{CH}_3(\text{CH}_2)_{16}\text{COOCH=CH}_2$ Vinyl stearate	27	122	[18]
$\text{CH}_3\text{COOH}$ Acetic acid	16.7	184	[16]
$\text{H}(\text{OC}_2\text{H}_2)_n\text{OH}$ Polyethylene glycol 600	20-25	146	[16]

## 2.1.2 Inorganic PCMs

Inorganic PCMs such as salt hydrates are considered as alloy of inorganic salts and water. They are characterized by a typical formula  $M.nH_2O$  and considered attractive materials for thermal energy storage due to their high volumetric storage density ( $350\text{ MJ/m}^3$ ), relatively high thermal conductivity ( $0.5\text{ W/m }^\circ\text{C}$ ) and moderate costs compared to paraffin waxes [19]. The major problems associated with salt hydrates as PCMs are: (1) supercooling phenomena which is resulting either from slow rate of nucleation or slow rate of growth of these nuclei, (2) incongruent melting and (3) high change in volume during phase transition. Table 2.4 listed of some inorganic substances with optional use as PCMs.

**Table 2.4** listed of some inorganic substances with optional use as PCMs [14]

PCM	Melting point ( $^\circ\text{C}$ )	Heat of fusion (kJ/kg)	Thermal conductivity (W/m.K)	Density (kg/m $^3$ )
$\text{Na}_2\text{CrO}_4.10\text{H}_2\text{O}$	18	n.a	n.a	n.a
$\text{KF}.4\text{H}_2\text{O}$	18.5	231	n.a	1447 (liquid, $20\text{ }^\circ\text{C}$ )
				1455 (solid, $18\text{ }^\circ\text{C}$ )
$\text{Mn}(\text{NO}_3)_2.6\text{H}_2\text{O}$	25.8	125.9	n.a	1728 (liquid, $40\text{ }^\circ\text{C}$ )
				1795 (solid, $5\text{ }^\circ\text{C}$ )
$\text{CaCl}_2.6\text{H}_2\text{O}$	29	190.8	0.540 (liquid, $38.7\text{ }^\circ\text{C}$ )	1562 (liquid, $32\text{ }^\circ\text{C}$ )
			1.088 (solid, $23\text{ }^\circ\text{C}$ )	1802 (solid, $24\text{ }^\circ\text{C}$ )
$\text{LiNO}_3.3\text{H}_2\text{O}$	30	296	n.a	n.a
$\text{Na}_2\text{SO}_4.10\text{H}_2\text{O}$	32.4	254	n.a	n.a
$\text{Na}_2\text{CO}_3.10\text{H}_2\text{O}$	33	247	n.a	n.a
$\text{CaBr}_2.6\text{H}_2\text{O}$	34	115.5	n.a	1956 (liquid, $35\text{ }^\circ\text{C}$ )
				2194 (solid, $24\text{ }^\circ\text{C}$ )
$\text{Na}_2\text{HPO}_4.12\text{H}_2\text{O}$	35.5	265	n.a	n.a
$\text{Zn}(\text{NO}_3)_2.6\text{H}_2\text{O}$	36	146.9	0.464 (liquid, $39.9\text{ }^\circ\text{C}$ )	1828 (liquid, $3\text{ }^\circ\text{C}$ )
				1937 (solid, $24\text{ }^\circ\text{C}$ )

n.a: not available

### 2.1.3 Eutectic mixtures

The development and improvement of PCMs with respect to their applications have been handled in many studies by preparing eutectic mixtures. Eutectic system is a mixture of chemical components (eutectic composition) that melts and solidifies (eutectic temperature) at specific single temperature. This temperature is lower than any of separate single eutectic composition melting temperature. Eutectic mixtures could be organic-organic, organic-inorganic and inorganic-inorganic mixtures as listed in Table 2.5. Table 2.6 shows a comparison of organic and inorganic materials for thermal energy storage.

**Table 2.5** Organic and inorganic eutectics with optional use as PCM [5, 14, 16]

Compound	Composition (wt. %)	Melting point (°C)	Heat of fusion (kJ/kg)
CH <sub>3</sub> (CH <sub>2</sub> ) <sub>8</sub> COOH + CH <sub>3</sub> (CH <sub>2</sub> ) <sub>10</sub> COOH	45 + 55	17-21	143
C <sub>14</sub> H <sub>28</sub> O <sub>2</sub> + C <sub>10</sub> H <sub>20</sub> O <sub>2</sub>	34 + 66	24	147.7
CaCl <sub>2</sub> + NaCl + KCl + H <sub>2</sub> O	48 + 4.3 + 0.4 + 47.3	26.8	188
CH <sub>3</sub> CONH <sub>2</sub> + NH <sub>2</sub> CONH <sub>2</sub>	50 +50	27	163
Triethylolethane + urea	62.5 + 37.5	29.8	218
CH <sub>3</sub> COONa.3H <sub>2</sub> O + NH <sub>2</sub> CONH <sub>2</sub>	40 + 60	30	200.5

**Table 2.6** Comparison of organic and inorganic materials for thermal energy storage [14]

Organic	Inorganic
<u>Advantages</u> <ul style="list-style-type: none"> <li>• No corrosive</li> <li>• Low or none supercooling</li> <li>• Chemical and thermal stability</li> </ul> <u>Disadvantages</u> <ul style="list-style-type: none"> <li>• Low phase change enthalpy</li> <li>• Low thermal conductivity</li> <li>• Inflammability</li> </ul>	<u>Advantages</u> <ul style="list-style-type: none"> <li>• High phase change enthalpy</li> </ul> <u>Disadvantages</u> <ul style="list-style-type: none"> <li>• Supercooling and corrosion</li> <li>• Phase separation and segregation</li> <li>• Lack of thermal stability</li> </ul>

## 2.2 Criteria of PCMs selections

The melting temperature and phase change enthalpy of existing PCMs are shown in Figure 2.3. From the melting temperature point of view it can be seen that, the potential use of PCMs in building are paraffin, fatty acids, salt hydrates and eutectic mixtures.

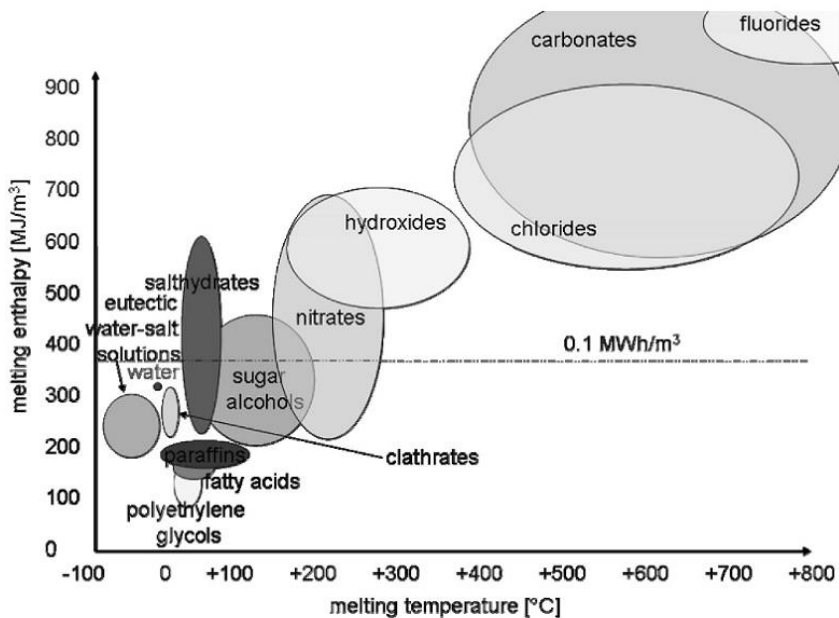


**Figure 2.3** Classification of materials that can be used as PCM, melting enthalpy and melting temperature [20]

Selection of proper PCMs not only depend on good latent heat capacity and narrow melting temperature range for a particular purpose, but should also fulfil a number of criteria such as thermochemical, chemical, kinetic and economic properties as listed in Table 2.7.

**Table 2.7** Criteria of PCMs selections [4]

Thermodynamic properties	<ul style="list-style-type: none"> <li>Melting temperature in desired range</li> <li>High latent heat of fusion per unit volume</li> <li>High thermal conductivity</li> <li>High specific heat and heat density</li> <li>Small volume change during phase change</li> <li>Congruent melting</li> </ul>
Kinetics properties	<ul style="list-style-type: none"> <li>High nucleation rate to avoid supercooling</li> </ul>
Chemical properties	<ul style="list-style-type: none"> <li>Complete reversible freezing/melting cycle</li> <li>Chemical stability</li> </ul>

	<ul style="list-style-type: none"> <li>• No degradation after freezing/melting cycle</li> <li>• No corrosiveness</li> <li>• No toxic, no flammable and no explosive materials</li> </ul>
Economic properties	<ul style="list-style-type: none"> <li>• Effective cost and large scale-availability</li> </ul>

## 2.3 Application of PCMs in Building

There are several applications where PCMs have been used for thermal energy storage, such as heating /cooling of water [21], smart textiles [22], biomaterials and biomedical applications [23], electronics [24], Automotive industry [25], space applications [26], food industry [27] and building application [5, 28, 29]

Building application has been recognized as one of the most foreseeable applications of PCMs. The use of PCMs within building materials could be helped in two ways: (1) Active solar energy stores (less energy consumption). In this way a temperature fluctuation of surrounding environment should be above and below the melting temperatures of PCMs during a day and night respectively. During a day when the sun is available the PCMs absorbs the heat and prevent indoor temperature to rise up, while in the night when the temperature drop down the energy absorbed during a day is released and rising up indoor temperature, thus no or less cooling and heating required. (2) electricity peak-load shifting (saving money) [8]. In most of countries around the world the price of electricity is changed over a day according to the demand by industry, commercial and residential activates. The use of PCMs in building could be helped in shifts most of the load coming from residential air conditions from peak to off-peak electricity tariffs. In the building applications, the PCMs melting temperature within the range of human comfort temperature (18–30 °C) are preferred. Some potential PCMs are listed in Table 2.8 including organic PCMs, salt hydrates and eutectics mixture, as well as potential commercial PCMs (Table 2.9).

**Table 2.8** Thermal properties of potential PCMs for building application

PCMs	Type	Melting point (°C)	Heat of fusion (KJ/Kg)	Specific heat (KJ/Kg K)	Thermal conductivity (W/m K)	Ref.
Paraffin C16-C18	Organic	20-22	152	-	-	
Paraffin C13-C24	Organic	22-24	189-2.1	2.1	0.21	[30]
Paraffin C18	Organic	28	244	2.16	0.15	[14]
Butyl stearate	Organic	19	140	-	-	[31]
1-Dodecanol	Organic	26	200	-	-	[30]
n-Octadecane	Organic	28	200	-	-	[14]
Vinyl stearate	Organic	27-29	122	-	-	[31]
Polyglycol E600	Organic	22	127.2	-	0.19 (l)	[31]
45/55 capric + lauric acid	Fatty acid eutectic	21	143	-	-	[30]
Propyl palmitate	Fatty acid	19	186	-	-	[14] [31]
KF.4H <sub>2</sub> O	Hydrate salts	18.5	231	1.84(s) 2.39(l)	-	[5]
Mn(NO <sub>3</sub> ).6H <sub>2</sub> O	Hydrate salts	25.8	125.9	-	-	[31]
CaCl <sub>2</sub> .6H <sub>2</sub> O	Hydrate salts	29.7	171	1.45(s)		[5]
CaCl <sub>2</sub> .6H <sub>2</sub> O+Nucleat+MgCl <sub>2</sub> .6H <sub>2</sub> O	Inorganic eutectic	25	127	-	-	[31]

**Table 2.9** Thermal properties of potential commercially PCMs for building application

PCM name	Type	Melting temperature (oC)	Heat of fusion ( KJ/Kg)	Specific heat (KJ/Kg K)	Thermal conductivity (W/m K)	Source
Rubitherm®RT21	Paraffin	21	134	-	-	Rubitherm
Rubitherm®RT25	Paraffin	25	147	2.9(s) 2.1(l)	1.02(s) 0.56(l)	
Rubitherm®RT27	Paraffin	27	179	1.8(s) 2.4(l)	0.2	Rubitherm
Rubitherm®RT31	Paraffin	31	157	-	-	Rubitherm
Rubitherm®SP22 17	Paraffin	22	150	-	-	Rubitherm
Rubitherm®SP25A8	Paraffin	25	180	-	-	Rubitherm
DuPont™ Energain®	Paraffin	22	170	-	-	DuPont™
ClimSel C15	n.a	15	130	-	-	Climator
ASTorstat HA16	Paraffin	18	n.a	-	-	Astor
ClimSel C23	Salt hydrate	23	148	-	-	Climator
AStorstat HA18	Paraffin	27	n.a	-	-	Astor
AC.27	Eutectic salt	27	200	-	-	Cristopia
PT24	Fatty acid ester	24	185	-	-	Pure Temp

# **Background on Microencapsulation of Phase Change Materials (PCMs) for Thermal Energy Storage Systems**

**3**

## **Abstract**

Phase change materials (PCMs) are organic or inorganic compounds, which melt and solidify with a melting range suitable for the specific application. They have the ability to absorb and release large amount of heat during phase transition. However in order to use them they must be well contained to prevent them from leaking out when melted. In this chapter, we will discuss the most important methods of microencapsulation, which are applicable to these PCMs.

### **3.1 Introduction**

Encapsulation is a process of engulfing the materials of solids or droplets of liquids or gases in a compatible thin solid wall. The material inside the capsules is referred to as the core, internal phase, or fill, whereas the wall is sometimes called a shell, coating, or membrane. Normally, encapsulation of materials is classified as nanocapsules, microcapsules and macrocapsules based on the capsule size diameter. The size diameter of microcapsules varies from 1 um to 1 mm, while the capsules smaller than 1 um are classified as nanocapsules and those larger than 1 mm as macrocapsules [32]. The encapsulation of materials has evolved from examples in nature; the simplest example of a macrocapsules is a bird egg and a cell along with it is content as a microcapsules. The applications of microencapsulation are numerous and it began with the carbonless copy papers, whereas the top sheet of the carbonless is coated with dye or ink microcapsules and the bottom layer sheet is coated with reactive clay. Though as time passed, the encapsulation technology have emerged and developed in many fields such as pharmaceutical industry [33], food [34], cosmetic [35], textile industries [22] and recently encapsulation of PCMs for thermal energy storage applications [36].

### **3.2 Morphology of the capsules**

The morphology of the capsules depends on the core materials and the deposition process of the shell. Figure 1 shows the morphology of three possible types of capsules with their

nomenclature [37]. The classical core/shell model of a microcapsule is given in Figure 1a. The capsule in Figure 1b differs slightly from the previous example in that the core is now divided into many separate regions. This may be called a multi-nuclear microcapsule. Figure 1c shows a micro-matrix particle, wherein the core material is evenly distributed through the particle and there is no surrounding shell coating.

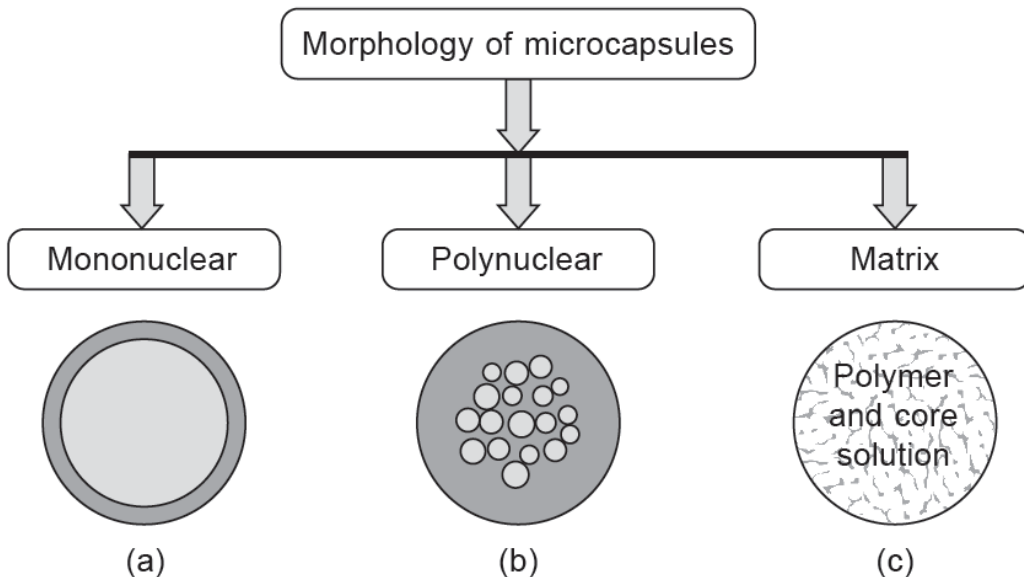


**Figure 3.1** Scheme diagrams of several different types of morphology of microcapsules [37]

### 3.3 Microencapsulation of phase change materials (MEPCMs)

Phase change materials (PCMs) are organic or inorganic compounds, which melt and solidify with a melting range suitable for the specific application. They have the ability to absorb and release large amount of heat during phase transition. However, to effectively use these materials, they need to be contained in inert and highly durable capsules. Recently, microencapsulation has been shown to provide an effective encapsulation of PCM, through an increasing heat transfer area, reducing PCMs reactivity towards the outside environment and prevent PCM from leaking when it is in liquid state.

Microencapsulation has already been proven as a successful technology in commercial applications such as in the pharmaceutical and agrochemical industries and recently, in the textile industry and thermal energy storage applications. In general, microencapsulation may be categorized into three groupings, namely chemical, physico-chemical and physico-mechanical processes (Table 3.1) [37]. In this chapter, we will discuss the most important methods of encapsulation, which are applicable to PCMs.

**Table 3.1** Methods used for microencapsulation [37]

Chemical processes	Physical processes Physico-chemical	Physico-mechanical
<ul style="list-style-type: none"> <li>Suspension, dispersion and emulsion polymerization</li> <li>Polycondensation</li> </ul>	<ul style="list-style-type: none"> <li>Coacervation</li> <li>Layer-by-Layer (L-B-L) assembly</li> <li>Sol-gel encapsulation</li> <li>Supercritical CO<sub>2</sub>-assisted microencapsulation</li> </ul>	<ul style="list-style-type: none"> <li>Spray-drying</li> <li>Multiple nozzle spraying</li> <li>Fluid-bed coating</li> <li>Centrifugal techniques</li> <li>Vacuum encapsulation</li> <li>Electrostatic encapsulation</li> </ul>

### 3.3.1 Interfacial polymerization (polycondensation)

This method is characterized by wall formation via rapid polymerization of monomers at the surface of the droplets of dispersed core material. Droplets are first formed by emulsifying an organic phase consisting of core materials and oil-soluble reactive monomer, which is usually isocyanate or acid chloride, in an aqueous phase. By adding water-soluble reactive monomer rapid reaction takes place between the two monomers at the interface of the droplets to form a polymer shell as shown in Figure 3.2.

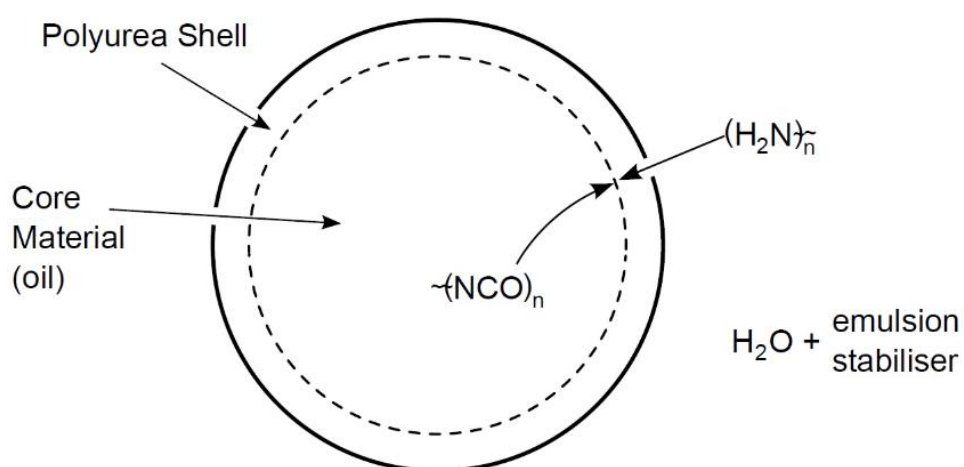


**Figure 3.2** Schematic formation of the MEPCM by interfacial polymerization [38].

The interfacial polymerization or polycondensation is a kind of popular method and it has been used for encapsulation a wide range of core materials, including oils [39], liquid crystal [40], pigment [41], proteins [42], peptides [43], and recently PCMs [44]. The preparation of polyurea microcapsules containing octadecane as PCM by interfacial polymerization was reported [44]. Toluene 2, 4-diisocyanate and diethylenetriamine were used as reactive monomers in disperse phase and aqueous phase, respectively. Multiple reactions occur during the formation polyurea shell. Polyurea microcapsules were formed not only by reaction toluene 2, 4-diisocyanate with diethylenetriamine, but also by the reaction of toluene 2, 4-diisocyanate with hydrolysed toluene 2, 4-diisocyanate at the interface and the excess of toluene 2, 4-diisocyanate with hydroxyl group of the non-ionic surfactant (NP-10) (Figure 3.3). The resulting polyurea microcapsules had a small size range of 0.1-1 um. The same method and materials were also employed, along with the addition of styrene-maleic anhydride copolymer as a dispersant [45]. Capsules ranged from 1-20  $\mu\text{m}$  in diameter.

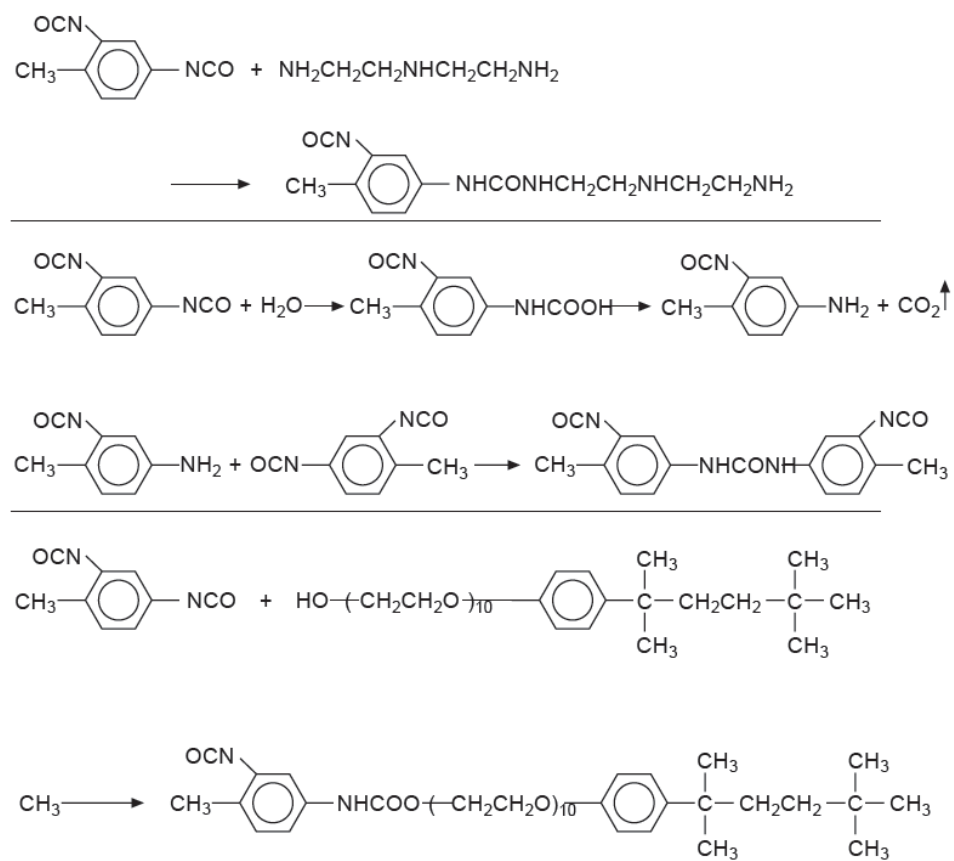


**Figure 3.3** Wall formation reaction of polyurea microcapsules: (a) reaction between TDI and DETA, (b) reaction between TDI and hydrolysed TDI and (c) reaction between TDI and NP-10 [44].

Different types of diamine water-soluble reactive monomers were investigated for preparing wall shell PCM microcapsules using interfacial polymerization method [46]. Ethylenediamine, 1, 6-hexane diamine and their mixture as water-soluble reactive monomers and toluene 2, 4-diisocyanate as oil-soluble monomer were used. The reported results show that, the encapsulation efficiency and thermal energy storage capacity of the PCM microcapsules reach highest when ethylene diamine was employed. In few years later, PCMs microcapsules based on n-octadecane as core material and polyurea as shell polymer using toluene 2, 4-diisocyanate as oil-soluble monomer and various amines containing different soft segments in the molecular chain (ethylene diamine, diethylene triamine and amine-terminated polyoxypropylene (Jeffamine T403)) as water-soluble monomers by polycondensation method were synthesised [47]. The morphological investigation (Figure 3.4) shows that the microcapsules synthesized using Jeffamine as the amine monomer have a smoother and more compact surface than those using ethylene diamine and diethylene triamine. Furthermore, large mean particle size, higher encapsulation efficiency and better anti-osmosis have achieved using Jeffamine.

A facile and an effective approach for fabricating highly monodisperse PCM polyurea microcapsules using a tubular microfluidic technique was prepared [48]. At the tip of the needle, spherical monodisperse droplets formed, stabilized under the action of emulsifier in the continuous phase, and then detached by a shear force caused by the cross-flowing continuous phase to produce an O/W emulsion. The O/W droplets were then partially solidified by polycondensation along the tube length and finally received in a collecting reservoir to perform the remainder polycondensation reaction (Figure 3.5). The resulting microcapsules were highly monodisperse and the particle size distribution ranged from 35 to 500  $\mu\text{m}$ . The size and morphology of the PCM microcapsules were controlled by changing the flow rates of the two immiscible fluids. In addition, adding conductor filler ( $\text{Fe}_3\text{O}_4$  NPs) into the organic phase depressed the supercooling of PCM microcapsules.

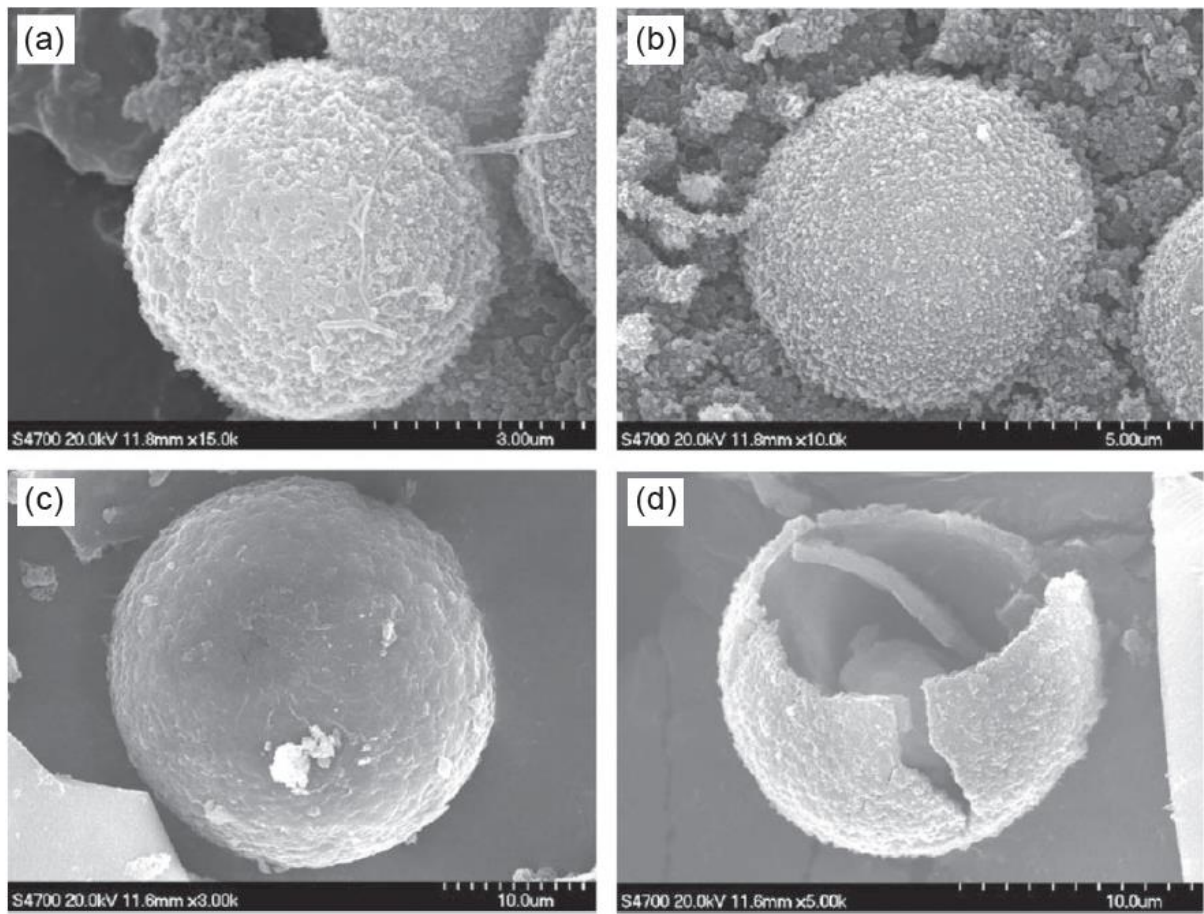


**Figure 3.4** SEM images of the microcapsules synthesized using different amine monomers: (a) EDA, (b) DETA, (c) Jeffamine, and (d) Cracked microcapsule Particle [47].

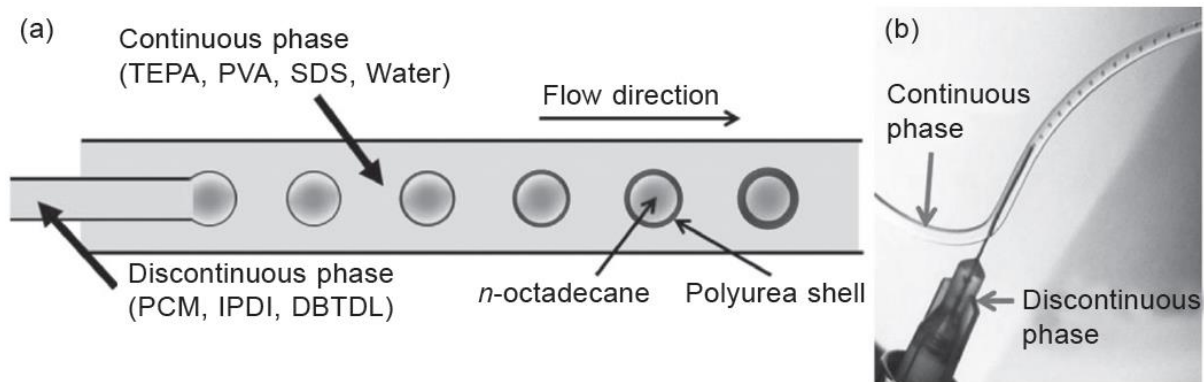


**Figure 3.5** (a) Schematic diagram of the fabrication of monodisperse PCM polyurea microcapsules in a tubular microfluidic device and (b) photograph of O/W PCM droplets produced at the tubular junction [48].

The microcapsules based on a polyurea shell have gathered much concern as an effective method for preparation PCMs microcapsules, since the polymerization reaction happened quickly and the produced PCMs microcapsules are relatively small and uniform in size. However, the microcapsules shell brittleness limited the practical applications of PCMs microcapsules using this technique. In an attempt to improve the polymer shell strength, a series of paraffin double-shell microcapsules with relatively low shell permeability were prepared using interfacial polymerization method [49]. The inner shell is formed through the reaction between polypropylene glycols and toluene 2, 4-diisocyanate and the outer through the reaction between toluene 2, 4-diisocyanate and amines (water-soluble reactive monomers) added in the aqueous phase. The same method and materials were also employed for the preparation of double-shell microcapsules along with the addition of styrene-maleic anhydride copolymer as a dispersant and butyl stearate as a PCM [50]. The reported results show that, the encapsulation efficiency has a maximum value of 95% at core to monomer ratio of 2, and the surface morphology of the microcapsules were smooth and compact with size range from 1-5  $\mu\text{m}$  in diameter. Furthermore, the latent heat was 85 kJ/kg with reasonable PCM weight content of 70 wt. %. The stability of the double-shell microcapsule against anti-ethanol wash and anti-heat are obviously improved compared to those of single-shell microcapsule [51]. Furthermore, novel PCMs microcapsules with styrene-divinylbenzene copolymer as inner shell and polyurethane as outer shell was investigated, where styrene and divinylbenzene were employed both as co-solvent and shell-forming monomers [32]. The mechanical strength of the shell microcapsules was slightly improved when double shell was fabricated.

### **3.3.2 In-situ polymerization**

In-situ polymerization is similar to the interfacial polymerization; except there are no reactive monomers in the organic phase, all polymerization takes place in the continuous phase rather than in the interface of the droplets as in the interfacial polymerization. The most common example of this method is the condensation polymerization of urea or melamine with formaldehyde to form cross-linked urea-formaldehyde or melamine-formaldehyde capsule shells. In this method, droplets are first formed by dispersing core material (PCMs) into an aqueous phase containing a small fraction of emulsifier, following that adding proper monomers or pre-polymers of urea with formaldehyde or melamine with formaldehyde. After the pH of the system is lowered, the polycondensation reaction starts, yielding cross-linked

urea-formaldehyde or melamine-formaldehyde resins. When the resin reaches a high molecular weight, it becomes insoluble in the aqueous phase, precipitates out and deposits at the oil-water interface of the droplets. The resin then hardens, forming the shell of the microcapsules as shown in Figure 3.6.

A number of articles have been published over the last few years on microencapsulation of PCMs using in-situ polymerization method. Melamine-formaldehyde microcapsules containing low melting temperature PCMs for used in cold energy transportation media by in-situ polymerization method was prepared [52]. Few years later, the same method and materials along with the addition of styrene-maleic anhydride monomethyl maleate copolymer as emulsifier was used [53]. The experimental result shows that the mixer speed in the emulsifying step was one of the most important factors affecting the size and size uniformity distribution of the PCMs capsules. By increasing the mixer speed, the size of the microcapsules is decreased and the uniformity size distribution is improved. The optimum emulsifying condition was found 8000 rpm with a capsule diameter of 4.2  $\mu\text{m}$ .

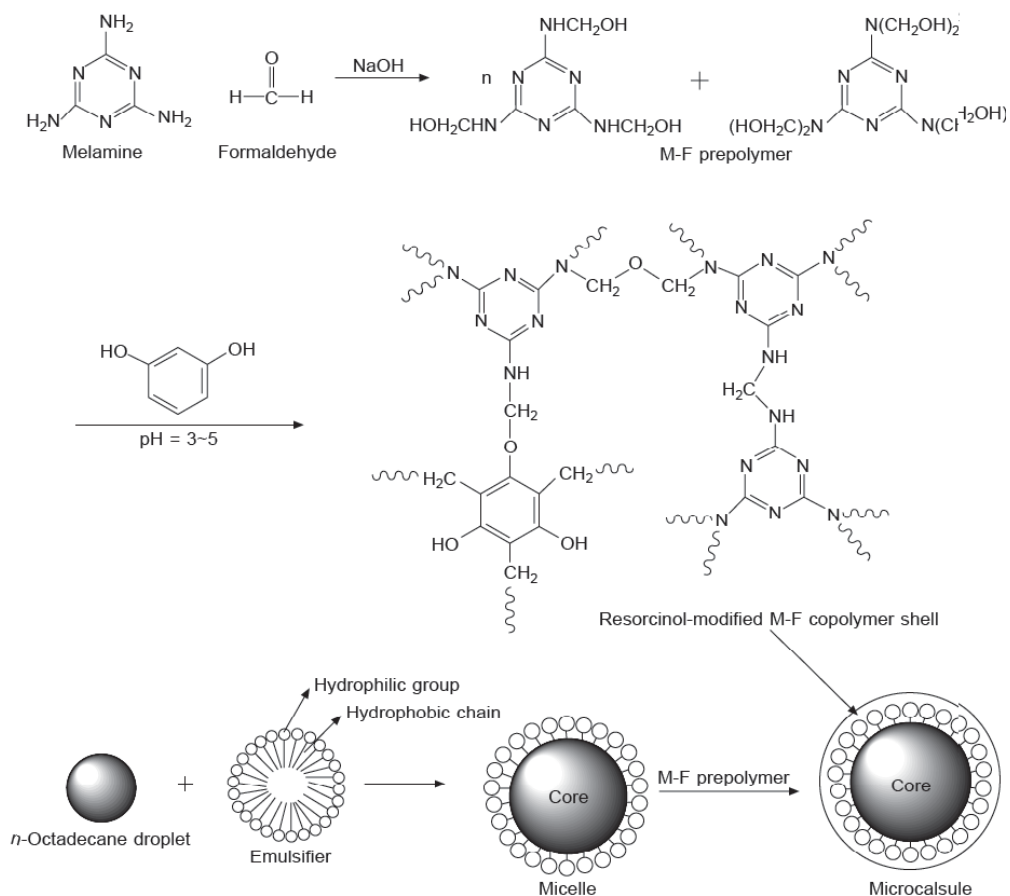


**Figure 3.6** Schematic formation of the n-octadecane microcapsules by in-situ polymerization [54].

A series of PCMs microcapsules articles have been published by a group of Chinese researchers based at Tianjin Polytechnic University using in-situ polymerization method [55–58]. The effects of stirring rate, contents of emulsifier and cyclohexane on diameters, morphology surface, phase change properties and thermal stabilities of the capsules were studied [57]. The diameters had less effect on the melting behaviour of microcapsules and significant effects on the crystallization behaviour. As the diameters of the microcapsules decreased, two crystallization peaks were observed from the DSC cooling curves (Figure 3.7). The ratio of the integrated area of the peak in the lower temperature increased with the decrease in diameters of microcapsules. The thermal stability of micro or nanocapsules rises with the increase of stirring rates and emulsifying content.

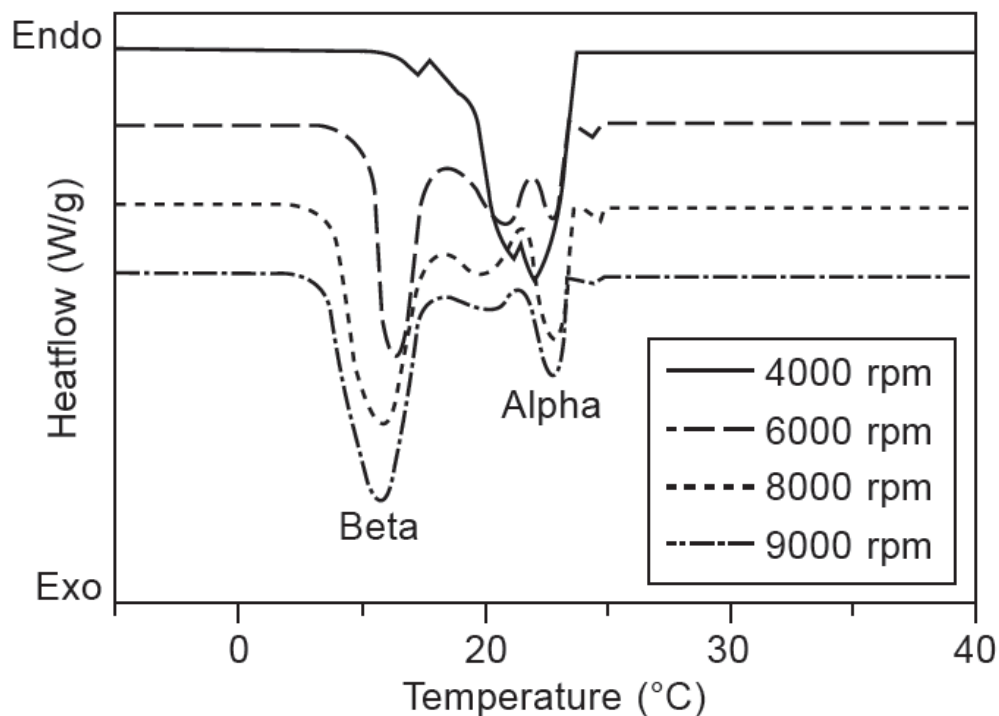


**Figure 3.7** DSC cooling curves of PCM microcapsules synthesized with various stirring rates [57].

Thermal stability of PCM microcapsules is crucial for practical applications. The effect of microcapsules diameter and urea-melamine-formaldehyde mole ratio on the thermal stability of PCMs microcapsules were investigated [55]. PCM microcapsules within the range of 0.4–5.6  $\mu\text{m}$  in size and urea-melamine-formaldehyde mole ratio of 0.2:0.8:3 have the highest thermal stability temperature. Furthermore, mixed 30–40 wt. % of cyclohexane with oil phase followed by heat-treatment at a suitable conditions produced a free expansion space inside the microcapsules (5–28 vt. %); thus improves the thermal stability of the PCMs

microcapsules. The existence of expansion space in the microcapsule allows the *n*-octadecane to expand freely when the temperature goes up without exerts stresses on the shell; thus thermal stability of *n*-octadecane microcapsules is enhanced [56, 58].

Thermal stability of the PCM microcapsules when silver nano particles (NCPCMMs) used was studied [59]. The surface morphology of the PCMs microcapsules becomes rough when silver nano particles were used as shown in Figure 3.8. However, the thermal stability of the PCMs microcapsules is improved as shown in Figure 3.9a. Furthermore, the percentage of weight loss under 130 °C at different time interval decreased in comparison to conventional PCMs microcapsules (Figure 3.9b). This could be attributed to the nano-composite structure of the microcapsules, in which metal silver nano particles mixed homogenously with a polymer shell; thus increase wall toughness and strength.

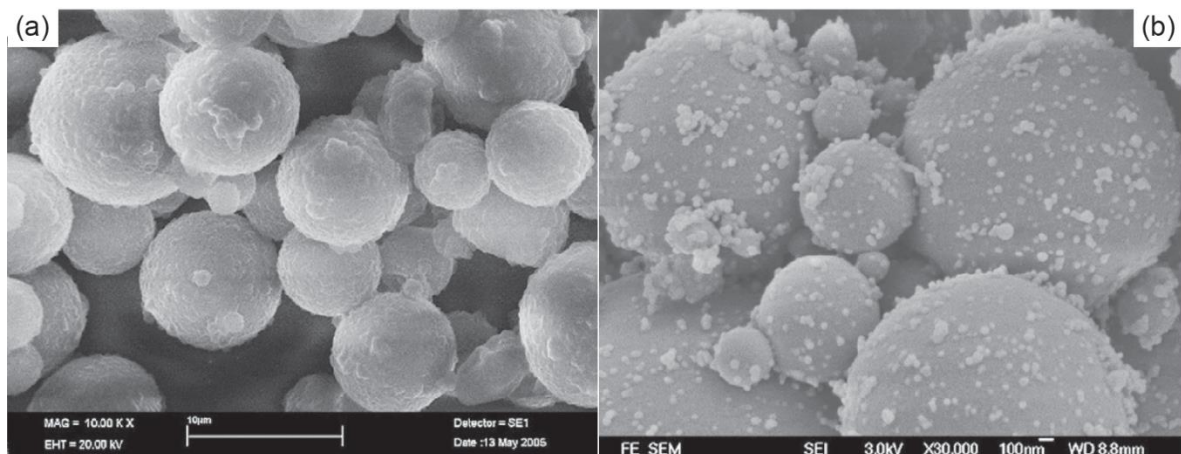
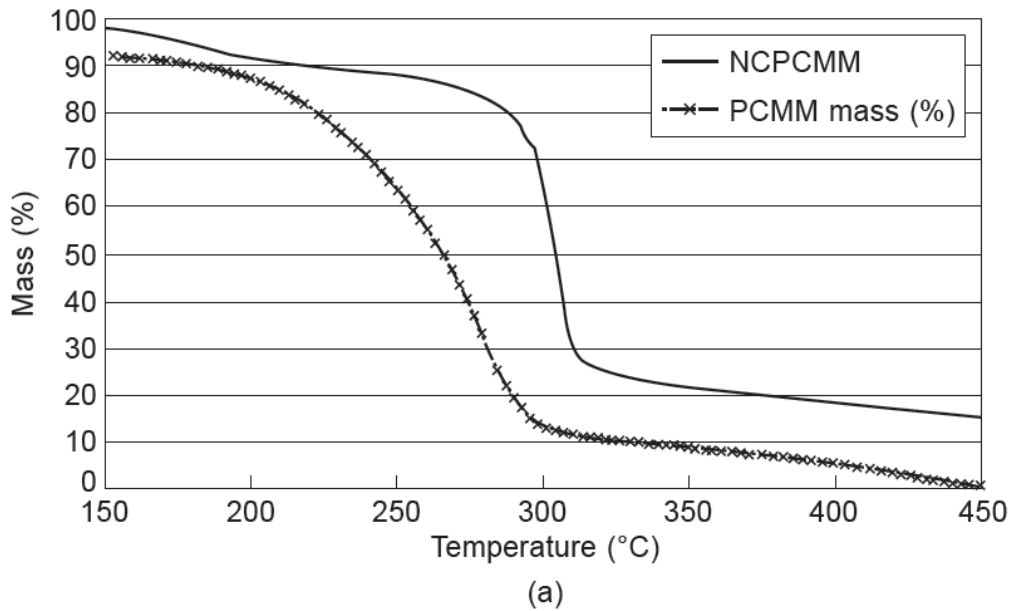
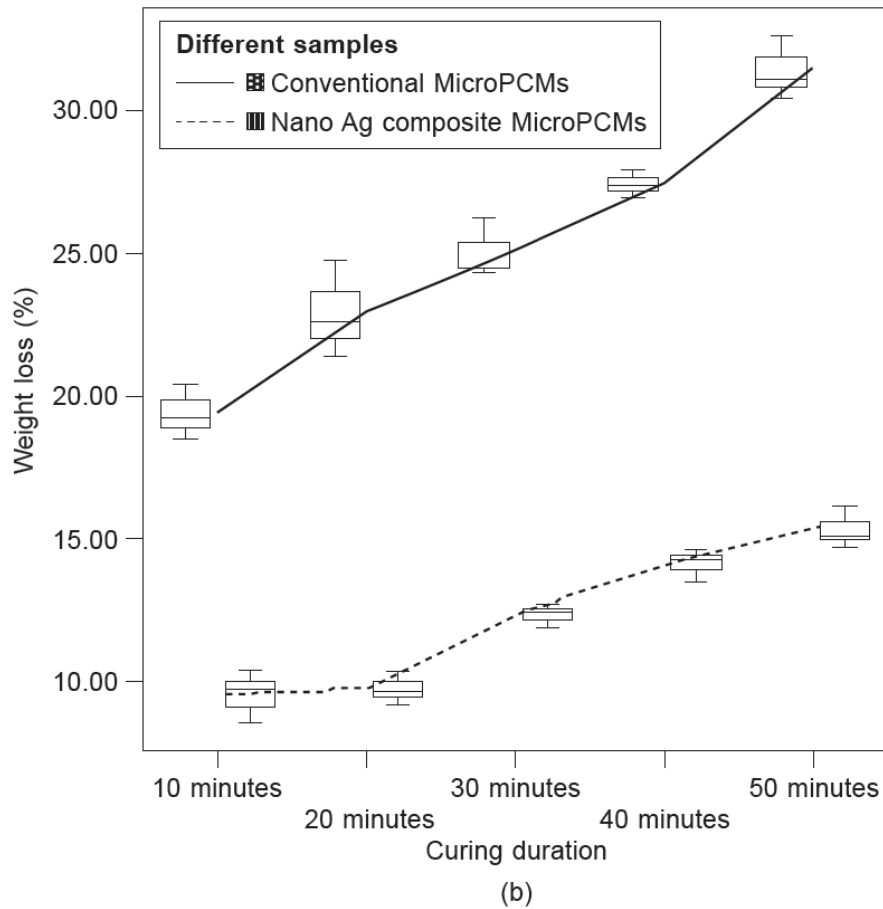


**Figure 3.8** SEM photos of (a) conventional PCM microcapsules and (b) silver-nanoparticles PCM microcapsules [59]



(a)



(b)

**Figure 3.9** (a) TGA curves of silver nanoparticles-PCM microcapsules and conventional PCM microcapsules and (b) weight loss trends of silver nanoparticles-PCM microcapsules and conventional PCM microcapsules at 130 °C [59].

Urea-formaldehyde or melamine-formaldehyde resins are one of the promising polymers used for microencapsulation of PCMs. However, formaldehyde based microcapsules do require significant preparation and strict safety precautions due to the fact that formaldehyde is known to be toxic. In addition, some of the residues of these formaldehyde resin in shells can cause environmental and health problems. Japan and European countries put a list of the maximum allowed residue limits of formaldehyde in textiles and similar products as reported in Table 3.2. Efforts have been made to reduce the remnant formaldehyde content in the PCMs microcapsules. Microcapsules containing n-octadecane with low remnant formaldehyde content was fabricated through intensified the system with melamine [60], using ammonia as a scavenger [61] or using methanol-modified melamine-formaldehyde pre-polymer as a shell material [62-64]. The results show that the remnant formaldehyde content in the PCMs microcapsules is still significant.

**Table 3.2** Examples of maximum allowed residue limits of formaldehyde in textiles and similar products [61]

	<b>Infant garments (ppm)</b>	<b>Garments that contact skin (ppm)</b>	<b>Other garments or fabrics (ppm)</b>
Japan Law No. 112	20	75	
European Union eco-label	30	75	300
Oeko-tex standard 100	20	75	300
EU restrictions on the use of dangerous chemicals	30	100	300
DIN CERTCO certification scheme for textile products	20	75	300
EU eco-label for footwear			textile 75 leather 150
EU eco-label for bed mattresses			mattress 30
EU eco-label for furniture			leather 150

ppm = parts per million, mg/kg, ng/g.

### 3.3.3 Suspension polymerization

Suspension polymerization is one of the encapsulation processes under the category of chemical methods. This method is used for production many common commercial resins, such as polyvinyl chloride (PVC), polystyrene and poly (methyl methacrylate). Through as

time passed, suspension polymerization used comprehensively for synthesis functional microspheres [65] and recently for fabrication PCMs microcapsules [66].

The mechanism formation of PCM microcapsules using free radical suspension polymerisation within a single droplet was described elsewhere [38]. The organic phase, which consists of PCM, water-insoluble monomers and free radical oil-soluble initiator are dispersed in the aqueous phase as droplets by high shear homogenization along with the use of small amounts of suspending agents. When the temperature reaches the decomposition temperature of free radical initiator, the reaction start takes place inside the droplets and the generated polymer precipitates out of the PCM-monomer mixture to form polymer particles. These particles continue to grow in number and size as polymerisation continues, and deposit at the oil/water interface by the action of hydrophobicity to form the capsule shell as shown in Figure 3.10.

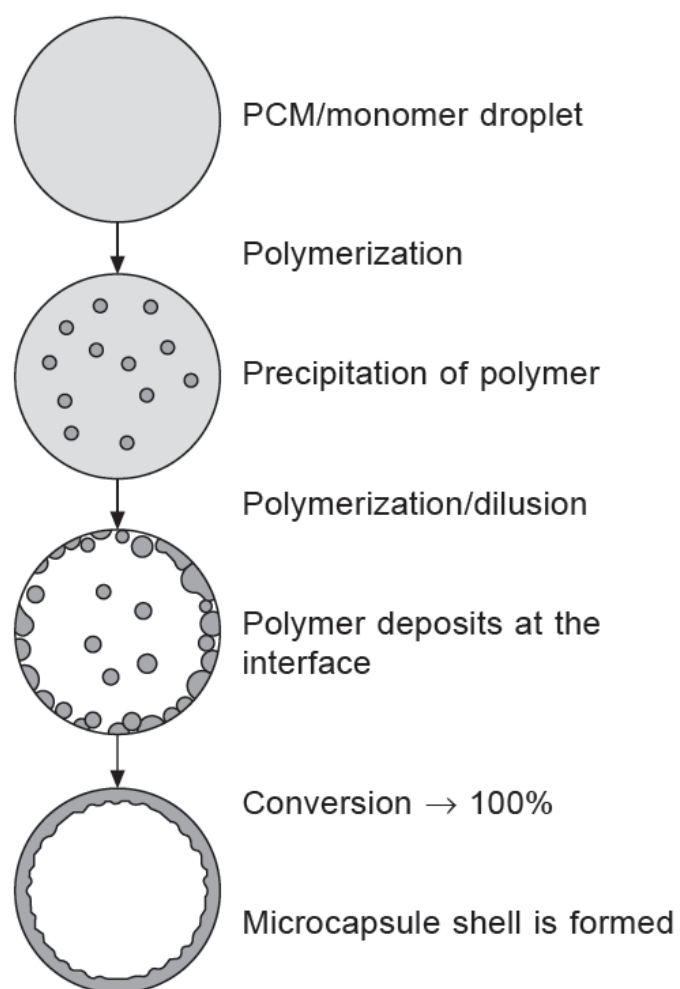


**Figure 3.10** Schematic diagram showing mechanism of capsule formation using suspension polymerisation [38].

At the beginning of the new century, microcapsules containing hexadecane as PCM and poly (styrene-co-N, N-dimethylaminoethyl methacrylate) as polymer shell was prepared using free radical suspension polymerization method [66]. SEM images show that hexadecane was completely encapsulated when the conversion was high, irrespective whether a hydrophilic co-monomer (N, N-dimethylaminoethyl methacrylate) was used.

Selecting proper shell materials for encapsulation PCMs is crucial for manufacturing fabulous PCMs microcapsules. Intensive work has been done for microencapsulation of PCMs using different shell materials (organic or inorganic shells). Polystyrene (PolySt) was used as a polymeric shell for microencapsulation different kinds of PCMs using suspension polymerization method [67]. This method allows encapsulating non-polar PCMs, while it was not possible to encapsulate polar PCMs. The microcapsules PCM content depends on the type of PCM used, with a possibility to obtain microcapsules with 50% by weight PCM. The same method of encapsulation has been used along with the use of poly (divinylbenzene) as shell material instead of polystyrene [68-70]. Poly methyl methacrylate (PMMA) microcapsules containing PCMs have been produced by Turkish researchers group based on Gaziosmanpasa University [71-74]. Furthermore, PMMA was used for encapsulating paraffin based on ultraviolet irradiation-initiated (UV) [75, 76].

The internal structure and surface morphology of the PCMs microcapsules depend on the core and shell materials type as well as the method of encapsulation (deposition process of the shell). The polarity and interfacial tension of the formed polymer inside the PCM droplets when the suspension polymerization technique was used are crucial for forming core/shell morphology. A composite salami-like morphology (large spheres encasing within the large capsule) was observed (Figure 3.11a) [67]. The values of polarity and interfacial tension of polystyrene are quite similar to paraffin wax, and thus core/shell morphology was not thermodynamically favoured during the polymerization process.

In an attempt to increase the polarity gap between polymer formed and PCM mixed of monomers with different polarity has been used. Microencapsulation of PCMs with a styrene-methyl methacrylate copolymer shell using suspension polymerization technique were prepared [77]. The internal structure of the large PCM microcapsules shows similar internal structure (salami like structures) when polystyrene microcapsules was used as shown in Figure 3.11b. However, the energy storage capacity of poly (styrene-methyl methacrylate) microcapsules was higher than polystyrene microcapsules at the same conditions. The higher

reactivity and polarity of methyl methacrylate compared to styrene favour paraffin microencapsulation. Two morphological features were observed when monopolymer of methyl methacrylate was used as a polymer shell of PCMs microcapsules: (1) inner structure with uniform mixture of paraffin and poly methyl methacrylate (Figure 3.11c) and (2) bumpy and irregular outer shell (Figure 3.11d) [77]. From a thermodynamic point of view the morphology of PMMA/paraffin microcapsules should be resemble a core/shell morphology, but Figure 3.11.d shows this was not the case. The rapid chain growth of MMA has produced a chain polymer with high molecular weight; thus facing a difficulty to diffuse and create core/shell morphology.

Further increase in the polarity of the chain polymer shell using ter-polymerization of methyl methacrylate, methyl acrylate and methacrylic acid (MMA-co-MA-MAA) was investigated [78]. The acrylic polymer appears to have formed seed-like spheres with thin and continuous shell (3  $\mu\text{m}$  in diameter) inside the large capsule and wrinkled exterior shell of the capsules (Figure 3.11e). The use of acrylic monomers to be part of the polymer shell reduced the wet glass temperature of the chain polymer; thus slightly enhanced the chain diffusion of the polymer to the interface. However, no significant difference in molecular weight of the chain polymer before and after used acrylic monomers was observed; thus minor enhancement of phase separation was achieved, but not sufficient enough to produce core/shell morphology. DSC results show that the PCMs microcapsules heat capacity when acrylic monomers were used increased twice than that of styrene based encapsulation.

A series of PCMs microcapsules articles have been published by a group of Chinese researchers from Tsinghua University using suspension polymerization method [79-82]. The effect of copolymerization of acrylic monomers with different side chain length on the thermal stability and PCM content in the microcapsules were investigated. The findings show that, the payload content of n-octadecane in the microcapsules inversely proportional with the length side chain of the acrylic monomers, and reached a maximum value up to 77 wt. % in the case of poly (methyl methacrylate-co-butyl methacrylate) copolymer shell. On the other hand, poly (methyl methacrylate-co-stearyl methacrylate) copolymer shell displays the highest thermal resistance up to a temperature of 255 °C.

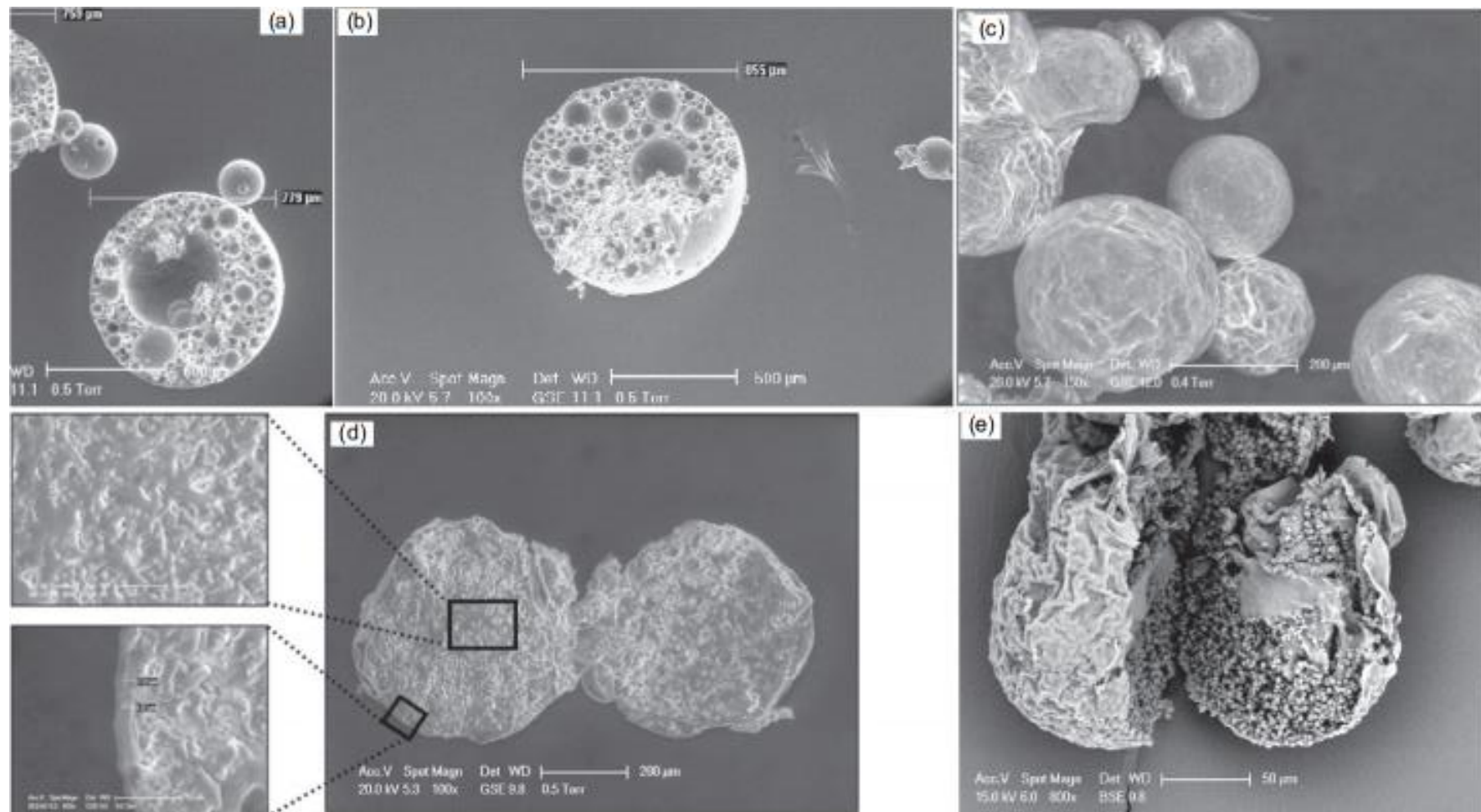


**Figure 3.11** SEM images of (a) cross-section of PolySt/ paraffin microcapsules, (b) cross-section of poly (St-MMA) /paraffin microcapsules, (c) general view of PMMA microcapsules, (d) cross-section of inner structure of PMMA/paraffin microcapsules and (e) cross-section of Poly (MMA-co-MA-co-MAA)/paraffin microcapsules [67, 77, 78].

### 3.3.4 Coacervation-phase separation method

Coacervation-phase separation method is one of the common methods of PCM encapsulation under a physic-chemical category. The polymer shell formed by cross linked two oppositely polyelectrolytes charge (polycation and polyanion) in an aqueous solution. Usually gelatin and gum arabic is the polycation and polyanion respectively. PCMs are dispersed in the gelatinous solution at an approximately 40-60 °C to form emulsion. Then Arabic gum was added slowly to the emulsion. Once, the pH adjusted with in the rage of 4.0-4.6 using acid; the phase separation is taken place and gel is formed around the oil droplets during the process of cooling. The formed gel was cross-linked using glutaraldehyde and becomes hard polymer shell then the prepared capsules separated. Schematic diagram of typical encapsulation process based on complex coacervation is shown in Figure 3.12 [38].

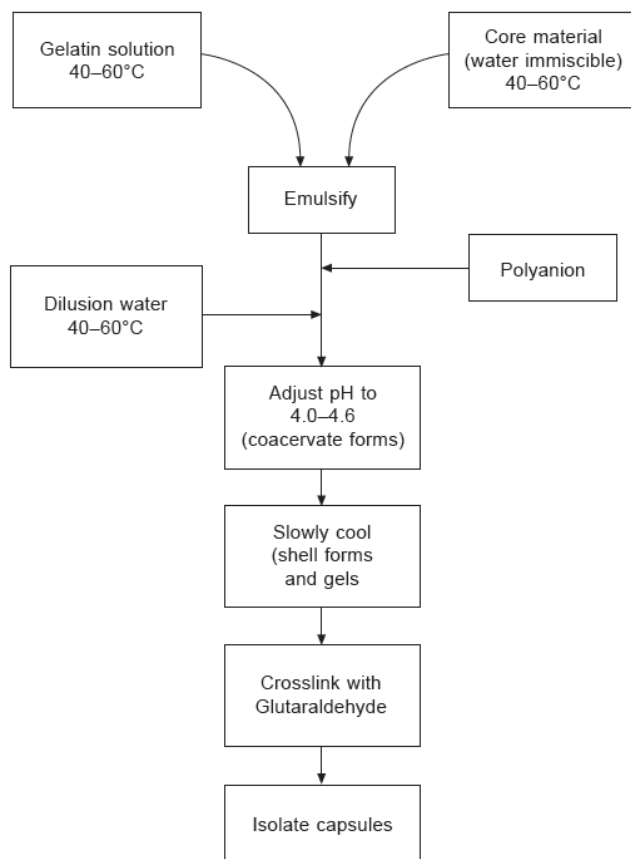


**Figure 3.12** Schematic diagram of typical encapsulation process based on complex coacervation [38].

In early 2000s, gelatinous microcapsules containing paraffin wax with diameter size of 50-100  $\mu\text{m}$  was prepared using complex coacervation method [36, 83]. Gelatin, gum arabic and formaldehyde were used as polycation, polyanion and cross-linker respectively. The results show that, the optimum emulsification rate of 1000 rpm for 10 minutes and the amount of cross linking agent is 6-8 ml. The PCM microcapsules energy storage and release capacities depend on the core/shell mass ratio, when the core/shell mass ratio of 1:1 the energy storage capacity was 213 J/g. Few years later, commercial Rubitherm RT27 microcapsules with two different coacervate compositions (Sterilized gelatin/Arabic gum and agar-agar/Arabic gum) using complex coacervation method were fabricated [84]. The RT27 mass content inside the microcapsules was similar with two different shells (48 wt. %), while the average particle diameter was 12  $\mu\text{m}$  and 4.3  $\mu\text{m}$  in the case of sterilized gelatin/Arabic gum and agar-agar/Arabic gum system respectively. Both systems degraded at the same temperature, but in the case of agar-agar/ Arabic gum system, the PCM microcapsules degraded in a more gradual way.

### **3.3.5 Spray-drying and other methods of PCMs microencapsulation**

As mentioned early in Table 1.1, spray-drying method is classified under mechanical process category and basically is suitable for heat-sensitive materials. Spray-drying method has been applied widely for microencapsulation of food [85], pharmaceutical ingredients [86] and recently PCMs [83].

Synthesis polymer microcapsules containing PCMs using spray drying method was reported [83]. Gelatin-acacia was used as polymer shell and paraffin wax as PCM. The microcapsules have high core loading up to 80% with a particle size range within 0.1–5  $\mu\text{m}$ . Furthermore, the microencapsulation efficiency between 60 and 92% and it's depending on the core-to-coating mass ratio. Low density polyethylene (LDPE) and ethylvinylacetate copolymer (EVA) were used as shell materials to encapsulate paraffin RT27 using spray drying method [87]. The operating conditions and formulation used to obtain the PCMs microcapsules were reported in the European patent EP2119498 (A1) [88]. A homogeneous liquid solution of PCM, polymer and dissolved polymer solvent was heated up above the melting point of PCM and then atomized using compressed  $\text{N}_2$  gas. The solvent was evaporated by a hot drying  $\text{N}_2$  in the drying chamber and then the polymer capsules were recovered in the collector (Figure 3.13). The properties of RT27 microcapsules depend on the location of microcapsules collection from the spray dryer. The PCM mass content in the

microcapsules produced using this method is similar to those produced by suspension polymerization method [67] and it is seemed to be more thermally stable after 3000 thermal cycles as shown in Figure 3.14.

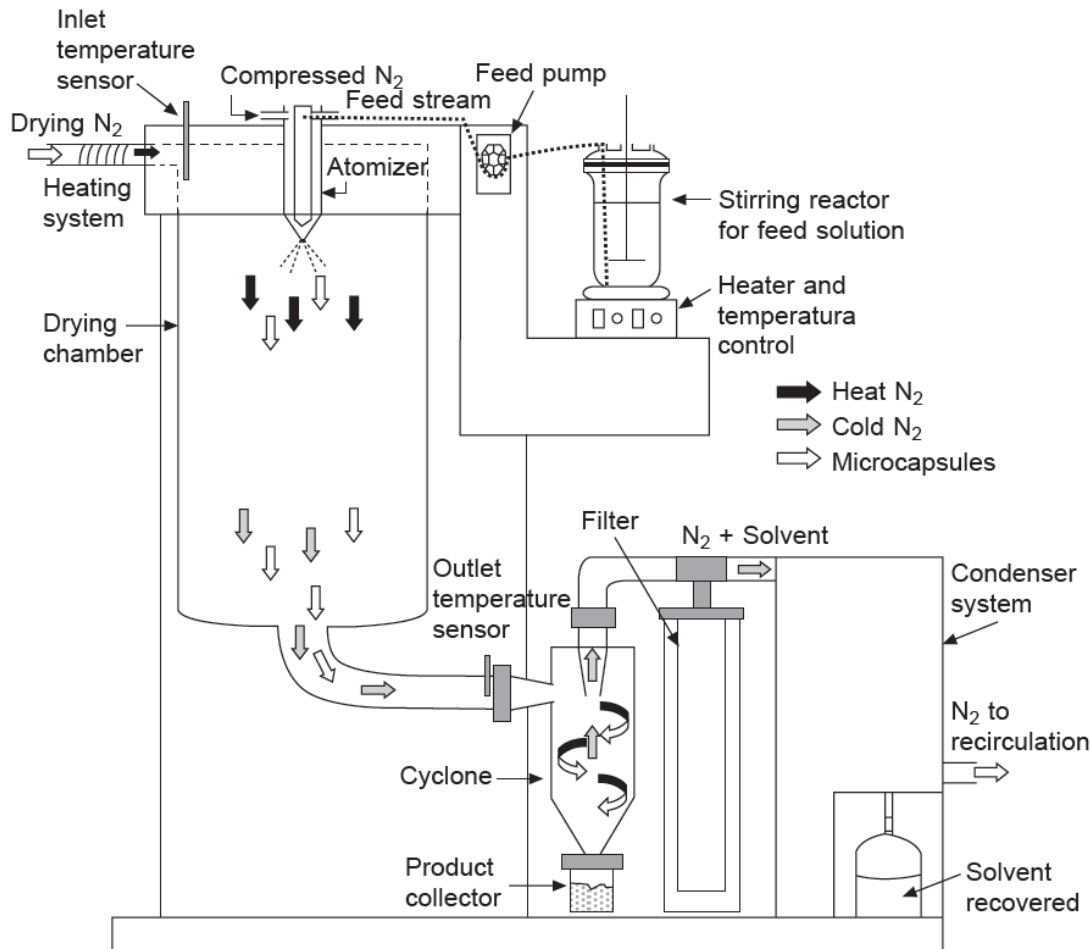


**Figure 3.13** Schematic representation of the spray drying equipment used for fabricated PCM microcapsules [87].

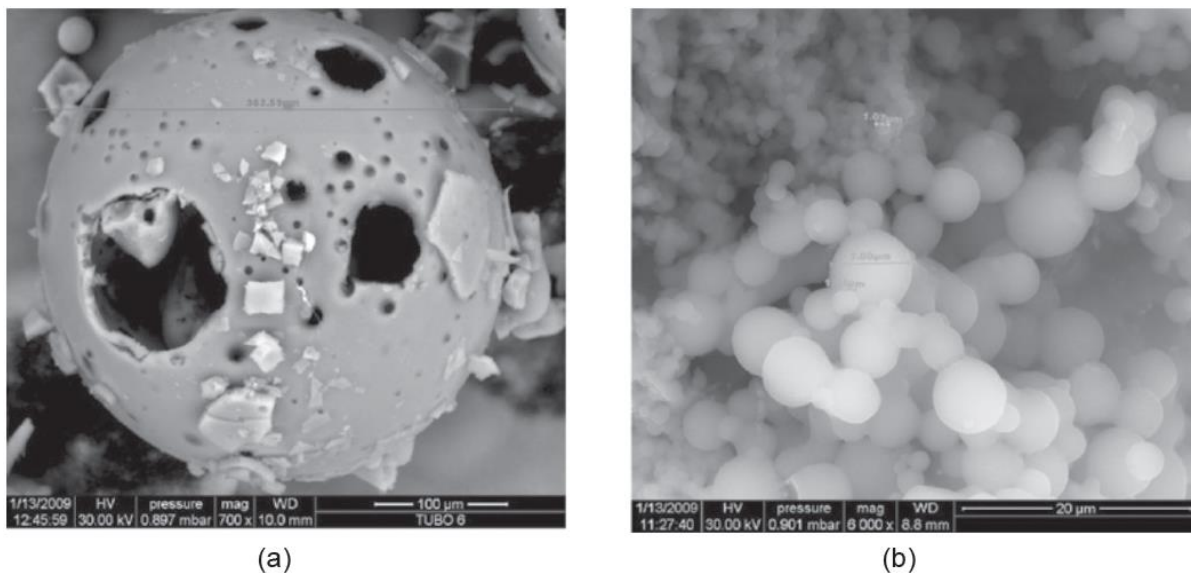


**Figure 3.14** SEM images of RT27 microcapsules produced using two different methods and shell materials after 3000 thermal cycles: (a) suspension polymerization method (polystyrene shell) and (b) spray drying method (LDPE–EVA shell) [87].

Other methods for microencapsulation of PCMs have been reported in the literature, for examples polycarbonate microcapsules containing stearic acid as PCM using solution casting method [89], n-tetradecane-microcapsules with different shell materials using phase separation method [90], PMMA-network-silica hybrid as polymer shell [91] via Sol-Gel process and n-eicosane microcapsules coated with polysiloxane using co-emulsification method [92].

### 3.4 Conclusion

This chapter discussed the most important methods of microencapsulation, which are applicable to the PCMs. The microcapsules based on polyurea shell have gathered much concern as an effective method for preparation PCMs microcapsules, since the polymerization reaction happened quickly and the produced PCMs microcapsules are relatively small and uniform in size. However, the microcapsules shell brittleness limited the practical applications of PCMs microcapsules using this technique. Urea-formaldehyde or melamine-formaldehyde resins are the shell materials used for microencapsulation of PCMs using in-situ polymerization method. Formaldehyde based microcapsules do require significant preparation and strict safety precautions due to the fact that formaldehyde is known to be toxic. In addition, some of the residues of these formaldehyde resin in shells can cause environmental and health problems. Gelatine and agar are the main materials used in coacervation method. These materials are prime mediums for bacterial growth alongside have the

ability to absorb water, which changes the physical properties of the shell capsules. These drawbacks limited the widespread applications of PCMs microcapsules produced using this method. Reducing the cost of manufacturing PCM microcapsules is considered a main issue and should be taken into account. High cost of production, coalescence problem and wide particle size distribution are inhibiting the chances of widespread use of spray drying method. Among the different methods of synthesis PCMs microcapsules, suspension polymerization has gained more attention recently as it is considered simple, safe and nontoxic materials used as well as provides the easy path to scale up production; thus this method will be used in this study for fabricating cross-linking of PMMA microcapsules containing Rubitherm<sup>®</sup> RT21.

# **Emulsion Stability and Cross-linking of PMMA Microcapsules Containing Phase Change Materials (PCMs)**

**4**

## **Abstract**

The microencapsulation of paraffin as a phase change material (PCM) using poly methyl methacrylate (PMM) as a shell was investigated by means of suspension polymerization. The increase in the emulsion stability by using mixed surfactants was studied. It was observed that a mixed surfactants system induces long-term emulsion stability and monodisperse droplets size distribution. Also, the use of mixed surfactants reduces significantly the buckles in microcapsules significantly. The effect of using pentaerythritol tetraacrylate (PETRA) as a cross-linker agent on the diverse properties of PCM microcapsules such as morphology, energy storage density, shell permeability and thermal stability has been investigated. Adding PETRA to the system improves the surface morphology and produces microcapsules with a much higher PCM content. For example, the core/shell mass ratio of 2:1 produces microcapsules with regular spheres having smooth surfaces. TGA results show two steps thermal degradation of microcapsules. The mass loss was similar to the non-encapsulated PCM until all the PCM was dissipated (step 1). Following that the microcapsules experienced lower rate of mass loss of the shell, which depends on its thickness (step 2).

## 4.1 Introduction

In an attempt to reduce the amount of energy consumption by heating and cooling in buildings, considerable efforts have been made to use phase change materials (PCMs) within the building envelope [5]. PCMs are organic or inorganic compounds, which melt and solidify with a melting range suitable for a given application. They have the ability to absorb and release large amounts of heat during their phase transition. The use of PCMs in buildings increases their thermal inertia, and therefore improves thermal comfort, reduces internal temperature fluctuation reduces heating and cooling requirements. However, in order to use them practically, they must be well contained to prevent them from leaking out when melted. Microencapsulation has been shown as the effective engulfing of PCM [93].

Microencapsulation is a well-known technology and has been developed in many fields such as pharmaceutical industry [33], food [34], cosmetics [94], textile industries [95] and thermal energy storage applications [36]. A number of articles have been published for microencapsulation of PCMs using different techniques with different shell materials [44, 83, 96]. A method was developed based on suspension free radical polymerization for microencapsulation hexadecane by using poly (styrene-co-N, N-dimethyl amino ethyl methacrylate) as shell [66]. Paraffin wax microcapsules were produced using gum arabic-gelatin mixture (as a shell material) by means of spray drying and complex coacervation methods [83]. Polycarbonate microcapsules containing stearic acid as PCM was fabricated using solution casting method [89]. N-tetradecane-microcapsules with different shell materials were synthesized by using phase separation method [90]. Poly methyl methacrylate (PMMA) network-silica hybrid microcapsules containing PCM was fabricated via Sol-Gel process [91]. A series of PMMA microcapsules containing different kind of PCMs were prepared using emulsion polymerization method [71-74]. Tetradecane microcapsules using melamine formaldehyde as a shell material was prepared using in situ polymerization [53]. Polyurea microcapsules containing octadecane as PCM was fabricated using interfacial polymerization [44]. A facile and an effective approach for fabricating highly monodisperse PCM polyurea microcapsules were reported using a tubular microfluidic technique [48].

In all of microencapsulation methods that previously mentioned, the introduction of emulsifier to stabilise the emulsion has been critical. Different concentrations of polyvinylpyrrolidone (PVP) (K30, Mw 40,000 g/mol) as stabilizer were tested [78]. The average particle size decreased when

the surfactant concentration increased. The highest mass percentage of paraffin in the microcapsules (46.5 wt. %) was achieved at a core/shell mass ratio of 1.02 and PVP/monomer mass ratio of 0.091. The effect of different types of single surfactant on the PCM microcapsules properties (particle size distribution, morphology and thermal properties) were investigated [97]. Spherical microcapsules with smooth surface were obtained when polyvinylpyrrolidone (PVP) and gelatin was used. Nevertheless, Arabic gum and poly vinyl alcohol (PVA) shows irregular particles with a rough surface. PVP produced microcapsules with lowest value of mean particle diameter (204  $\mu\text{m}$ ) while Arabic gum produced microcapsules with the highest amount of PCM mass percentage content (67.9 wt. %).

A prerequisite for manufacturing good characteristics PCM microcapsules is the ability to produce stable emulsion with a well-controlled droplets size. Literature survey clearly indicates that in the majority of the investigations of PCM microencapsulation single surfactant was used [97-99]. Improving the stability of the emulsion through the use of mixed surfactants was not reported in the literature. Therefore, in this work, the emulsion stability and PCM microcapsules characterizations (morphology and thermal properties) were investigated in the presence of a mixture of surfactants (sodium dodecyl sulfate (SDS) and poly vinyl alcohol (PVA)).

A number of articles in the literature reported that the cross linking of PCM microcapsules exhibits a great improvement in shell mechanical strength and PCM payload [79, 80, 100]. Therefore, the effect of adding pentaerythritol tetraacrylate (PETRA) as cross linking agent on the PCM microcapsules characteristics such as morphology, shell permeability and thermal properties was investigated.

## 4.2 Experimental

### 4.2.1 Materials

Methyl methacrylate (MMA) (99%, contains  $\leq 30$  ppm monomethyl ether hydroquinone (MEHQ) as inhibitor, Sigma Aldrich, NZ) and pentaerythritol tetraacrylate (PETRA) (contains 350 ppm (MEHQ), Sigma Aldrich, NZ) were used as monomer and cross-linking agent respectively. Commercially available Rubitherm®RT21 ( $T_{\text{pm}} = 21^\circ\text{C}$ ,  $\Delta H_m = 135 \text{ J/g}$ , RUBITHERM® Technologies GmbH, Germany) was used as PCM. Polyvinyl alcohol (PVA) (Mw 85,000-124,000, Sigma Aldrich, NZ) and sodium dodecyl sulfate (SDS) (BioXtra, 99%, Sigma Aldrich, NZ) were

used as non-ionic and ionic surfactant respectively. Luperox® A75, Benzoyl peroxide (BPO) (75%, contains 25% water, Sigma Aldrich, NZ) was used as free radical thermal initiator. All chemicals were used as it is without any further purification.

## **4.2.2 Synthesis of PCMs Microcapsules**

### **4.2.2.1 Emulsification**

A standard procedure was used as reported elsewhere [67]. Wherein; an aqueous solution of surface-active agent (called aqueous phase) and a mixture of MMA, PETRA, BPO and PCM (called organic phase) were prepared separately. The organic phase was added to the aqueous phase and emulsified mechanically using a high shear mixer (Silverson L5M-A laboratory Mixer) equipped with a fine emulsor screen. A stirring rate of 3000 rpm for 5 minutes was chosen to achieve the required emulsification.

### **4.2.2.2 Polymerization**

The produced emulsion was transferred to a 2-L four-neck glass reactor (LR-2.ST laboratory reactor- IKA-Werke GmbH@Co.KG) consisting of EUROSTAR 200 control P4, Anchor stirrer LR 2000.1, HBR 4 digital heating bath as shown in Figure 4.1. The agitation speed was set at approximately 300 rpm; and the temperature of the water bath was maintained at 70 °C for 2 hours, and then adjusted to 85 °C for another 4 hours. The water bath was then switch off and allowed to cool down naturally to room temperature. After cooling, the suspension of PCM microcapsules was transferred to a clean glass beaker and washed three times with distilled water to remove the unreacted monomers and the PCM, which is not encapsulated. The separated microcapsules were spread on a tray and placed in an oven at 50 °C for 48 hours for drying. The dried microcapsules were then collected for testing.

## **4.2.3 Characterization of Microcapsules**

### **4.2.3.1 Scanning Electron Microscope (SEM)**

The microcapsules morphology was examined using a scanning electron microscope (SEM) (Philips XL30S FEG, Netherland) operating under low vacuum pressure of 0.9 torr. All samples were coated with gold prior to the investigation.



**Figure 4.1** Schematic diagram of LR-2.ST laboratory polymerization reactor

#### 4.2.3.2 Differential Scanning Calorimetry (DSC)

Phase change properties of the fabricated PCM microcapsules and the pure PCMs (such as melting and solidification temperatures and their phase change enthalpies) were determined using a SHIMADZU DSC-60 differential scanning calorimetry. The measurements were performed by varying the temperature from -15 to 40 °C with heating and cooling rate of 3 °C/min. Each sample was analysed for three times and the average was taken.

Consequently, the ratio of encapsulated PCM (core material) to polymer (shell material) can also be determined using DSC results from the following equation [78].

$$\% \text{ PCM in microcapsules by mass} = \frac{\Delta H_{\text{microcapsules}}}{\Delta H_{\text{Pure PCM}}} \times 100\% \quad (4.1)$$

Where,  $\Delta H_{\text{microcapsules}}$  (J/g) is the latent heat of the microcapsule containing PCM and  $\Delta H_{\text{Pure PCM}}$  (J/g) is the latent heat of pure PCM (before encapsulation). In equation 1, it is assumed that the latent heat of the microcapsule without PCM is zero, which is true if the shell does not go phase change.

#### **4.2.3.3 Particle Size and Particle Size Distribution (PSD)**

The particle size distribution of the microcapsules was measured using a laser Diffraction Particle Size Analyser (Mastersizer 2000, Malvern, UK). In such analysis, a small sample of suspended microcapsules was dispersed into deionised water bath. The water bath equipped with an ultrasonic probe to prevent particles agglomeration and a pump arm to circulate the suspended microcapsules into the measuring cell. Each sample was analysed for three times and the average was taken.

#### **4.2.3.4 Thermal Gravimetric Analyser (TGA)**

Thermal stability of pure PCM and PCM microcapsules were analyzed using SHIMADZU TGA-50 thermal gravimetric analyzer (TGA). Analyses were performed by raising the temperature from room temperature to 550 °C at a heating rate of 10 °C/min.

#### **4.2.3.5 Mass loss**

The permeability of PCM through the shell of microcapsules was tested via mass loss analyses. This was performed by placing a known mass of dried microcapsules into an aluminium pan and putting it into a drying oven at 50°C. The mass of the microcapsules was periodically measured over a month. Also, the mass loss of bulk RT21 was measured under the same conditions for comparison. The mass loss percentage was calculated by the following equation.

$$\% \text{ mass loss} = \frac{\text{Initial mass} - \text{Final mass}}{\text{Initial mass}} \times 100\% \quad (4.2)$$

### **4.3 Results and Discussion**

#### **4.3.1 Effect of surfactants on the emulsion stability, morphology and thermal properties of PCM microcapsules**

Emulsion stability is the ability of an emulsion to keep its properties over a certain period of time. However, as emulsions are thermodynamically unstable, changes of emulsion properties will occur. The more slowly the properties change, the more stable the emulsion is. There are many phenomena such as coalescence; flocculation and creaming that can alter the properties of an emulsion. The disruption of oil droplets depends on the oil-water interfacial tension; droplet break-up is facilitated when the interfacial tension is low. The presence of an emulsifier in the system may help to

decrease the interfacial tension and minimize the effects of interfacial forces by forming a protective layer around the oil droplet [101].

The emulsion stability over a day was assessed by optical observation and emulsion droplet size measurements. A small quantity of the PCM emulsion was placed in a small glass beaker (~250 mL of emulsion) and kept for one day under a fume hood without mixing. The volume fraction ( $V_{fcr}$ ), of the formed cream layer was measured by the following equation:

$$V_{fcr} = \frac{V_{cr}}{V_{em}} \quad (4.3)$$

Where,  $V_{fcr}$  the volume fraction of the formed cream layer,  $V_{cr}$  volume of the cream layer and  $V_{em}$  volume of the emulsion.

The emulsion stability through the use of mixed surfactants was studied and compared to a system where only a single surfactant (PVA) was used. The concentrations of materials used in the preparation of single and mixed surfactants emulsion are reported in Table 4.1. The use of mixed surfactants induced long-term emulsion stability since the appearance of a whitish layer at the top of the emulsion after one day was not observed as shown in Figure 4.2. In contrast, whitish layer has been observed in the case of using single surfactant as shown in Figure 4.3, with approximately 25 % of cream volume fraction after the same period of time.

**Table 4.1** Concentrations of materials used in the preparation of PCM microcapsules (PCMMCs)

	Single surfactant	Mixed surfactant	Cross linked PCMMCs	Un-cross linked PCMMCs
<b>Aqueous phase</b>	Mass (g)	Mass (g)	Mass (g)	Mass (g)
Deionized water	600	600	600	600
Polyvinyl alcohol (PVA)	6	6	6	6
Sodium dodecyl sulphate (SDS)	--	0.3	0.3	0.3
<b>Organic phase</b>				
Methyl methacrylate (MMA)	33.3	33.3	28.3	33.3
Pentaerythritol tetraacrylate (PETRA)	--	--	5	--
Benzoyl peroxide (BPO)	0.8	0.8	0.8	0.8
Rubitherm®RT21 (PCM)	66.6	66.6	66.6	66.6



**Figure 4.2** Digital camera photographs of the PCM emulsion stability in the case of mixed surfactants system at (a) 0 day and (b) after one day

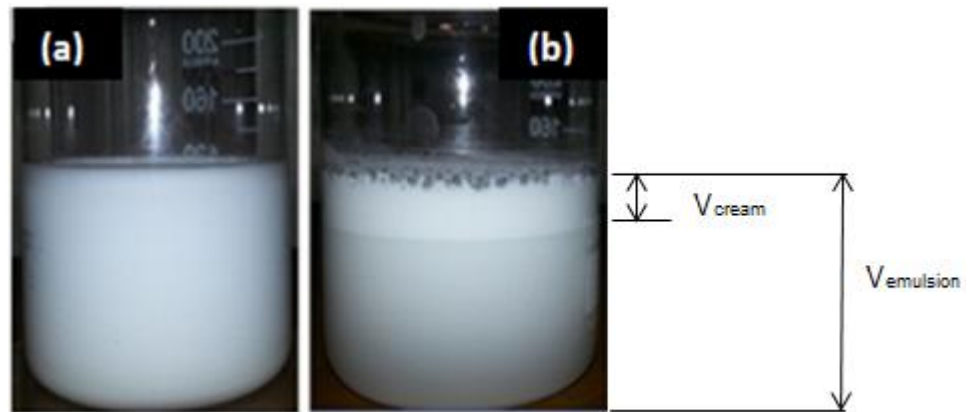


**Figure 4.3** Digital camera photographs of the PCM emulsion stability in the case of single surfactant system at (a) 0 day and (b) after one day

Visual observations may not be accurate enough to measure the emulsion stability. The instability of the emulsion is affected by droplet size. Thus, the droplet size measurement is important as it provides information about the emulsion properties. A mono-dispersed droplet distribution with no significant shifting of droplets size has been observed after one day in the case of mixed surfactant. In comparison, the single surfactant shows a poly-dispersed droplet size distribution with a dramatic increase in droplet sizes after the same period of time as shown in the Figure 4.4. The presence of a charged emulsifier (SDS) at the droplet interface could have induced a strong electrostatic repulsion between the droplets, which forms a thick protective interfacial film that prevents droplets contact and coalescence.

Aforementioned, the prerequisite for manufacturing good characteristics of PCM microcapsules is the ability to produce stable droplets with a uniform well-controlled size. The morphology and particle sizes of the PCM microcapsules were studied for both systems (single surfactant and mixed surfactants). It seems that the surface morphology and the particle size of the microcapsules are related directly to the emulsion stability, where the percentage of surface buckles and dimples on the surface of the microcapsules are reduced significantly in the case of mixed surfactant. The use of mixed surfactants reduced microcapsules size to almost half as shown in Figure 4.5. Existing of SDS in the system could have produced a uniform protective layer around the droplets and hence reducing interfacial tension between the organic phase and the aqueous phase.

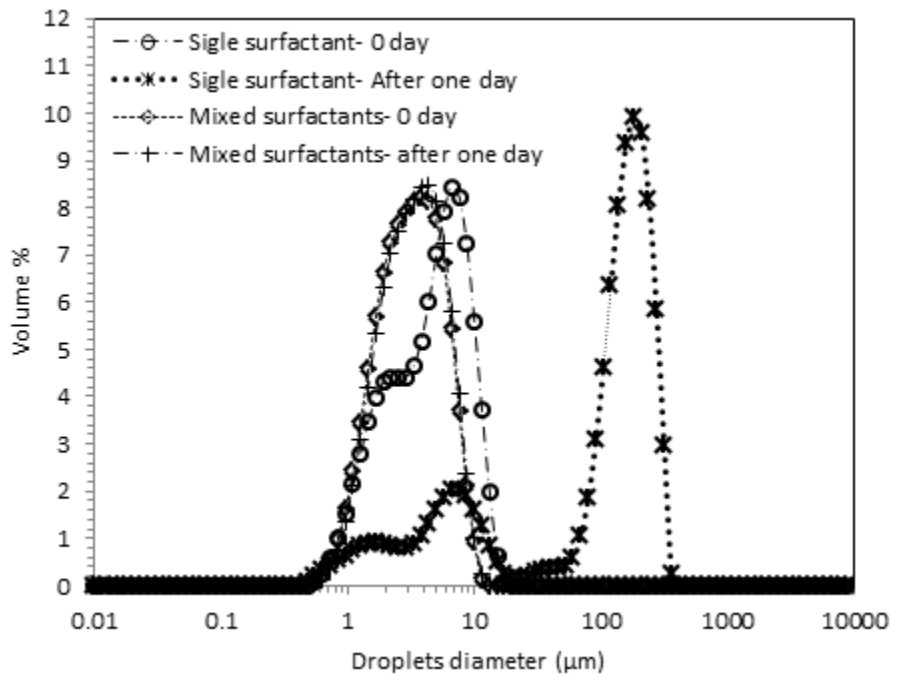


**Figure 4.4** Droplet size distributions of the PCM emulsion

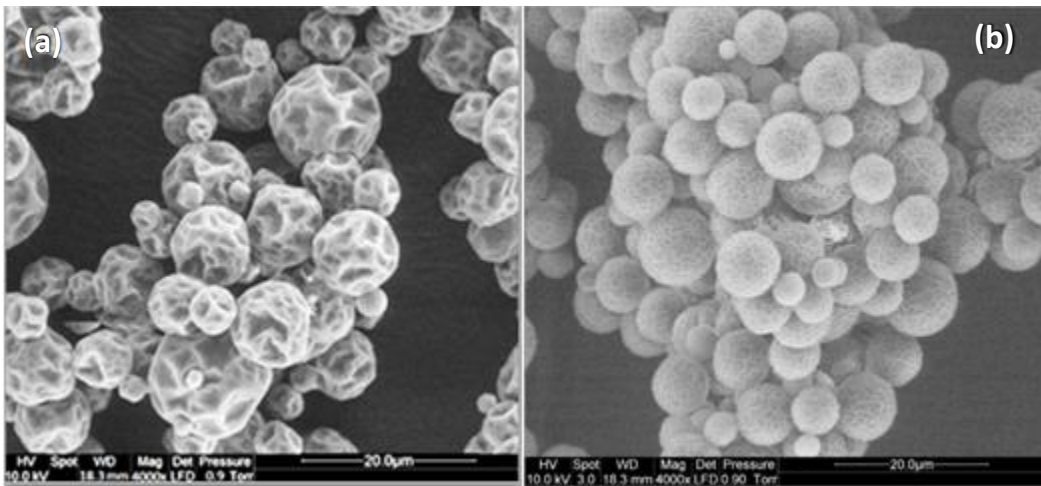


**Figure 4.5** SEM surface morphology micrographs of the PCM microcapsules: (a) Single surfactant and (b) Mixed surfactants

#### 4.3.2 Effect of cross linking agent on the morphology of microcapsules

The cross linking agent in polymer science is a substance that promotes or regulates the intermolecular covalent bonding between polymer chains, linking them together to create a more rigid structure. The effect of cross linking agent on the diverse properties of the microcapsules (morphology and thermal properties) was investigated in this work. The morphologies of the cross-linked and uncross-linked PCM microcapsules are shown in Figure 4.6. In the case of uncross-linked PCM microcapsules, the morphology appears to be similar to the wool ball with wrinkled and rugged surfaces as shown in Figure 4.6a. In contrast, adding a small amount of PETRA (cross-linker) to the system improves the surface morphology of the microcapsules to be smooth and compact as shown in Figure 4.6b.

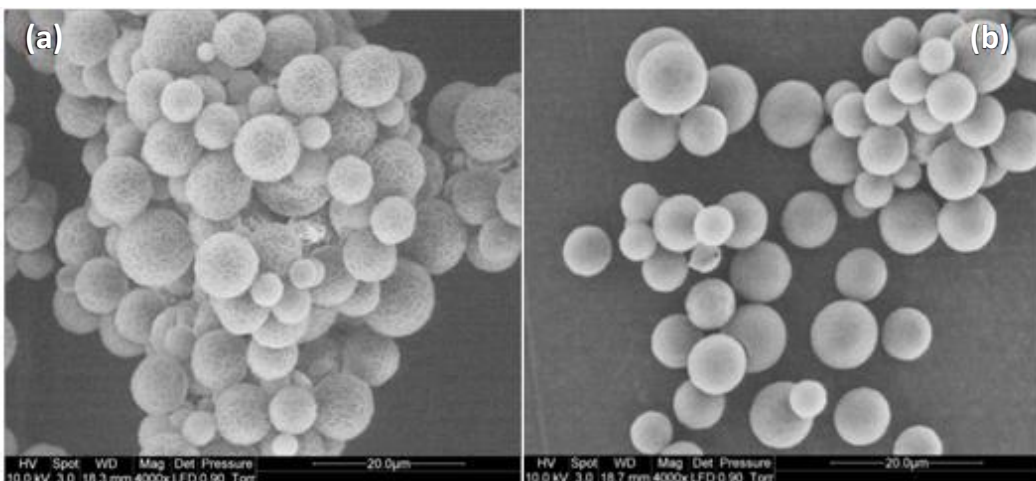


**Figure 4.6** SEM surface morphology micrographs of PCM microcapsules: (a) Uncross-linked microcapsules (b) Cross-linked microcapsules with PETRA

### 4.3.3 Effect of cross linking agent on the thermal properties of microcapsules

Thermal properties of pure RT21 and both systems (cross-linked and uncross-linked PCM microcapsules) were investigated using DSC as shown in Figure 4.7. The DSC results show an increase in thermal energy storage capacity of the microcapsules from 84.3 to 113.4 J/g when a small fraction of PETRA (cross-linking agent) was added to the system. The melting temperature of the RT21 in the microcapsules for both systems is similar to that of the bulk RT21. In contrast, the crystallization temperature of the PCM microcapsules was about 10°C lower than that of the bulk RT21 (super-cooling phenomena) in both cases as shown in Figure 4.7a and b. The supercooling of PCM in microcapsules has been reported [80]. The increase of the degree of super-cooling of RT21 microcapsules could be attributed either to the decrease in the amount of RT21 nuclei inside each microcapsule compared to the bulk RT21 [102] or due to formation of vacuum pockets space inside the microcapsules [103].

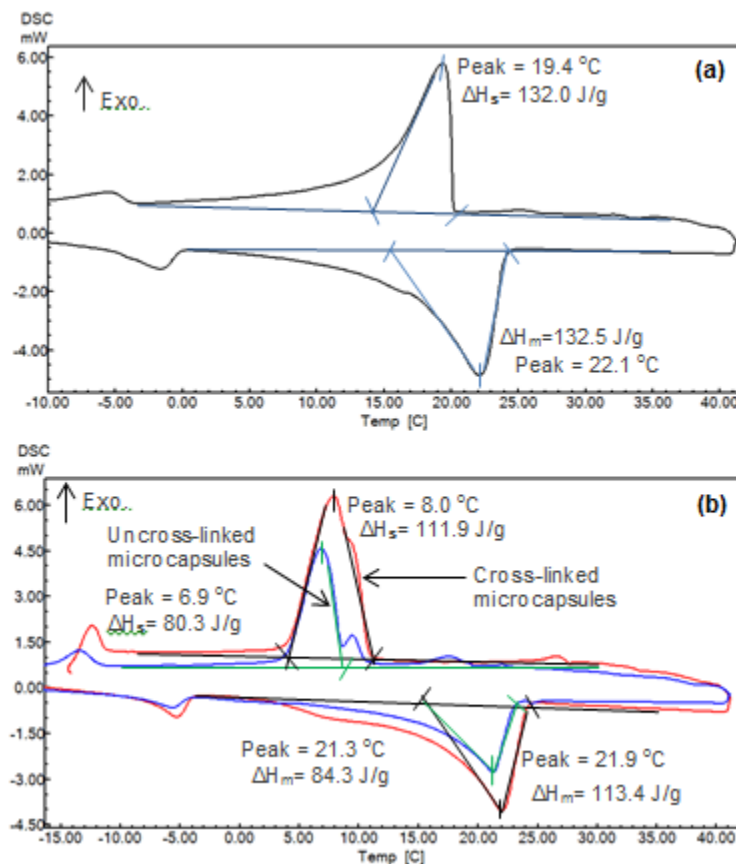


**Figure 4.7** DSC curves of (a) Bulk RT21 and (b) Cross linked PMMA/RT21 microcapsules (Red curve) and uncross-linked PMMA/RT21 microcapsules (Blue curve)

#### 4.3.4 Effect of core/shell mass ratio on the morphology of microcapsules

The effect of core/shell mass ratio on the diverse properties of cross-linked PMMA microcapsules containing PCM such as surface morphology and shell leaking test was investigated in this work. The chemical recipe ingredients used for preparation of PCM microcapsules (PCMMCs) with different mass ratio of PCM to monomers are shown in Table 4.2. SEM photos of PCM microcapsules with different core/shell mass ratio have been taken as shown in Figure 4.8. Rough surface with some buckles and dimples was observed when the core/shell mass ratio was set to 1:1. Further increase in core/shell mass ratio up to 2:1 improves morphology of the microcapsules and their surfaces become smooth and compact. Broken microcapsules were observed when the mass ratio was set to 3:1. This is probably due to the fewer polymers deposit on the surface of the droplet and thus did not form a sufficient shell thickness to envelope the entire PCM. The highest PCM content obtained in this work was 85.6 wt. % when the mass ratio was set to 2:1 , which is higher than the ones obtained in literature as shown in Table 4.3. Also, the size of the microcapsules was within the range of those reported in the literature as shown in Table 4.3.

**Table 4.2** Chemical recipe ingredients used for preparation of PCM microcapsules (PCMMCs) with different mass ratio of PCM to monomers

	Mass ratio of PCM to monomers			
	1:1	1.5:1	2:1	3:1
<b>Aqueous phase</b>	Mass (g)	Mass (g)	Mass (g)	Mass (g)
Deionized water	600	600	600	600
Polyvinyl alcohol (PVA)	6	6	6	6
Sodium dodecyl sulphate (SDS)	0.3	0.3	0.3	0.3
<b>Organic phase</b>				
Methyl methacrylate (MMA)	42.5	34	28.3	21.3
Pentaerythritol tetraacrylate (PETRA)	7.5	6	5	3.7
Benzoyl peroxide (BPO)	1.2	0.9	0.8	0.6
Rubitherm®RT21 (PCM)	50	60	66.6	75

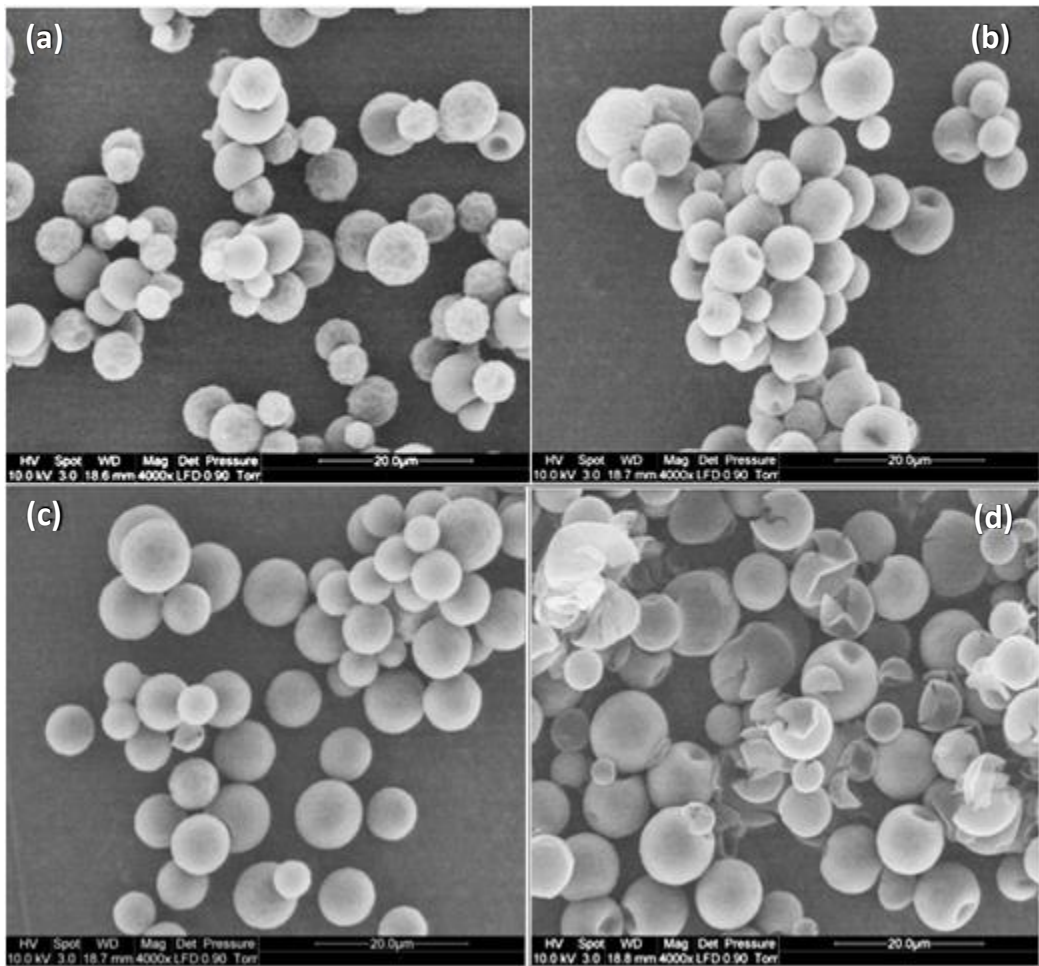


**Figure 4.8** SEM surface morphology micrographs of cross-linked PMMA microcapsules containing PCM with different mass ratio of PCM to monomer: (a) 1:1, (b) 1.5:1, (c) 2:1 and (d) 3: 1

#### 4.3.5 Effect of core/shell mass ratio on mass loss through microcapsules

A developed mass loss test was carried out by placing PCM and PCM microcapsules at 50°C in oven over a period of time (Figure 4.9). As shown in Figure 4.9a, bulk RT21 had lost 9 wt.% of its initial mass over a period of four weeks even under its flash point temperature (154 °C - manufacturers RT21® data sheet); this could be due to the fact that volatile components may exist in the RT21. As shown previously in Figure 4.7a, the DSC peak of the bulk RT21, was not very sharp, which suggests that there could be more than one chemical that makes up the composition of RT21.

The main target of the encapsulation is to provide a complete containment of the PCM inside the polymer shell. In this work mass loss test of RT21 microcapsules with different core/shell mass ratio was investigated. As shown in Figure 4.9b the mass loss gradually increased by increasing

**Table 4.3** Comparison between selected PCM microcapsules from the literature and RT21 microcapsules obtained in this work.

Shell Materials	Core Materials	Microcapsules Diameter ( μm)	PCM Content (wt. %)	Method of Encapsulation	References
Cross-linked PMMA	Rubitherm®RT21	5	85.6	Suspension polymerization	Present work
Cross linked PMMA	n-hexadecane	0.22 – 1.05	61.4	Emulsion polymerization	[100]
Cross linked PMMA	n-octadecane	-	75.3	Suspension polymerization	[80]
P (MMA-co-MA-co-MAA)	PRS paraffin wax	244	41.7	Suspension polymerization	[78]
P(St-MMA)	PRS paraffin wax	380	43.2	Suspension polymerization	[77]
PMMA	Paraffin	0.5-2	61.2	UV irradiation	[76]
PMMA	Paraffin wax	0.21	66	UV irradiation	[75]
PMMA-Silica Hybrid Shell	n-octadecane	10	73.3	Sol-Gel Process	[91]
Modified PMMA	(Na <sub>2</sub> HPO <sub>4</sub> ·7H <sub>2</sub> O) Hydrate Salt	6.8	84	Suspension copolymerization-solvent volatile	[104]
LDPE-EVA copolymer	Rubitherm®RT27	3.5	63	Spray drying	[87]
MF polymer	Dodecanol	1–16	40–70	In-situ polymerization	[63]
polyurea	n-octadecane	35-500	83	Interfacial polymerization	[48]

**Abbreviations:** PMMA- Poly methyl methacrylate, P (MMA-co-MA-co-MAA) - Tert-polymerization of methyl methacrylate, methyl acrylate and methacrylic acid and LDPE-EVA - Copolymer of low density polyethylene and ethyl vinyl acetate

core/shell mass ratio and become significant when the core/shell mass ratio is higher than two. This could be due to fewer polymers deposited on the surface of the droplet and thus did not form a complete encapsulation; resulting of leaking out PCM. The broken capsules shown in Figure 4.8d support these results. When the core/shell mass ratio was less than two, the mass loss was small and got stabilised after some time.

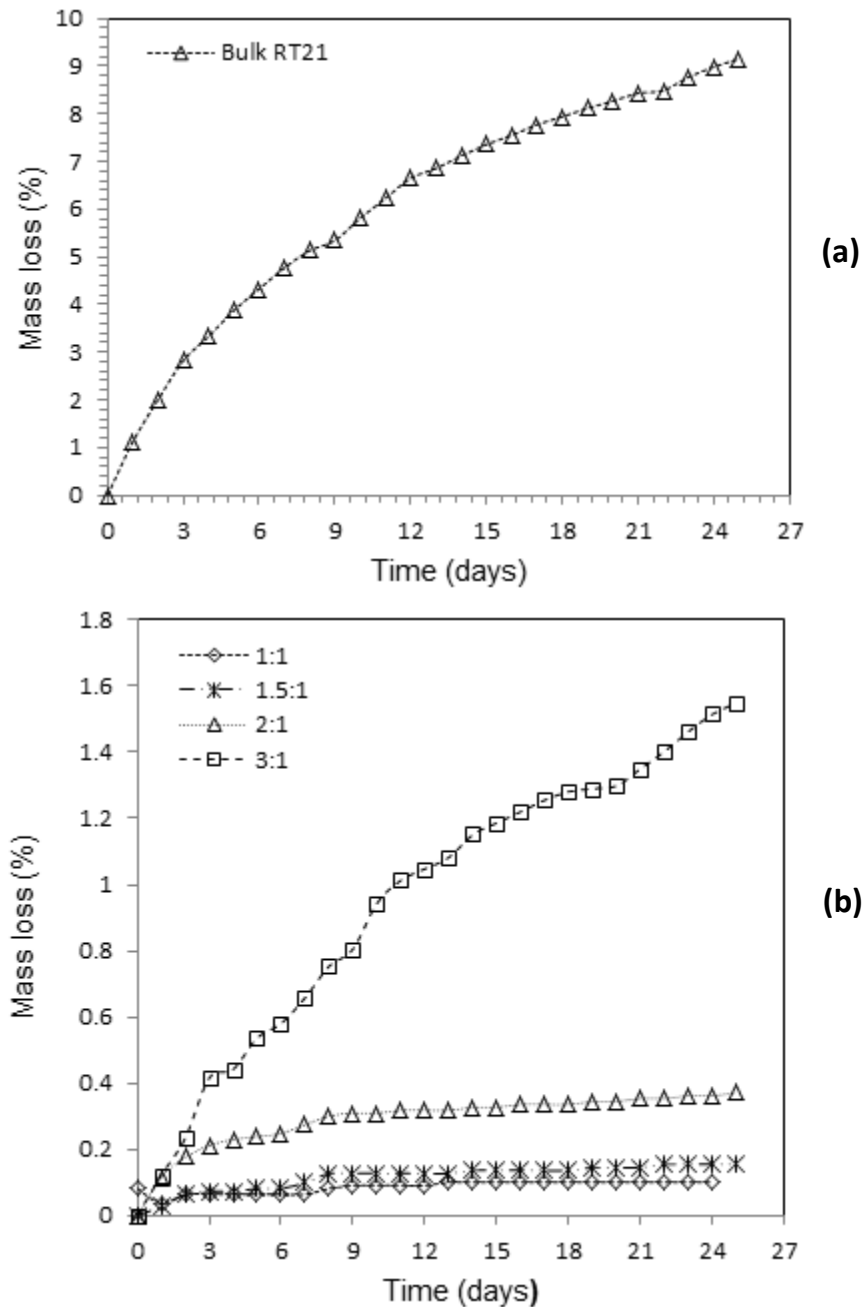


**Figure 4.9** Percentage mass losses of (a) bulk RT21 and (b) RT21 microcapsules with different core/shell mass ratio

#### 4.3.6 Effect of core/shell mass ratio on the thermal stability of microcapsules

Thermal stability of PCM microcapsules using TGA has been widely used to test the resistance of the microcapsules against thermal degradation. TGA curves of bulk RT21 and RT21 microcapsules with different core/shell mass ratio were obtained by heating the sample up to 550 °C at a rate of 10 °C/min. As shown in Figure 4.10, two steps thermal degradation of PCM microcapsules were observed. The mass loss was similar to the non-encapsulated PCM until all the PCM was dissipated (step 1). Following that the microcapsules experienced lower rate of mass loss of the shell, which depends on its thickness (step 2).

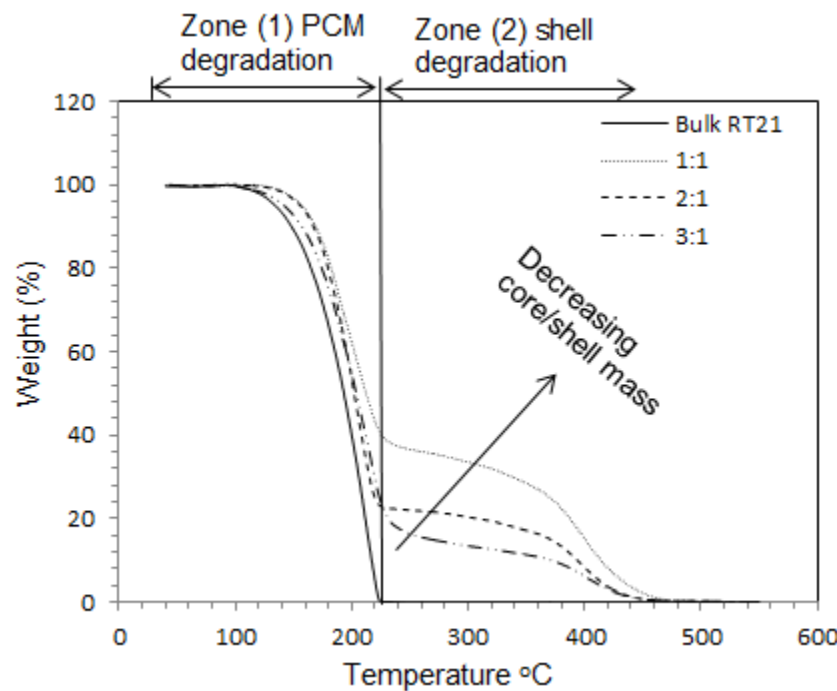


**Figure 4.10** TGA curves of Bulk RT21 and RT21microcapsules with different core/shell mass ratio

# **Supercooling Elimination of Phase Change Materials (PCMs) Microcapsules**

**5**

## **Abstract**

PCM microcapsules with supercooling have limited their widespread use as a latent heat storage system. In this study Rubitherm®RT58 and 1-octadecanol were selected as nucleating agents in an attempt to reduce or eliminate the supercooling issue of PCM microcapsules. The PCM microcapsules (PCMMC) were prepared using a suspension polymerization method. The DSC result shows that the onset crystallization temperature of PCMMC was approximately 10 °C lower than that of the bulk RT21. The supercooling of PCMMC containing Rubitherm®RT58 or 1-octadecanol was totally eliminated by shifting the onset crystallization temperatures of the PCMMC to be matched with the onset crystallization temperature of the bulk RT21. However, the PCM weight content of RT21 microcapsules in the presence of Rubitherm®RT58 was found to be higher than that of the microcapsules with 1-octadecanol. SEM images show no significant changes in the morphology of the PCMMC after introducing the nucleating agent. The mass loss gradually increased and became significant when 1-octadecanol was introduced to capsules. In contrast, the mass loss of the PCMMC when Rubitherm®RT58 was introduced was small and became stabilized after a short period of time. This study shows little change in the latent heat of fusion and melting temperature of PCMMC after 2000 thermal recycles with a consistent surface morphology.

## 5.2 Introduction

Supercooling is a state where liquids do not solidify below their normal freezing point. The supercooling of phase change materials (PCM) limits its widespread applications, therefore understanding the crystallization process is fundamental to advances in PCM research and technology. The crystallization process goes through several phases: induction phase, crystal growth phase and crystal regrowth phase. During the induction phase nuclei are formed and grow to a sufficient size to be stable (nucleation centres are formed). Next the material diffuses to form a nucleus which is adsorbed on its surface. The adsorbed material migrates along the surface and is incorporated into crystal form. These small crystals continue to grow and eventually become large enough and numerous enough to sustain a rapid rate of crystal growth. The rate of crystallization slows as the freezing process nears completion. Even after the material is totally frozen, redistribution processes continue to modify the particle shape and size distribution [105].

Inorganic PCM such as salts hydrate can sub-cool significantly but organic PCM such as paraffin do not experience serious supercooling [106]. However, when organic PCMs are encapsulated in microcapsules they tend to supercool severely, most likely due to the absence of nuclei in such small space. A significant lowering of the crystallization temperature has been observed in the cooling process of PCM microcapsules (PCMMCs) with various polymer shells [81, 107]. For example, PCMMCs using poly(divinylbenzene) and different copolymers as shell materials by means of suspension polymerization method were prepared [32, 108, 109]. Results have shown that the crystallization temperature of the PCMMCs was about 10 °C lower than that of bulk PCM, while the melting temperature was very slightly affected. The same results were reported using same method but with poly methyl methacrylate instead of poly(divinylbenzene) as a polymer shell [79, 80]. Different attempts have been attempted to reduce the supercooling of PCMMCs such as control the size of the PCMMCs [38, 52], adding nucleating agent or metal additives to the PCM prior encapsulation [102, 110, 111] or by optimizing the composition and structure of the capsules shell [112].

The crystal growth is governed and limited by the size of liquid droplets or PCMMCs after nucleation [113]. The effect of capsules size on crystallization temperature of the melamine-formaldehyde (MF)/ n-dodecane microcapsules was investigated [52]. The prepared microcapsules diameters were in the rage of 5-1000 µm. The degree of supercooling, which was defined as the

difference between the temperatures of melting and crystallization, was the same for the capsules in the range of 100-1000  $\mu\text{m}$ . In the range of 5-100  $\mu\text{m}$ , the degree of supercooling increased as the microcapsules sizes decreased which agreed with previous studies [102].

Controlling the size of the PCMMCs to be large is one of the realistic options for minimizing supercooling, but PCMMCs with large diameter do not function well in application of building industries due to the fact that they often rupture during mixing [114-116]. The objective of producing PCM microcapsules with a smaller diameter and a low degree of supercooling has received increasing attention. To overcome this problem of supercooling, mixing a nucleation agent with the PCM prior to encapsulation is an option.

The effect of adding a nucleating agent to the PCM prior to encapsulation on the crystallization temperatures of melamine-formaldehyde (MF)/ n-dodecane microcapsules and gelatin/n-tetradecane microcapsules were investigated. The degree of supercooling of PCMMCs was reduced dramatically when 2 wt. % of 1-tetradecanol (nucleating agent) was used [52]. Furthermore, different types of nucleating agents, i.e. sodium chloride, 1-octadecanol and paraffin, were tested [102, 111]. The reported results show that, super-cooling was prevented by feeding about 6 wt.% sodium chloride to the emulsion or 9 wt.% 1-octadecanol in the core material, but the surface of the microcapsules in both cases was very rough and the dispersion was poor. Nevertheless, adding approximately 20 wt. % of paraffin (melting point 62-65 °C) into the core material was able to prevent n-octadecane from super-cooling, and had no effect on the morphology and dispersion of the microcapsules. However, the effective latent heat of the PCM present in the microcapsules was sharply reduced due to the addition of a large quantity of non-PCM material.

Silica fume and tetradecanol as nucleating agents were used, and their effects on the supercooling suppression of n-tetradecane microcapsules were investigated [117]. Results indicate that silica fume at 0.2 wt. % is ineffective in suppressing the supercooling of microencapsulated n-tetradecane, whereas 1-4 wt. % of tetradecanol have greatly suppressed supercooling. Melamine-formaldehyde microcapsules containing two *n*-alkane PCMs, namely, n-dodecane (C12) or n-tetradecane (C14) were prepared by “*in situ* polymerization” [118]. A small amount of n-hexatriacontane (C36) was introduced as an organic gelator into the core of microcapsules to cope with the supercooling problem. DSC analyses demonstrated that pure n-alkanes crystallized at a higher temperature and the degree of supercooling was 4.1 and 2.9 °C for C12 and C14, respectively. After microencapsulated

alkanes the degree of supercooling was aggravated to 13.2 and 8 °C for C12 and C14 microcapsules respectively. The degree of supercooling was reduced to 5.8 and 2.9 °C for C12 and C14 microcapsules respectively when 3% (mass fraction) of C36 was mixed with PCM. The enthalpies of microencapsulated C12 and C14 containing C36 was reduced by 14.3 and 6.4 % respectively. Silver nano composite PCMMCs were fabricated in an attempt to suppress the supercooling of the PCMMCs [110] . The PCMMCs undergoes two phase change stages during cooling process (labelled  $\alpha$  and  $\beta$  peaks) and the stored energy is not released at one time. The first exothermic peak is called as “peak alpha”, corresponding to a heterogeneously nucleated liquid-rotator phase transition. The second exothermic peak is called as “peak beta”, corresponding to the homogeneously nucleated rotator-crystal transition. The supercooling can be depressed to about 1- 3 °C for the silver nano composite PCM microcapsules, thus; silver nanoparticles in the core likely act as a foreign nucleus in crystallization stage, as heterogeneous nucleation is still the main mechanism in crystallization.

Suppression of supercooling of PCMMCs was also carried out by optimizing the shell composition and structure [112]. The results show that a homogeneous nucleation can be mediated by shell-induced nucleation of the triclinic phase and the metastable rotator phase when the shell composition and structure are optimized, without the need for any nucleating additives. Three peaks, labelled  $\alpha$ ,  $\beta$ , and  $\gamma$  were observed on the DSC cooling curves of the octadecane microcapsules. These peaks are attributed to the shell-induced liquid-rotator and liquid-triclinic transition, rotator-crystal transition, and homogeneously nucleated liquid-triclinic transition. The onset of freezing temperature shifted from 21.3 to 23.4 °C when the mass ratio of formaldehyde to melamine was 1.25 at a pH of 8.5.

The main objective of this paper is to study the effect of adding different types and concentrations of nucleating agents to the PCM prior to encapsulation on the thermal properties, surface morphology and shell permeability of the PCM microcapsules. Adding nucleating agents to the PCM prior encapsulation has been reported as an efficient technique in decreasing supercooling of PCM microcapsules as aforementioned. However, the available literature shows only limited information about the PCM microcapsules testing, so in this paper accelerated thermal cycling test, developed mass loss test, beside DSC and SEM tests were used to assess the quality of the PCM microcapsules.

## 5.2 Experimental

### 5.2.1 Materials

Rubitherm®RT58 ( $T_{pm} = 58^\circ\text{C}$ , RUBITHERM® Technologies GmbH, Germany) and 1-Octadecanol (Reagent Plus®, 99%) were used as nucleating agents. The rest of chemicals used as were reported in the materials section in Chapter Four (see page 40).

### 5.2.2 Synthesis of PCMs Microcapsules

#### 5.2.2.1 Emulsification

The procedure used for preparing oil/water emulsion as was reported in Chapter Four (see page 41), along with the mixing nucleating agent with PCM prior emulsification. The percentage content of nucleating agent based on the mass of PCM was calculated using the following equation.

$$W_{na} = \frac{M_{na}}{M_{na} + M_{PCM}} \times 100\% \quad \dots \quad (5.1)$$

Where,  $W_{na}$  is the percentage content of nucleating agent based on the mass of PCM,  $M_{na}$  is the mass of nucleating agent and  $M_{PCM}$  is the mass of PCM. The chemical recipe of ingredients for preparing PCM microcapsules is listed in Table 5.1.

**Table 5.1** Chemical recipe ingredients of RT21 microcapsules containing a nucleating agent

	No nucleating agent	15 wt.% nucleating agent	5 wt.% nucleating agent
<b>Aqueous phase</b>	Mass (g)	Mass (g)	Mass (g)
Deionized water	600	600	600
Polyvinyl alcohol (PVA)	6	6	6
Sodium dodecyl sulphate (SDS)	0.3	0.3	0.3
<b>Organic phase</b>			
Methyl methacrylate (MMA)	28	28	28
Pentaerythritol tetraacrylate (PETRA)	5	5	5
Benzoyl peroxide (BPO)	0.8	0.8	0.8
Rubitherm®RT21 (PCM)	66	56.1	62.7
Nucleating agent)	--	9.9	3.3

### **5.2.2.2 Polymerization**

The polymerization reaction conditions as were reported in Chapter Four (see page 41).

### **5.2.3 Characterization of Microcapsules**

The morphology, thermal energy absorbs and release and permeability of PCM through the shell of microcapsules were analyzed using scanning electron microscope (SEM), differential scanning calorimeter (DSC) and mass loss analysis respectively. The analysis conditions and machines model used as were reported in Chapter Four (see page 41).

For practical application, PCM microcapsules are required to work for multiple melting and freezing cycles without any significant changes in their properties. Accelerated thermal cycling experiments of PCM microcapsules were performed in a controlled heating/cooling water bath at temperatures cycling between 2 and 40 °C as shown in Figure 5.1. These experiments were conducted by using 20 g of PCM microcapsules in a 50 ml sealed cylindrical plastic container with K-type thermocouple immersed in the centre of the PCM microcapsules and connected to a data logger and PC to measure the PCM temperature during cycling as shown in Figure 5.2.

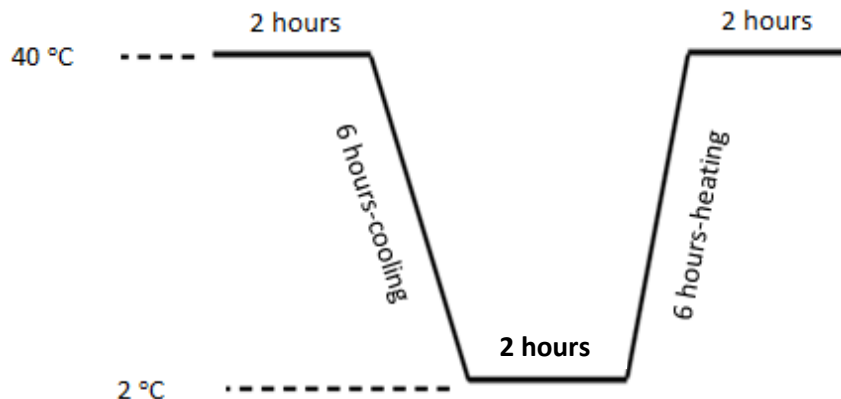


**Figure 5.1** Set temperatures of water bath



**Figure 5.2** Accelerated thermal cycling set-up

### 5.3 Results and Discussion

Thermal properties of bulk RT21 and RT21 microcapsules (RT21MCs) were investigated using DSC as shown in Figure 5.3. The melting temperature of RT21 in the microcapsules is similar to that of the bulk RT21. In contrast, the crystallization temperature of RT21MCs was about  $10^{\circ}\text{C}$  lower than that of the bulk RT21 (supercooling). The nucleating mechanism for PCM capsules with tiny volume is shifted from heterogeneous to homogeneous nucleation [119]. The reason for the shifting in the crystallization mechanism could be associated with the available number of foreign nuclei that usually cause heterogeneous nucleation in the bulk phase and are now distributed among a large number of isolated tiny microcapsules. The heterogeneous nucleation for PCM microcapsules is reduced because only a small number of nuclei contained in a single microcapsule. Therefore, the crystallization process cannot be finished in short time as in non-encapsulated PCM.

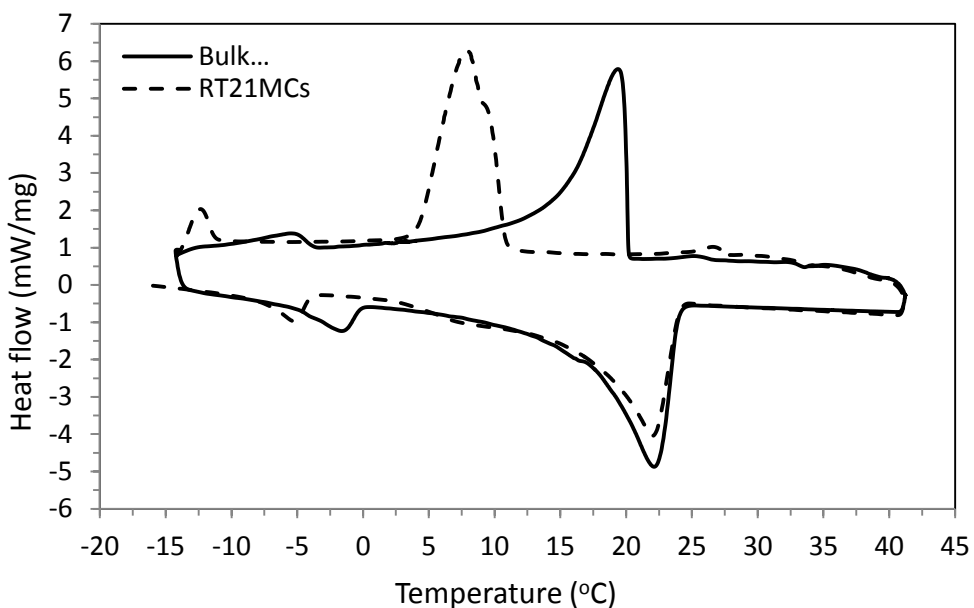


**Figure 5.3** DSC curves of bulk RT21 (solid line) and RT21MCs (dash line)

The supercooling of the PCM microcapsules is an obstacle for widespread applications and considerable efforts have been made to eliminate the supercooling of the PCM microcapsules. To reduce the supercooling of PCMMCs, additives were mixed with the PCM prior encapsulation to act as a nucleating agent. These nucleating agents are usually materials with a similar crystal structure as the solid PCM to allow the solid phase of the PCM to grow on their surfaces (surface-mediated) but with a higher melting temperature to avoid deactivation when the PCM is melted [120]. Figure 5.4 shows the DSC curve for the microcapsules containing two different crystal structures of nucleating agents. Commercial RT58 (paraffin) and 1-octadecanol (also known as stearyl alcohol) with peak melting temperatures of 58 and 59.5 °C respectively, were used as nucleating agents. The degree of supercooling has been reduced dramatically when either RT58 or 1-octadecanol was used, as shown in Figure 5.4 and Table 5.2. However, the addition of 1-octadecanol has influenced negatively the PCM thermal behaviors such as making the solidification to occur over wider range of temperature and less PCM contained in the microcapsules compared to the addition of RT58 (see Table 5.2). This could be due to the PCM losses during the encapsulation process when 1-octadecanol was used.

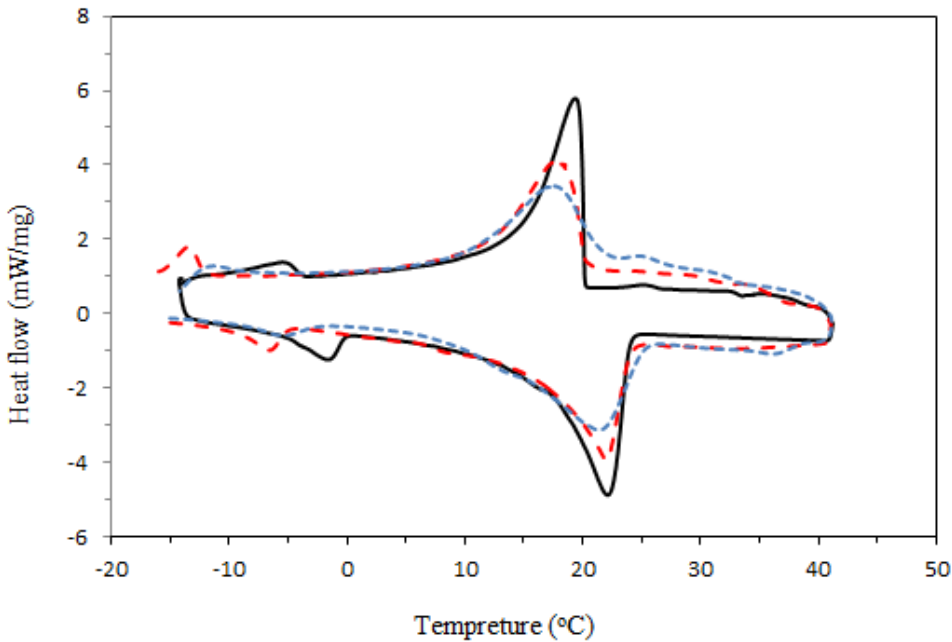


**Figure 5.4** DSC curves of the bulk RT21 (black solid line), RT21MC-15wt. % RT58 (Red dash line) and RT21MC-15wt. % 1- octadecanol (blue dot line)

Figure 5.5 shows the SEM micrographs of the PCM microcapsules and the PCM microcapsules containing a nucleating agent. The surface morphology of the PCM microcapsules without a nucleating agent shows a smooth surface. However, buckles and dimples on the surface of the PCM microcapsules were observed when the nucleating agent was introduced. The number of buckles and dimples reduce significantly when 5 wt. % RT58 was used (Figure 7d). The mass ratio of core (PCM + nucleating agent) to shell material was kept constant in all samples (see Table 1). The nucleating agent solidifies at significantly higher temperature about 58°C, while the shell is still soft. This is most likely to be the cause of the dimples shown in Figure 7, caused by the volume reduction in the nucleating agent during solidification. The volume reduction in RT58 is 12.5% based on the MSDS sheet reported by the manufacturing company Rubitherm. Based on the solid and liquid density of the RT58, which are 880 and 770 kg/m<sup>3</sup> respectively, the corresponding volume change of the capsules will be 1.8 %., which is probably sufficient to cause the dimples shown in Figure 5.

The main target of encapsulation is to provide complete containment of the PCM inside the polymer shell. The permeability of PCM through the shell of microcapsules was tested via mass loss analysis. Figure 5.6 compares the mass losses of the PCM from microcapsules with and without the use of nucleating agent. The mass loss gradually increased and became significant when 1-

octadecanol was used. 1-octadecanol works as a nucleating agent, however it seems to affect the shell negatively. In contrast, the mass loss of the PCM microcapsules containing RT58 was small. The presence of RT58 in the core material may have created a protective layer inside the microcapsules, thus provides a complete containment of the PCM beside the polymer shell. This suggests that adding RT58 not only to prevent supercooling but could also improve the properties of the capsule shell.

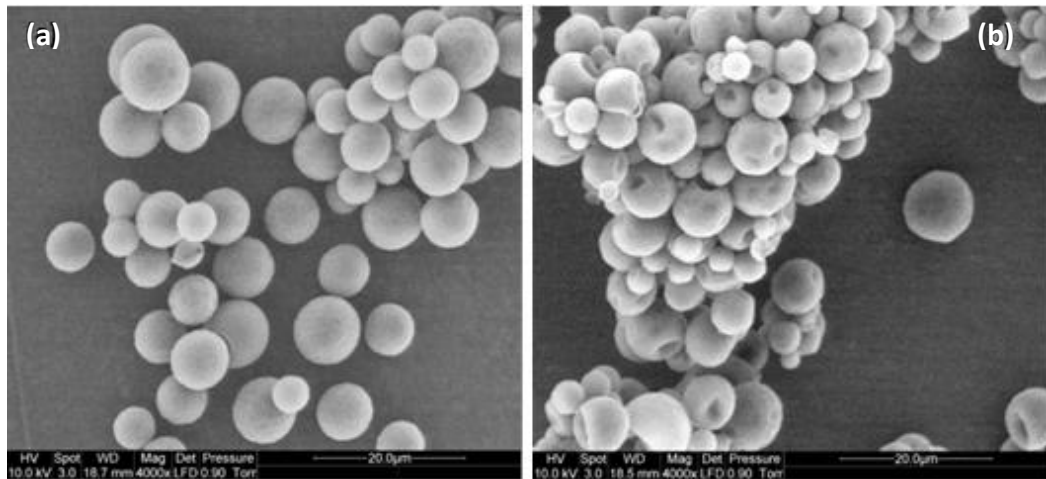


**Figure 5.5** SEM photos of (a) RT21MC and (b) RT21MC-15wt. % RT58

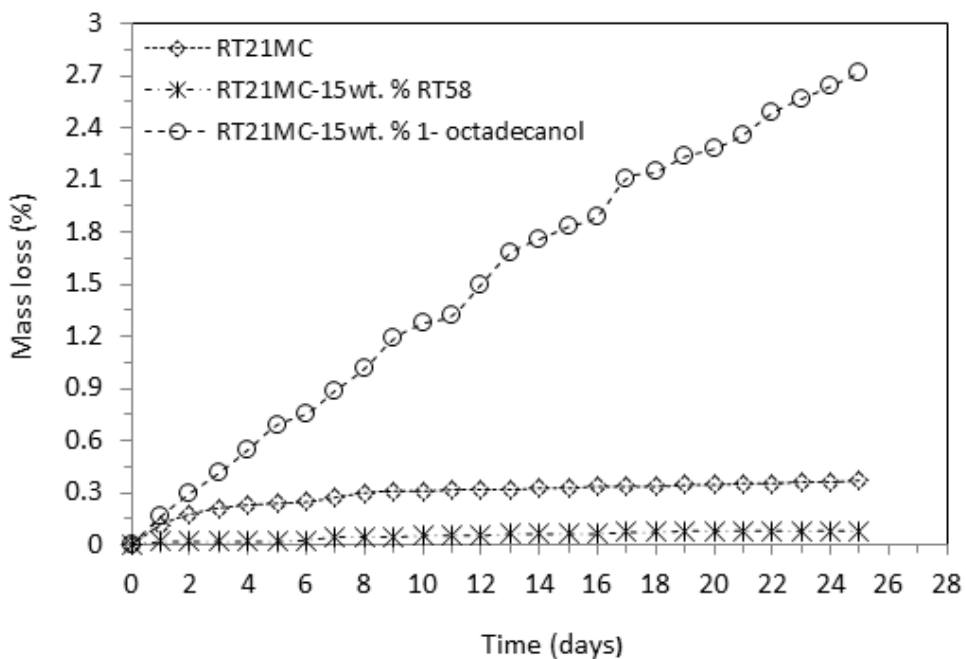
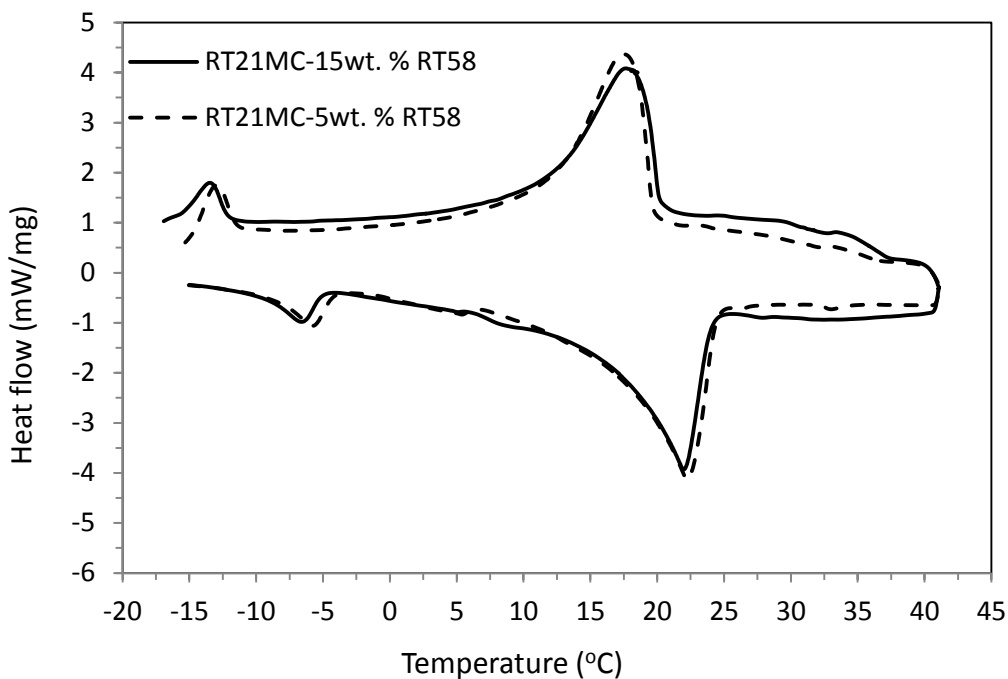


**Figure 5.6** Percentage mass losses of RT21MC, RT21MC-15wt. % RT58 and RT21MC-15wt. % 1-octadecanol

**Table 5.2** Thermal properties of RT21 microcapsules

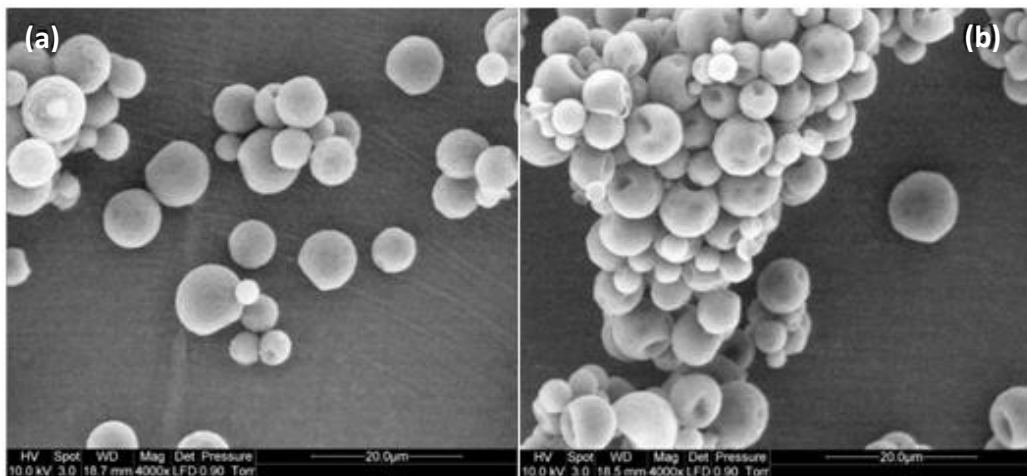
	Heating process				Cooling process				PCM wt.% content in microcapsules	Theoretical PCM wt.% content in microcapsules
	T <sub>onset</sub> (°C)	T <sub>peak</sub> (°C)	T <sub>endset</sub> (°C)	ΔH <sub>m</sub> (kJ/kg)	T <sub>onset</sub> (°C)	T <sub>peak</sub> (°C)	T <sub>endset</sub> (°C)	ΔH <sub>c</sub> (kJ/kg)		
Bulk RT21	16.5	22.1	23.8	132	20.1	19.3	14.5	132.4	--	--
RT21MC	16.6	21.9	23.9	113.4	10.8	7.9	4.1	111.8	85.9	66.6
RT21MC-15wt.% RT58	16.4	21.9	23.9	104.7	20.2	17.6	11.0	102.2	79.3	56.1
RT21MC-15wt.% 1-Octadecanol	16.4	21.9	24.4	80.2	21.2	17.5	10.9	78.5	60.7	56.1
RT21MC-5wt.% RT58	16.1	22.2	24.2	110.4	19.7	17.5	11.4	108.3	83.6	62.7

Many researchers have reported to reduce the supercooling of PCM microcapsules by adding different kinds of nucleating materials. The drawback of using this technique is the drop in the effective latent heat of the PCM microcapsules due to the relatively large amount of nucleating agent added. In an attempt to prepare PCM microcapsules with high phase change enthalpy and no supercooling, capsules containing 5 wt. % of nucleating agent were tried. Figure 5.7 shows the DSC curves for the PCM microcapsules containing 5 and 15 wt. % of nucleating agent (RT58). It is clear that 5 wt. % of RT58 is sufficient to eliminate totally the supercooling of the PCM microcapsules. However, PCM wt. % content in microcapsules has increased up to 83.6 wt. % as reported in the Table 5.2. The highest PCM content obtained in this work was 83.6 wt. %, which is higher than the ones obtained in literature [102]. Also, one primary solidification peak of PCMMCs was observed in this work, whereas were multi solidification peaks have been reported in the literature [38, 111].



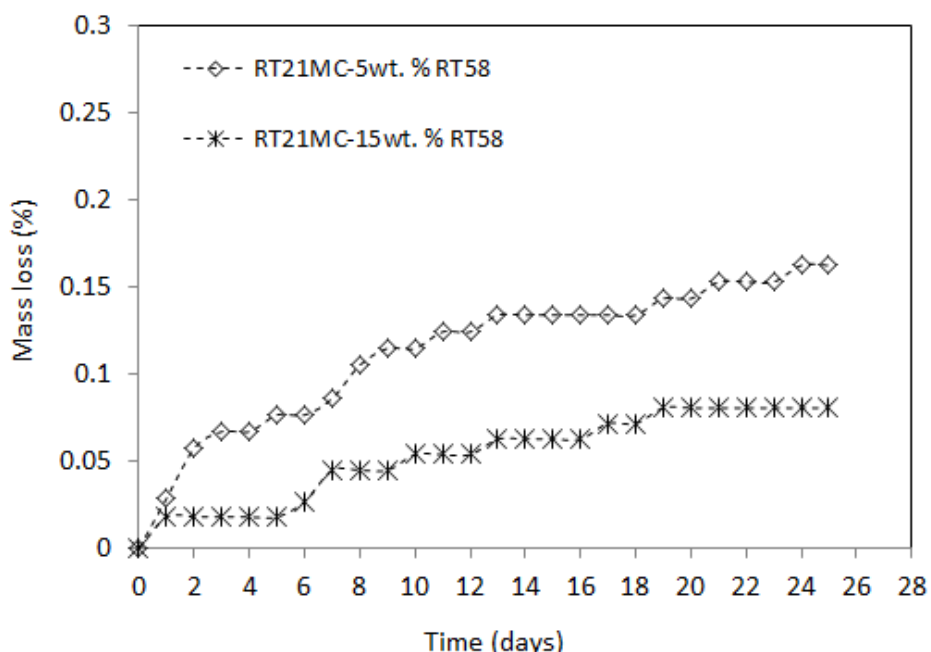
**Figure 5.7** DSC curves of PCM microcapsules containing a) 5 wt. % RT58 (dash line) and b) 15 wt. % RT58 (solid line)

Figure 5.8 shows the SEM photos of the PCM microcapsules in presence of 5 and 15 wt. % of nucleating agent (RT58). When 5 wt. % RT58 was used, the number of buckles and dimples appear on the surface of the microcapsules was reduced significantly.



**Figure 5.8** SEM photos of a) RT21MC-5 wt. % RT58 and b) RT21MC-15wt. % RT58

The mass loss experiments were carried out for the RT21microcapsules containing different concentrations of the nucleating agent (RT58). Figure 5.9 shows low mass loss of PCM from the capsules containing 5 wt. % and 15 wt. % RT58. As the RT58 concentration in the PCM increases, the mass loss decreases. The higher freezing point is likely to come from the blocking of pore, which are in the poly methyl methacrylate coat.



**Figure 5.9** Percentage mass losses of RT21MC-5wt. % RT58 and RT21MC-15wt. % RT58

The most important criteria that have prevented the widespread use of latent heat are the long-term life of the PCM microcapsules and the number of cycles they can withstand without any significant changes in their properties such as latent heat, solidification and melting temperatures and capsules morphology. Figure 5.10 shows the DSC curves of the

RT21 microcapsules containing 5 wt. % RT58 before and after 1000 and 2000 thermal cycles. In the first 1000 cycles, the onset melting temperatures of the microcapsules increased by 0.16 °C and the onset crystallization temperature decreased by 0.91 °C. However, no further change was observed between 1000 and 2000 cycles (see Table 5.3). These changes in temperatures in the beginning of 1000 cycles could be due to the formatting of new crystal orientation and placement of the PCM crystal inside the capsules.

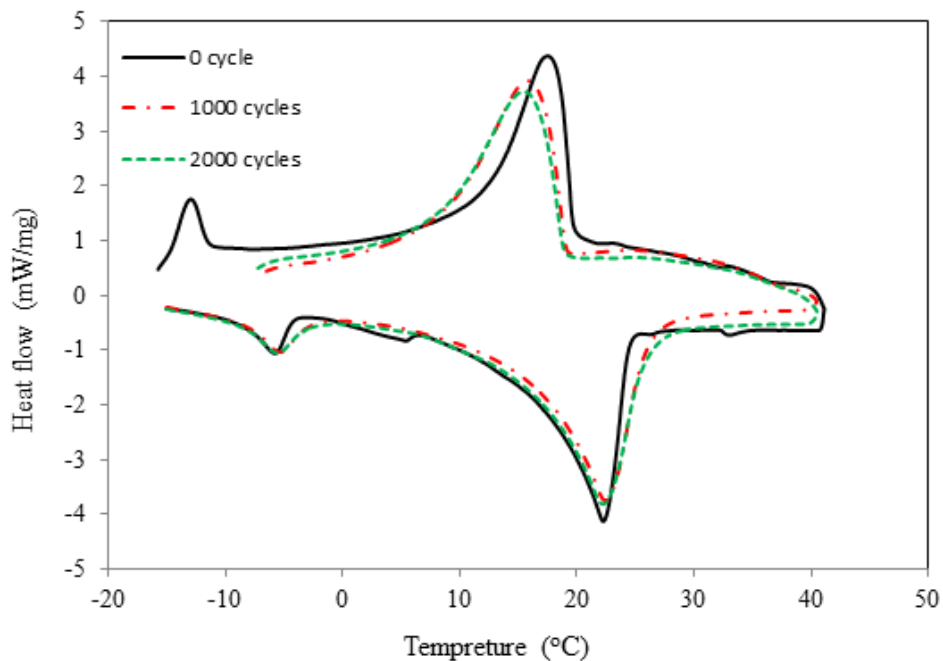


**Figure 5.10** DSC curves of PCM microcapsules before and after thermal cycling

The latent heat of PCM microcapsules has a minor change between 1 % and 2 % after 1000 and 2000 cycles, compared with zero cycle (Table 5.3). These changes in temperatures and enthalpies are very small and acceptable for use in the building application.

**Table 5.3** Thermal properties of the RT21 microcapsules before and after thermal cycling

Number of cycles	Melting process				Crystallization process			
	T <sub>onset</sub> (°C)	T <sub>peak</sub> (°C)	T <sub>endset</sub> (°C)	ΔH <sub>f</sub> (kJ/kg)	T <sub>onset</sub> (°C)	T <sub>peak</sub> (°C)	T <sub>endset</sub> (°C)	ΔH <sub>c</sub> (kJ/kg)
0	16.11	22.28	24.28	110.42	19.79	17.51	11.42	108.30
1000	16.27	22.44	25.97	109.15	18.88	15.79	9.44	106.02
2000	15.26	22.21	25.79	108.07	19.01	15.47	9.23	105.15

Figure 5.11 shows the SEM micrograph of RT21 microcapsules before and after thermal cycling. SEM photos show that the capsule shape remained spherical and no shell cracks were observed after repeating 2000 cycles. Only a few buckles and dimples on the surface of the PCM microcapsules were seen after 2000 cycles.

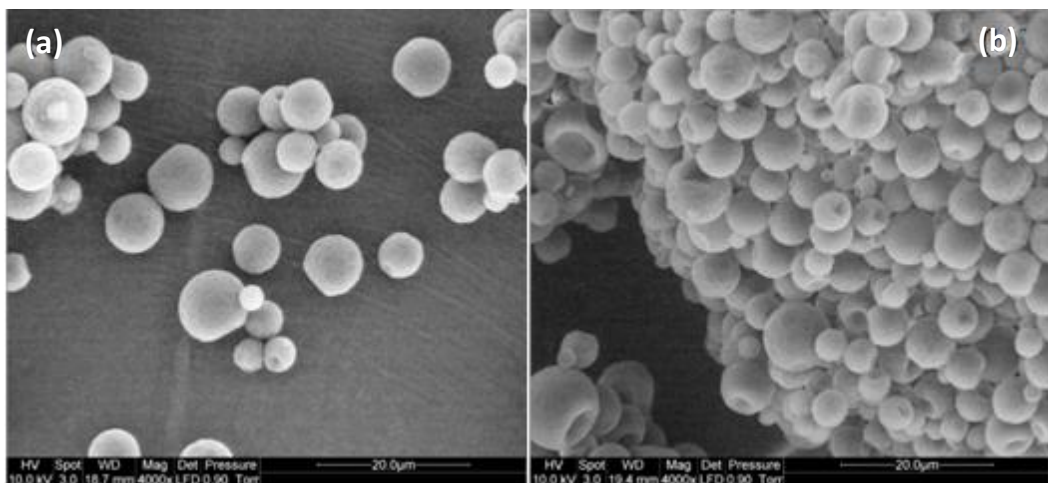


**Figure 5.11** SEM photos of RT21 microcapsules with 5 wt.% RT58: (a) 0 cycle (b) 2000 cycles

Thermal energy storage and release performance of the PCM microcapsules after 1000 and 2000 cycles were measured using a cyclic heating/cooling water bath as shown in Figure 5.2. According to Figure 5.12, it can be observed that the PCM microcapsules have heat storage and release processes seen from the deviation of the temperature-time line at the melting and

freezing points of the PCM. The results show that slight changes in phase transition temperatures of the PCM microcapsules after 1000 cycles compared to zero cycles. However, the PCM microcapsules become stabilized without any changes in the phase transition temperature after 2000 cycles compared to 1000 cycles which agrees with the results obtained using DSC (Figure 5.10).

The phase change time can be roughly estimated from the temperature-time curves of the PCM and PCM microcapsules by plotting the outer tangent lines. The interval time between two points of intersection is defined as the phase change time. The temperature-time curves undergo a freezing processes in the bulk RT21 and RT21 microcapsules as shown in Figure 5.13. For the freezing process, it took approximately 55 and 75 minutes for the bulk RT21 and RT21 microcapsules respectively to complete the solidification of the PCM. This time ratio measurement reflects the effective latent heat, which is smaller for microcapsules based on same mass.

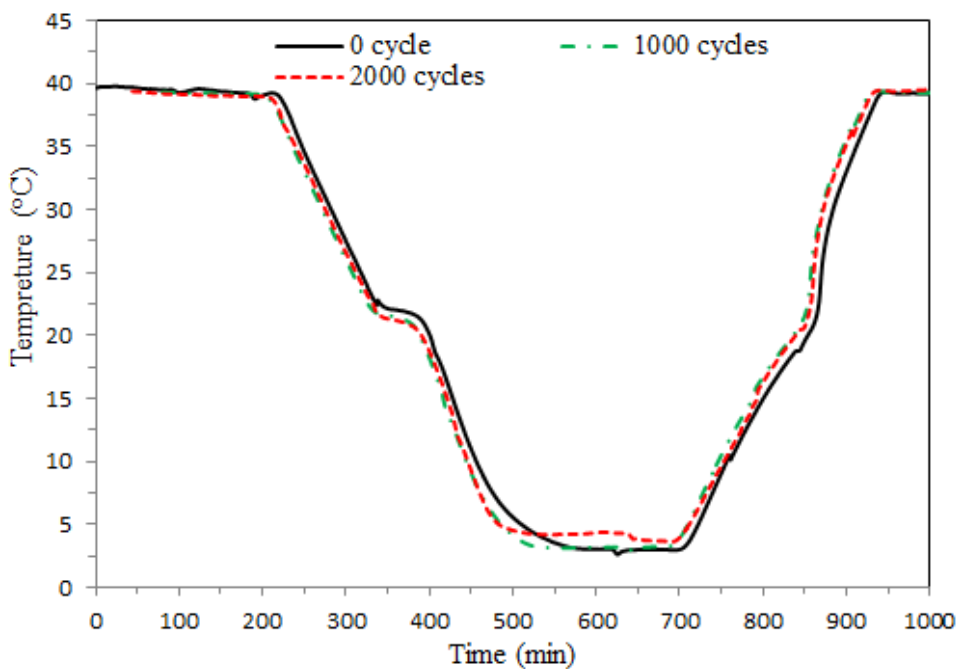


**Figure 5.12** Heat storage and release performance of RT21 microcapsules before and after thermal cycling

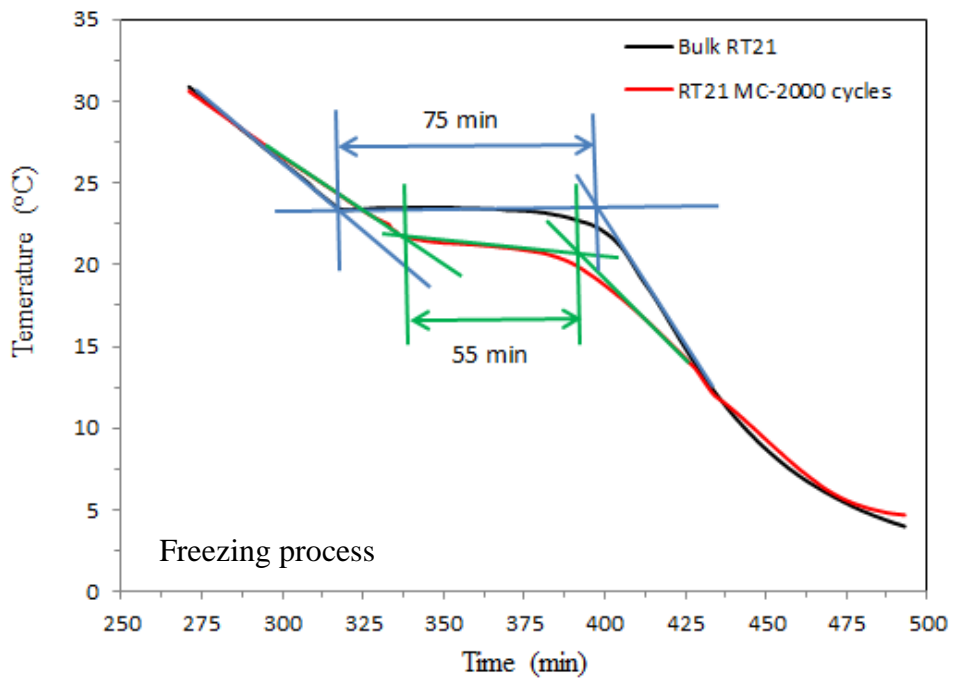


**Figure 5.13** Heat realease curve of RT21 and RT21 microcapsules

# The Use of Thin Film Closed Loop UV Reactor for Microencapsulation of Phase Change Materials (PCMs)

6

## Abstract

Thermal-initiated free-radical polymerization method is commonly used in dispersion polymerization for microencapsulating PCMs. In this method the polymerization reaction initiated at elevated temperatures and usually needs a long time to achieve a high monomer conversion. Efforts have been made to shorten the reaction period of dispersion polymerization by using photo-induced polymerization at room temperature [121]. This chapter presents a novel process of microencapsulating PCMs using a falling thin film closed loop UV reactor. Commercial Rubitherm<sup>®</sup>RT21 ( $T_{pm}= 22\text{ }^{\circ}\text{C}$  and  $\Delta H_m= 135\text{ J/g}$ ) and cross-linked polymethyl methacrylate were used as PCMs and shell materials respectively. Two methods of emulsion preparation were investigated. In method ‘1’ the emulsion was prepared by emulsifying a mixture of monomer, cross linking agents, organic soluble photoinitiator and PCMs in aqueous solution containing stabilizing agents, in method ‘2’ the PCMs were firstly emulsified in aqueous solution containing stabilizing agents and water-soluble photoinitiators, after which a mixture of monomer and cross linking agents were added. SEM images show a large percentage of the microcapsules were agglomerated with only small amount of microcapsules available under method ‘1’ conditions. However, smooth, compact and dry spherical microcapsules were produced, when method ‘2’ was used. Furthermore, DSC measurements showed an increase in the thermal energy storage capacity of the microcapsules when the emulsion was prepared based on method ‘2’. The effect of the cross linking agent with different numbers of cross-linking functional moieties such as ethylene glycol dimethacrylate (EGDM) and pentaerythritol tetraacrylate (PETRA) on the properties of RT21 microcapsules was studied. The higher number of crosslinking functional moieties (PETRA) has produced microcapsules with smooth and compact surfaces with an increased thermal energy storage capacity of the PCM. No serious change in the surface morphology of the RT21 microcapsules were observed when the irradiated time was reduced from 2 hours to 1 hour. However, the heat storage capacity of the RT21 microcapsules increased from 80.5 to 90.3 J/g when the irradiated time decreased from 2 hours to 1 hour respectively. This could be due to the less monomer conversion; thus producing PCMs microcapsules with thinner shells.

## 6.1 Introduction

As the word implies, photo induced polymerization involves a polymerization reaction that takes place under a specific stimulus of light. Applications in which photopolymerization is used include films and coatings [122], inks [123], adhesives [124], fiber optics [125], and dentistry [126]. Photopolymerization is classified as photochemical condensation polymerization and photoinduced active centre polymerization as shown in Figure 6.1. Photochemical condensation reactions occur through the direct irradiation of a monomer species or by using a photo-generated catalyst. However, photoinduced active centre polymerization (addition polymerizations) occurs by means of a chain reaction mechanism involving the propagation of an active centre interacting with the monomer. The active centre consists of reactive species, typically, a radical, a cation, or an anion. Typical subsequent reaction steps of photoinitiated addition polymerization are represented in equations 1-3. The active species ( $R^*$ ) is generated by a homolytic or a heterolytic bond cleavage of the photoinitiator (I) under the specific stimulus of light (equation 1).  $R^*$  is the true initiator that induces polymerization of the monomer (M) by opening a multiple bond or a ring (equation 2). During this process, the active centre is conserved by producing a new reactive species,  $RM^*$ . In the subsequent reaction of  $RM^*$  with monomer the polymer chain lengthens (equation 3). Depending on the type of active centre present in the polymerization and the reaction conditions, a variety of chain termination or transfer processes may also occur; those stop or disrupt the progress of the growing chain [127].



### 6.1.1 Photoinitiator

In order to produce free radicals that initiate polymerization, a light of a certain spectra emission needs to attack and overlap the photoinitiator absorption spectra. Upon absorption, the photoinitiator molecule is promoted from the ground electronic state to either a singlet or triplet excited electronic state. This excited molecule undergoes either cleavage or reaction with another molecule to produce initiating free radicals [128].

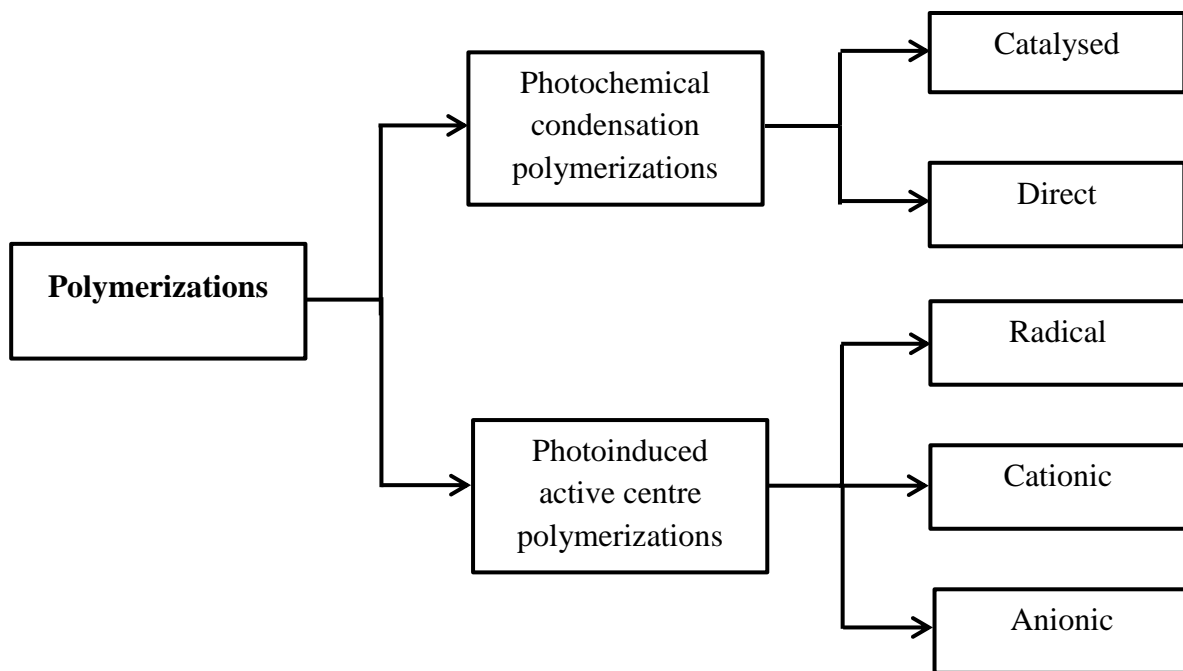


**Figure 6.1** Categories of photopolymerizations reactions [129]

The selection of the ideal photoinitiator is critical to achieve the desired reaction speed and conversion of monomer. For photo initiation to proceed efficiently the absorption bands of the photo initiator must overlap with the emission spectrum of the source and there must be minimal competing absorption by the components of the formulation at the wavelengths corresponding to photo initiator excitation [130].

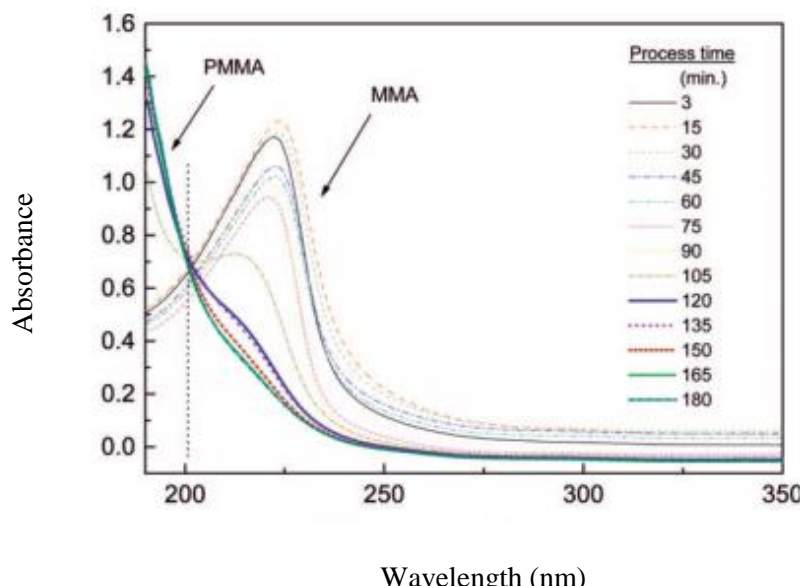


**Figure 6.2** UV absorption spectra of MMA and PMMA in mini-emulsion polymerization during polymerization [131]

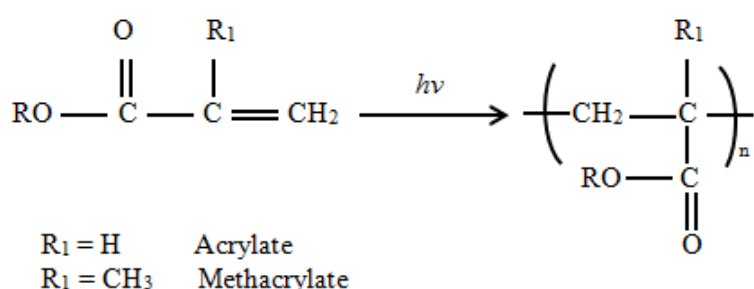
Figure 6.2 Shows UV absorption spectra of methyl methacrylate (MMA) and poly methyl methacrylate (PMMA) in mini-emulsion polymerization during polymerization. MMA has a strong UV absorption with a maximum value at a wavelength of 225 nm, while PMMA absorbs at a lower wavelength. MMA and PMMA have an identical absorptivity at 200 nm wavelength. Based on these results, there is a clear optical window to select a UV lamp has emitted a light within the range of 250-350 nm in wavelength and a photoinitiator absorb a light within the same range without absorption competition of monomer and polymer; thus no absorption peak observed in that range for monomers and polymer as shown in Figure 6.2. Numerous photoinitiators have been developed to meet the needs of a variety of photopolymerization systems. Commercial highly efficient free Radical photoinitiator that are concerned in this research are listed in Table 6.1.

**Table 6.1** Commercial photoinitiators used in this study

Commercial Name	Chemical Class	Chemical Identity	Appearance	UV/Vis Absorption Peak (nm) in Methanol
IRGACURE 1173	$\alpha$ -Hydroxyketone	2-Hydroxy-2-methyl-1-phenyl-1-propanone	clear, light yellow liquid	245, 280, 331
IRGACURE 2959	$\alpha$ -Hydroxyketone	2-Hydroxy-1-[4-(2-hydroxyethoxy) phenyl]-2-methyl-1-propanone	off-white powder	276
IRGACURE 369	$\alpha$ -Aminoketone	2-Benzyl-2-(dimethylamino)-1-[4-(4-morpholinyl)phenyl]-1-butanone	slightly yellow powder	324
IRGACURE 907	$\alpha$ -Aminoketone	2-Methyl-1-[4-(methylthio) phenyl]-2-(4-morpholinyl)-1-propanone	white to light beige powder	304

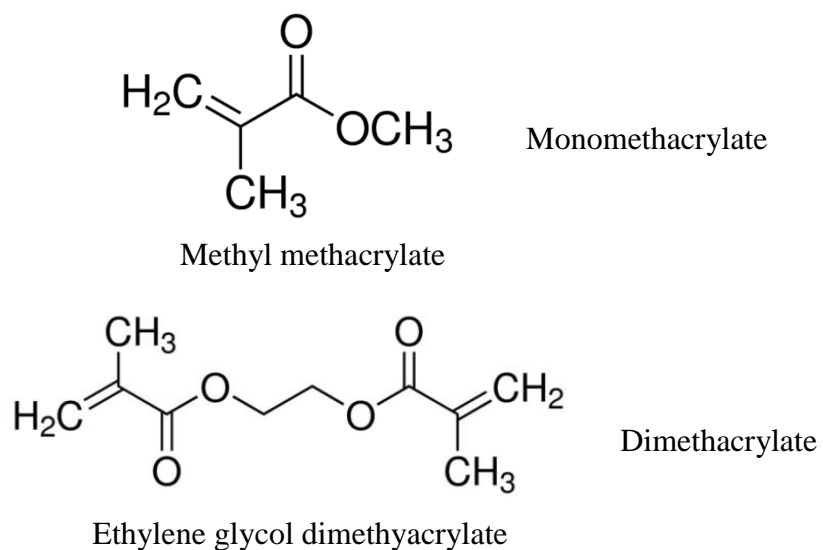
## 6.1.2 Monomers

Photopolymerization systems, like thermally initiated systems, contain initiator, monomer, and other additives that impart the desired properties. Photoinitiated radical polymerization of unsaturated monomers such as acrylate and methacrylate monomers has gained more attention in industrial use since their first introduction. The highly reactive free-radical active centres attack carbon–carbon double bonds in unsaturated monomers to form polymer chains as shown in Figure 6.3. Mixed monoacrylates (one C=C group per molecule) with multiacrylates (two or more C=C groups per molecule) are commonly used to produce a polymer with desirable properties.



**Figure 6.3** Molecular structures of monoacrylate or monomethacrylate monomer and its corresponding polymer repeat unit

Multiacrylates increase the mechanical strength and solvent resistance of the ultimate polymer by forming cross-linked networks rather than linear polymer chains. Monoacrylates also reduce the viscosity of the prepolymer mixture making it easier for processing [128]. Figure 6.4 shows a molecular structure of monomers with varying numbers of acrylate/methacrylate reactive groups.



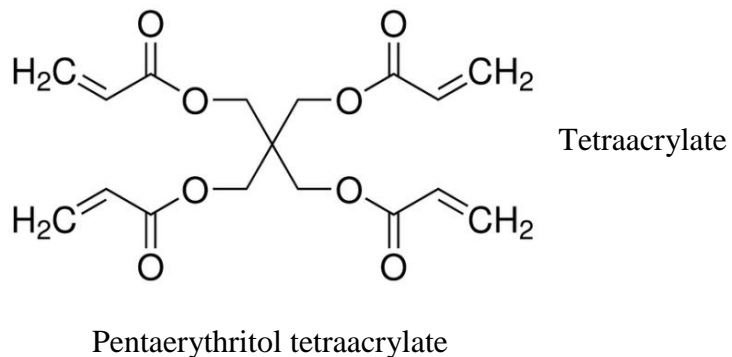


**Figure 6.4** Molecular structures of monomers with varying numbers of acrylate reactive groups.

### 6.1.3 Effect of oxygen on photopolymerization

The presence of oxygen in the reaction mixture plays a significant effect on the photopolymerization reaction rate as it's considered as a powerful inhibitor. It has ability to react efficiently with radicals and molecules in their excited triplet states. The photopolymerization could be inhibited efficiently at ambient molecular oxygen especially under specific conditions such as low film thickness, low light intensity and low cure dosage [132].

The influence of oxygen on the polymerization reaction rate of methyl methacrylate was investigated [38]. The results show that the presence of oxygen inhibited the reaction by increasing the duration of the induction period. A number of techniques have been used to overcome the oxygen inhibition, including the use of (1) high intensity UV cure dosage, (2) inert atmosphere (purging the system with nitrogen) and (3) additives such as amines [132].

### 6.1.4 Microencapsulation of PCMs using UV curing

As discussed in chapter 3, thermal-initiated free-radical polymerization is commonly used for producing PCM microcapsules, where the reaction time can take up to 24 hours to achieve a high monomer conversion. Efforts have been made to shorten this reaction time through the use of photo-induced polymerization. Spherical-like poly methyl methacrylate (PMMA)/paraffin microcapsules were successfully prepared using UV-initiated emulsion polymerization [76]. Span80 and Tween20 were used in combination as emulsifiers in oil phase (45 wt. % Span 80 and 55 wt. % Tween 80) and photocure 2959 as water-soluble photoinitiators. The photopolymerization was carried out in a tailored low columned quartz container, and was irradiated using a UV light with 1000 W under magnetic stirring at the

speed of 600 rpm for 30 minutes. The UV light source was positioned at a height of 25 cm above the surface of the container. The SEM photos indicated that the prepared microcapsules have smooth and compact surfaces with diameters ranging from 0.5 to 2  $\mu\text{m}$ . Furthermore the DSC result shows that the PMMA microcapsules contained 61 wt. % of paraffin.

This method has also been employed for the preparation of paraffin wax/cross-linked polymethyl methacrylate microcapsules [75]. Polyethylene glycol octyl phenylether (TX-100) and poly (vinyl alcohol) (PVA) were used as surfactant and dispersing agents, respectively. Ethylene glycol dimethacrylate and 2-hydroxyl-2-methyl-1-phenyl acetone (1173) were used as cross-linker agents and oil-soluble photoinitiators respectively. The photopolymerization was carried out in 250 ml a round bottom flask. The prepared O/W emulsion was irradiated by UV light of 250 W at temperature higher than the melting temperature of paraffin wax, 60 °C, for 30 minutes. SEM images show a coagulated paraffin/PMMA microcapsule with a regular spherical shape and smooth surface without edges or sharp dents. Furthermore, particle size distribution (PSD) in volume show unimodal distributions of particle sizes ranging in the interval between 0.13  $\mu\text{m}$  to 0.32  $\mu\text{m}$  with an average diameter of 0.21  $\mu\text{m}$ . The melting temperature and latent heats of the PCM microcapsules were measured using DSC as 55.8 °C and 106.9 J/g respectively. The microencapsulation ratio of the paraffin wax in the microcapsules was 66 wt. %. In addition, the DSC curves of paraffin/PMMA microcapsules show that the melting temperature of microcapsules increased by 0.3 °C and 0.7 °C and the freezing temperature increased by 0.1 °C and 0.3 °C after being subjected to 1500 and 3000 heating/cooling cycles respectively.

As reported in the previous work, the photopolymerization was carried out in 250 ml a round bottom flask. The photopolymerization conditions such as UV irradiated time and the PCMs microcapsules properties depend on the batch volume. Falling thin film closed loop UV reactor is an interesting alternative to the UV batch reactor, since the thin film UV reactor configuration present advantages over UV batch reactor including (1) easy for scale up production, (2) decrease the thickness of O/W emulsion to insure a good penetration of the UV light and (3) increase the surface area of the emulsion to facilitate the mass transfer of the inert gas to the liquid phase, where N<sub>2</sub> purging is essential in the photopolymerization reaction as it increases the overall efficiency of the photopolymerization reaction as previously discussed. This chapter presents a novel process for microencapsulating PCMs

using the thin film closed loop UV reactor. Two different methods of emulsion preparation were used and investigated. The effect of adding cross linking agents with different numbers of cross-linking functional moieties, ethylene glycol dimethacrylate (EGDM) and pentaerythritol tetraacrylate (PETRA) and their mixture to the methyl methacrylate monomer on the morphology surface and thermal properties of RT21 microcapsules were investigated. Furthermore, the effect of UV dose on the PCM microcapsules properties was studied by circulating the emulsion for different period of time.

## **6.2 Experimental**

### **6.2.1 Materials**

Methyl methacrylate (MMA) (99%, contains  $\leq$ 30 ppm monomethyl ether hydroquinone (MEHQ) as inhibitor, Sigma Aldrich, NZ), ethylene glycol dimethacrylate (EGDM) (98%, contains 90-110 ppm monomethyl ether hydroquinone as inhibitor) and pentaerythritol tetraacrylate (PETRA) (contains 350 ppm (MEHQ), Sigma Aldrich, NZ) were used as cross linking agents. Commercially available Rubitherm®RT21 ( $T_{pm}$ = 21 °C,  $\Delta H_m$ = 135 J/g, RUBITHERM® Technologies GmbH, Germany) was used as a PCM. Polyvinyl alcohol (PVA) (Mw 85,000-124,000, Sigma Aldrich, NZ) and sodium dodecyl sulfate (SDS) (BioXtra, 99%, Sigma Aldrich, NZ) were used as non-ionic and ionic surfactant. IRGACURE® 2959 (2-Hydroxy-1-[4-(2-hydroxyethoxy) phenyl]-2-methyl-1-propanone) and IRGACURE® 1173 (2-Hydroxy-2-methyl-1-phenyl-1-propanone) were used as water-soluble and oil-soluble photoinitiators.

### **6.2.2 Preparation of emulsion**

Two different methods have been followed for preparing emulsion mixture as described hereunder.

#### **6.2.2.1 Method ‘1’**

Aqueous phase and organic phase were prepared separately. 5.6 g PVA and 0.25 g SDS were dissolved into 1.5 L of deionized water and were defined as aqueous phase. 125 g of a mixture of monomer (MMA) and cross-linking gent (PETRA) (the mass ratio of MMA to PETRA is set as 1:1), 0.5 g IRGACURE® 1173 and 75 g Rubitherm®RT21 were assembled as organic phase. The emulsion was prepared by slowly adding the organic phase to the aqueous phase under mechanical stirring at 5000 rpm. The emulsification process was

continued for 5 minutes using a high shear mixer (Silverson L5M-A laboratory Mixer) equipped with a fine screen.

### **6.2.2.2 Method ‘2’**

Three phases were prepared separately in this method. 5.6 g PVA, 0.25 g SDS and 3 g water soluble photoinitiator (IRGACURE® 2959) were dissolved into 1.5 L of deionized water (phase ‘1’). 75 g of Rubitherm® RT21 was weighted (phase 2). 125 g of mixed monomers with different mass ratios were prepared (phase 3). In this approach, PCM emulsions were prepared firstly by slowly adding the PCMs to phase ‘1’ under mechanical stirring at 5000 rpm. The emulsification was continues for 5 minutes, after which phase ‘3’ was added slowly to the PCM emulsion under the same rate of mechanical stirring for a further 5 minutes.

### **6.2.3 Photopolymerization**

PCMs emulsion is cloudy and therefore not transparent to UV light. To increase the UV light penetration through the emulsion, a falling thin film closed loop UV reactor was designed and constructed. It has been reported that any opaque liquid may be considered transparent to UV light if it is in the form of a liquid film with a thickness less than 1.6 mm [133]. Figure 6.5 shows the overall sketch diagram of the falling thin film closed loop UV reactor used in this study.

The UV reactor was designed and manufactured at the workshop of Qatar University. The designed reactor consists of several parts: (1) collection tank, (2) magnetic pump (IWAKI AMERICA Inc.), (3) emulsion flow distributor at the top of the inclined glass plate, (4) four UV lamps (MH module, 250W mercury lamp, Heraeus Noblelight GmbH) (Figure 6.6), (5) cooling fan and (6) circulating cooling system.

In a typical experiment, 1.5 L of prepared PCM emulsion was used. The emulsion was introduced at the start of the experiment in the collection tank which was surrounded with a cooling jacket and equipped with a mechanical stirrer and inlet nitrogen. The magnetic pump recirculated the emulsion from the tank to the flow distributor at flow rate of 1.5 L/min. The flow distributor was located at the top of the flat inclined plate. The flat inclined plate surface was made from glass, on which the prepared PCMs emulsion flowed as a thin film (Figure 6.6) and back into the tank. Four UV lamps (MH module, 250W mercury lamp, Heraeus Noblelight GmbH) were positioned 300 mm above the surface of the thin film emulsion. The

total values at maximum in 300 mm distance [w/m<sup>2</sup>] of the mercury UV lamp are listed in Table 6.2. The UV reactor was purged with nitrogen during the photopolymerization reaction for deoxygenating the emulsion. The recirculating time of PCMs emulsion was kept for two hours at 35 °C.

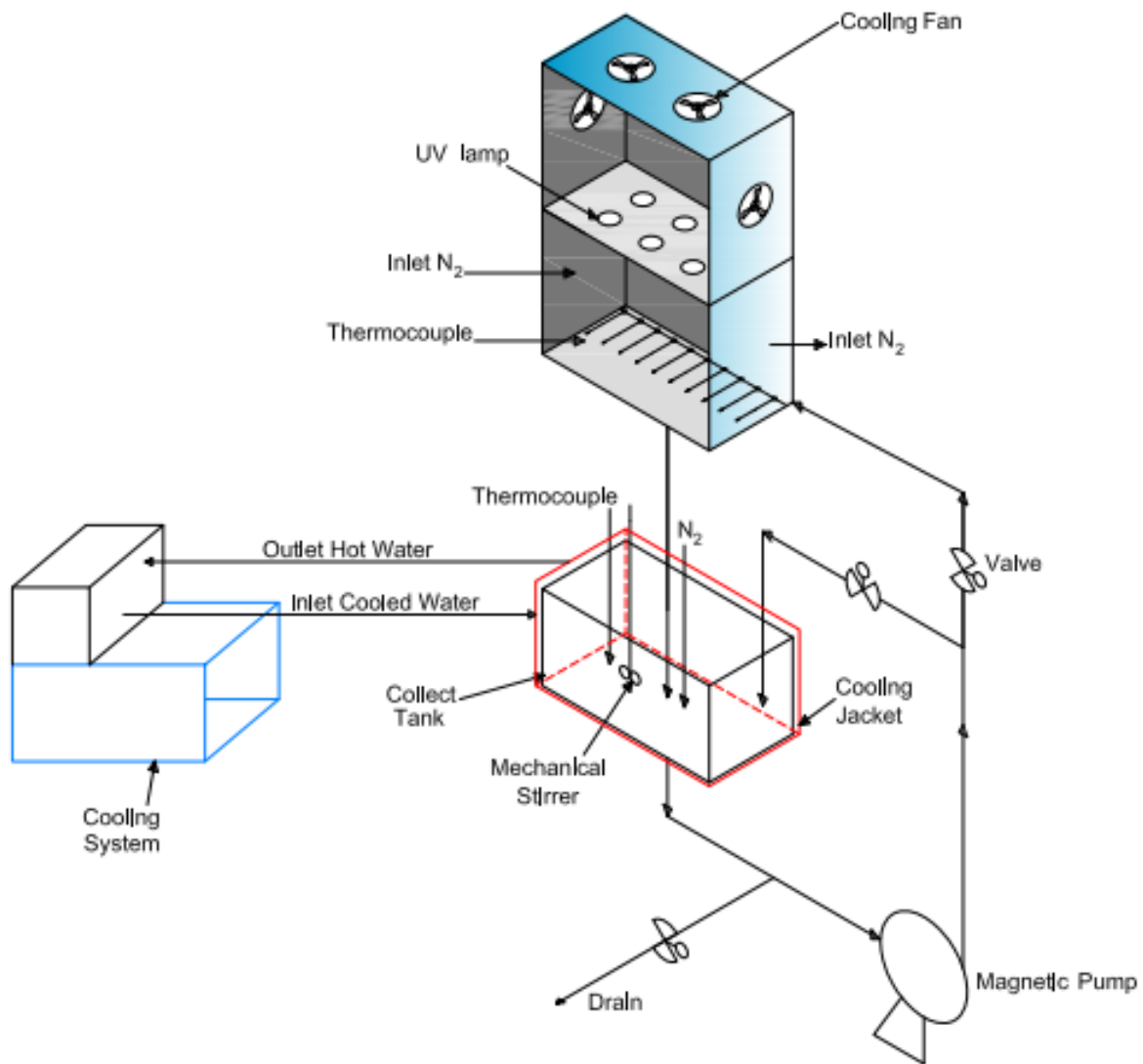


**Figure 6.5** Overall sketch diagram of the falling thin film closed loop UV reactor.

**Table 6.2** Total values at maximum in 300 mm distance [ $\text{w/m}^2$ ] of the mercury UV lamp

Range	Mercury lamp
UVC (250-280 nm)	193
UVB (280-315 nm)	148
UVA (315-400 nm)	174
VIS (400-450 nm)	153

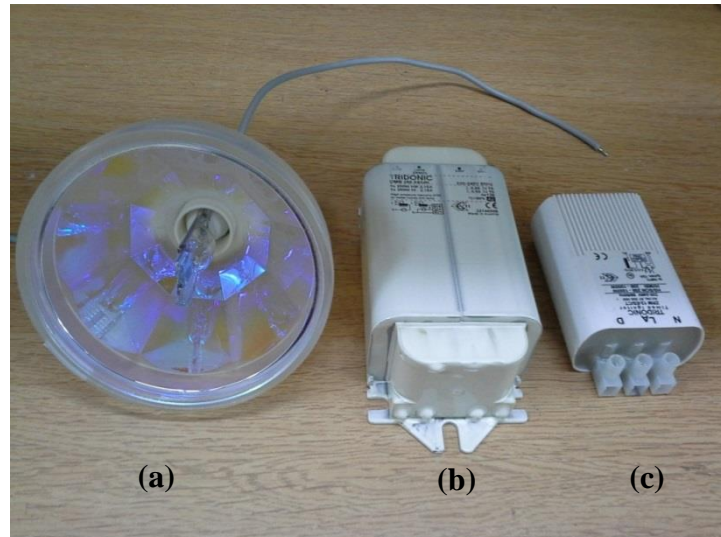


**Figure 6.6** Camera photos of (a) MH module, 250W mercury lamp, (b) Ballast and (c) igniter.



**Figure 6.7** A thin film PCMs emulsion flow.

The produced PCM microcapsule suspension was transferred to a clean glass beaker for a washing process. PCM microcapsule suspensions were washed three times with distilled water to remove any unreacted monomer and any PCM, which had not been encapsulated.

The separated microcapsules were spread on a tray and placed in an oven at 50 °C for 48 hours to dry. The dried microcapsules were then collected for testing.

### **6.3 PCM microcapsules characterizations**

#### **6.3.1 Scanning Electron Microscope (SEM)**

The surface morphology of the microcapsules was investigated by using a Nova NanoSEM 450 scanning electron microscope (SEM). All samples were coated with a thin layer of gold prior to testing.

#### **6.3.2 Differential Scanning Calorimetry (DSC)**

Phase change thermal properties of PCM and PCMs microcapsules including melting and crystallizing points and phase change enthalpies were measured using a differential scanning calorimetry (DSC) (Perkin Elmer DSC 7). The measurements were performed by varying the temperature from -15 to 40 °C with heating and cooling rate of 3 °C/min.

## **6.4 Results and Discussion**

### **6.4.1 Effect of emulsion preparation method on microencapsulation of RT21**

Two methods have been used for preparing PCMs emulsion. In method ‘1’ droplets of monomers and PCM mixture are formed in a solution of surfactant and water. The photopolymerization of prepared emulsion occurs in the core of the droplet and a polymer shell forms outside of the core. However, in method ‘2’ PCM droplets are formed in the solution of surfactant and water and then a mixture of monomers is added. The photopolymerization in method 2 takes place in two areas: (1) the micelles of the PCM droplets; where some of the monomers are diffused and located and (2) in the aqueous phase. Organic-soluble and water-soluble photoinitiators were used in method 1 and 2 respectively. The mass ratio of PCM to monomers (0.6:1) was kept constant in both methods.

SEM images and corresponding digital camera photographs of RT21 microcapsules prepared using the two different methods of emulsion preparation have been taken as shown in Figure 6.8. The results show that most of the particles are agglomerated into lumps and a small amount of microcapsule was obtained when the emulsion was prepared using method ‘1’. This could be due to the low monomer conversion. The UV light attacks the mixture of

photoinitiator and monomers that are concentrated in the droplets micelles and produced a very thin polymer shell. The produced shell is non-transparent, so prevents UV light from going inside the droplet and completes the photopolymerization of the monomer rest. This very thin polymer shell is not strong enough to contain the PCM inside the capsules, so most of the capsules agglomerated into lumps and PCM leaked out as shown in Figure 6.8a. However smooth, compact and dry spherical capsules were produced, when the emulsion was prepared using method ‘2’ as shown in Figure 6.8b.

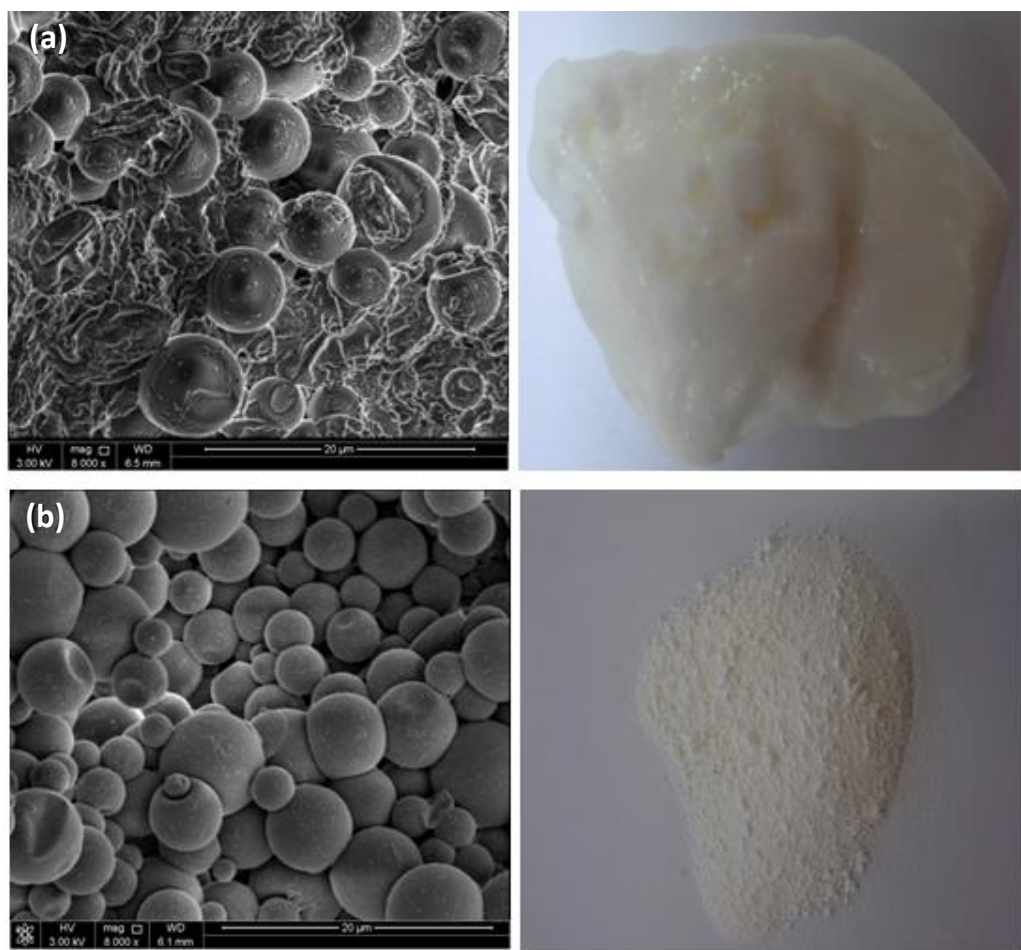


**Figure 6.8** SEM images and digital camera photographs of RT21 microcapsules prepared using the two different methods of emulsion preparation: (a) Method ‘1’ and (b) Method ‘2’

Phase change properties of bulk PCM and PCM microcapsules were measured using a differential scanning calorimeter (DSC) as shown in Figure 6.9. The DSC measurements show that energy storage capacity of the microcapsules produced using method ‘2’ is significantly higher than those produced using method ‘1’.

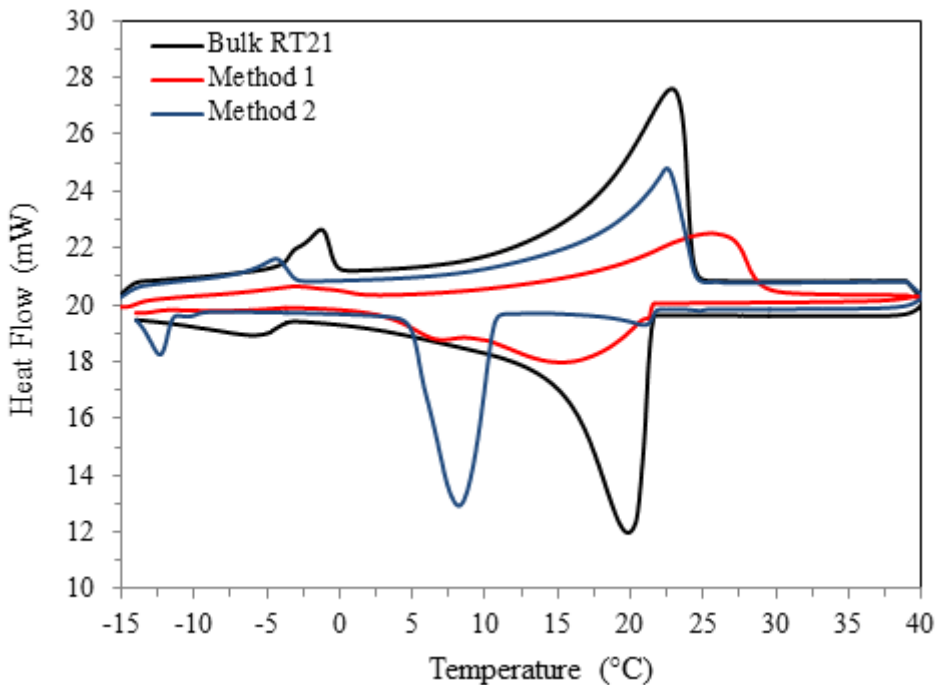


**Figure 6.9** DSC curves of RT21 microcapsules prepared using the two different methods of emulsion

**Table 6.3** Thermal properties of RT21 microcapsules prepared using the two different methods of emulsion preparation

	Method 1		Method 2		Bulk RT21	
	Heating	Cooling	Heating	Cooling	Heating	Cooling
T <sub>onset</sub> (°C)	15.19	21.51	16.02	10.63	15.41	21.42
T <sub>peak</sub> (°C)	25.63	15.38	22.5	8.2	22.82	19.82
T <sub>endset</sub> (°C)	28.90	2.4	24.48	4.9	24.24	14.58
ΔH (kJ/kg)	70.6	79.5	103.6	94.3	135	133.6

The melting temperatures of the RT21 microcapsules increased, and become higher than the bulk RT21 when the PCMs emulsion was prepared using method ‘1’. However, there was no change in the melting temperatures of RT21 microcapsules prepared using method ‘2’ as reported in Table 6.3 and shown in Figure 6.9.

The thermal characteristics (i.e. melting range and latent heat of fusion) of bulk RT21 was tested following an exposure to heating at temperatures of 30 and 55 °C. The results obtained indicated that RT21 experienced a significant irreversible physical change with time. The

data collected and analysis indicated a shift in the peak melting point from 22.5 to 28 °C due to loss of low molecular mass paraffin present in over a period of 120 days when kept at a temperature of 55 °C [17]. The well containment of the RT21 inside the polymer shell produced using method ‘2’ prevented such loss.

The drawback of method ‘2’ is the formation solid polymer microspheres (monomers losses) as observed particles precipitated during the process of washing. DSC measurement of these particles shows no peaks within the temperature range of RT21 phase transition (Figure 6.10), suggesting that they contain no PCM. Approximately 30-35 % of the total monomer was converted to polymer microsphere instead of PCM microcapsules (the monomer losses were calculated using equation 6.1). Further investigation is needed to minimize this monomer loss.

$$\text{monomer losses} = \frac{\text{mass of dry soild polymer microsphere}}{\text{mass of monomers(MMA+PETRA)}} \dots\dots\dots (6.1)$$

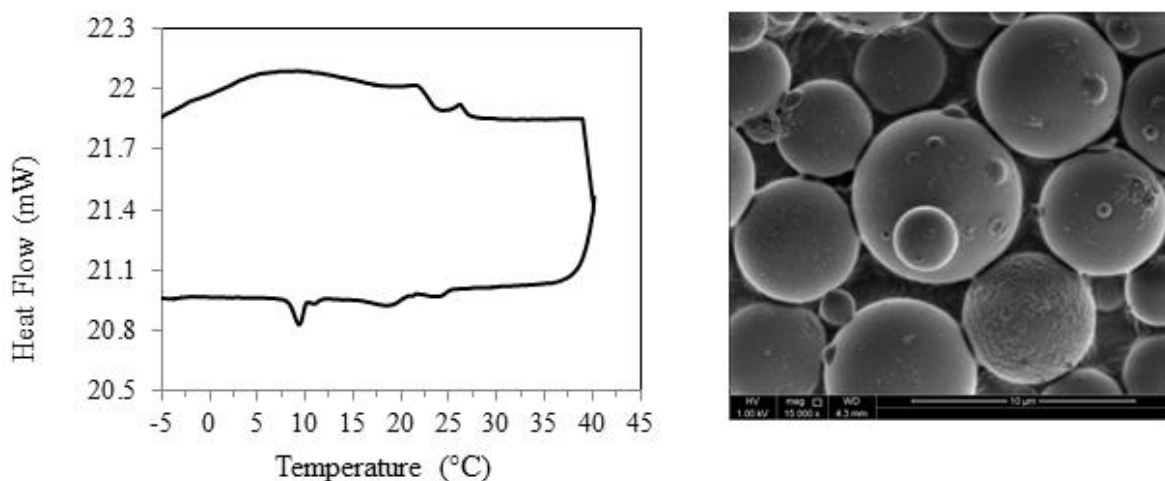


**Figure 6.10** DSC curve and SEM photo of the produced microspheres

#### 6.4.2 Effect of adding cross linking agent with different numbers of cross-linkable functional moieties on the properties of RT21 microcapsules

As stated early, unsaturated monomers, which have one C=C group per molecule (monomethacrylate monomer) tend to be mixed with monomers having two or more C=C group per molecule (multiacrylate monomer) to produce a polymer with reasonable properties (such as high mechanical strength). In this study, cross linking agent with different numbers of cross-linkable functional moieties such as ethylene glycol dimethacrylate (two C=C reactive group) and pentaerythritol tetraacrylate (three C=C reactive group) was mixed

with methyl methacrylate (MMA) (one C=C reactive group). Figure 6.11 shows SEM photos of RT21 microcapsules produced at 1:1 mass ratio of cross linking agent to monomer.

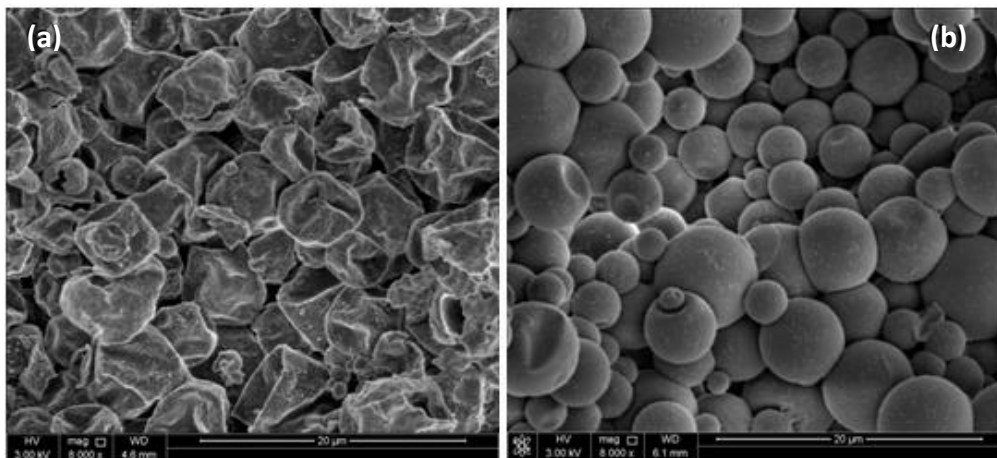


**Figure 6.11** SEM photos of RT21 microcapsules produced using (a) EGDM and (b) PETRA

Broken and shrinkage microcapsules were observed when EGDM was used (Figure 6.11a). However, smooth and compact microcapsules with very limited dimples on their surfaces were obtained when PETRA was used as shown in Figure 6.11b. This result indicates that the larger the number of crosslinking functional moieties, the higher the degree of cross-linking of the polymer shell of the microcapsules and thus the stronger shell. Not only the higher number of crosslinking functional moieties has a positive effect on the microcapsules morphology, but it also increases the thermal energy storage capacity of the PCM microcapsules from 83.2 to 103.6 J/g (Figure 6.12). This may be due to the well containment of PCM inside the microcapsules, so prevent the mass loss of PCM through the shell.

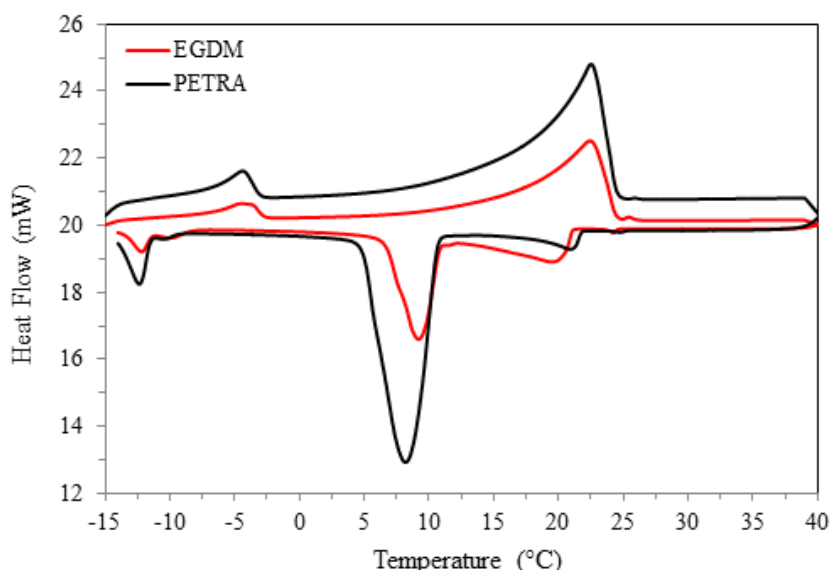


**Figure 6.12** DSC curves of RT21 microcapsules produced using (a) EGDM and (b) PETRA

### 6.4.3 Effect of PETRA concentrations on the RT21 microcapsules properties

In order to explore the effect of PETRA concentrations on the properties of PCMs microcapsules, a series of experiments were carried out using PETRA concentrations from 0 to 50 wt. %. SEM photos of RT21 microcapsules are shown in Figure 6.13. Particles are agglomerated to lumps and no microcapsules formed when only MMA was used (Figure 6.13a). However, spherical microcapsules with porous structure appeared when 15 wt. % of PETRA was used (Figure 6.13b). The surface morphology of the microcapsules was improved by increasing PETRA concentration. Helmet shape microcapsules with smooth and dense surface were observed when the amount of PETRA increased up to 30wt. % (Figure 6.13c). Further increase in PETRA up to 50 wt. % improved the sphericity of the microcapsules to be totally sphere with smooth and compact surface (Figure 6.13d).

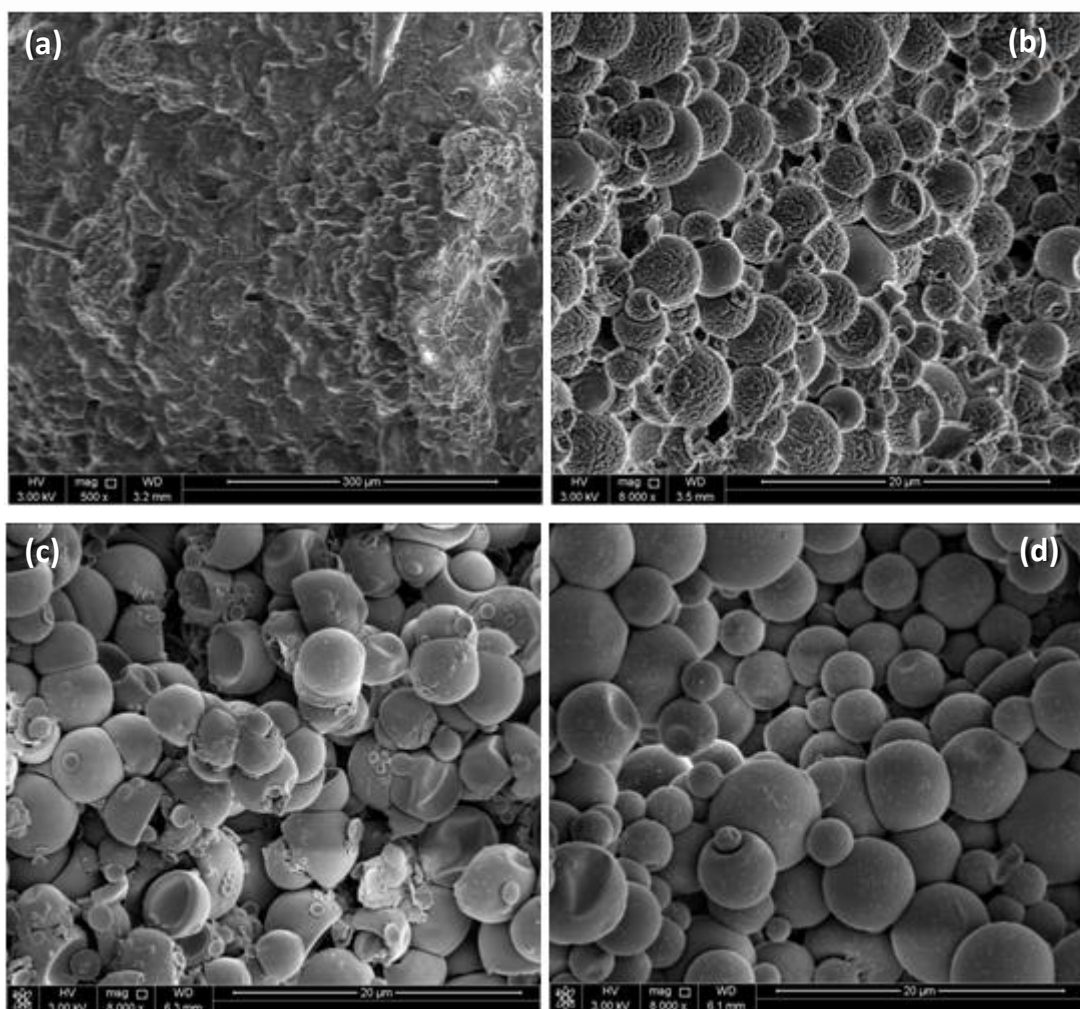


**Figure 6.13** SEM photos of RT21 microcapsules with different PETRA concentrations: (a) 0 wt. %, (b) 15 wt. %, (c) 30 wt. % and (d) 50 wt. %

Thermal properties of RT21 microcapsules prepared with different PETRA concentrations are shown in Figure 6.14 and are summarized in Table 6.4. It is clear that the endothermic peaks of RT21 microcapsules increased by 3.14 and 0.97 °C in comparison to the bulk RT21 when 0 and 15 wt. % of PETRA were used respectively. However, no shifting in peak melting temperature of the RT21 microcapsules has been observed once 50 wt. % of PETRA was used as shown in Figure 6.13 and Table 6.4. It is also obvious that increasing PETRA concentration led to an increase in the latent heat of the RT21 microcapsules. RT21 microcapsules prepared using 50 wt. % PETRA has the highest latent heat of fusion (103.6 J/g), which corresponds to 76.7 wt. % PCM (Table 6.4). These results imply that higher crosslinking degree increases the strength of the polymer shell, and hence enhanced the containment of RT21 inside the microcapsules; thus preventing light compositions of RT21 from vaporizing.

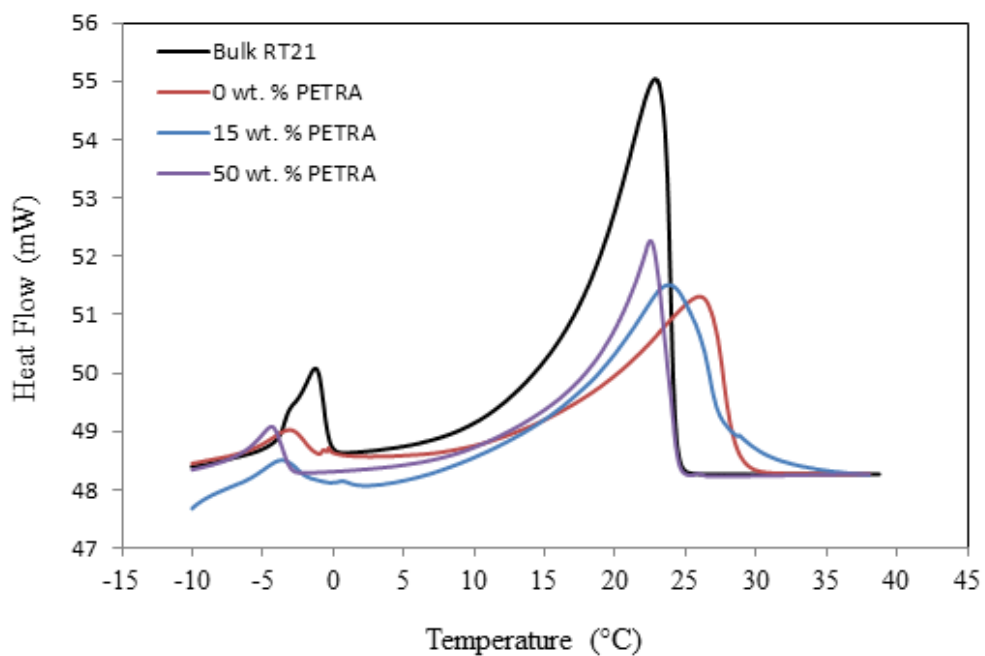


**Figure 6.14** DSC heating curves of RT21 microcapsules with versus PETRA concentrations:  
 (a) 0 wt. %, (b) 15 wt. %, (c) 30 wt. % and (d) 50 wt. %

**Table 6.4** Thermal properties of RT21 microcapsules with versus PETRA concentrations

	Heating			
	T <sub>onset</sub> (°C)	T <sub>peak</sub> (°C)	T <sub>endset</sub> (°C)	ΔH (kJ/kg)
Bulk RT21	15.41	22.82	24.24	135
0 wt. % PETRA	15.03	25.96	28.52	83.8
15wt. % PETRA	14.27	23.79	28.08	89.4
50 wt. % PETRA	16.02	22.5	24.48	103.6

#### 6.4.4 Effect of cross-linking agents mixture concentrations and emulsion circulating time on the RT21 microcapsules properties

EGDM is a hydrophilic difunctional methacrylate offering low viscosity, low shrinkage, adhesion, flexibility and high crosslinking density. Incorporation of EGDM into polymeric shell of the PCM microcapsules improves their thermal and mechanical properties [100]. PETRA is a hydrophilic tetraacrylate monomer, which has four C=C reactive groups per molecule, and commercially used as a light crosslinking and branching agent for comonomers to prepare crosslinking polymers [134]. Thermal properties and shell mechanical strength of PCM microcapsules were enhanced when PETRA was used [80]. So mixtures of cross linking agents, EGDM and PETRA, and their effect on the RT21 microcapsules properties were investigated.

Figure 6.15a and b show the morphology of RT21 microcapsules prepared with different concentrations of mixture of EGDM and PETRA. The mass ratio of PCM to monomers (MMA, EGDM and PETRA) was kept constant in both mixtures (0.6:1). The RT21 microcapsules surface morphology was enhanced when a mixture of 35 wt. % PETRA 15 wt. % EGDM and 50 wt.% MMA (mixture ‘A’) was used. However, bukles and dimples were observed when a mixture of 15 wt. % PETRA, 35 wt. % EGDM and 50 wt. % MMA (mixture ‘B’) was used. The absence of RT21 microcapsules surface dimples when a mixture ‘A’ was used could be due to the enhancement of the mechanical strenght of the polymer shell; thus preventing shrinking of the polymer shell during phase transition of the PCM. The thermal energy storage capacity of RT21 microcapsules is high when mixture ‘A’ was used (Table 6.5). The monomers losses of mixture ‘B’ in comparasion to mixture ‘A’ was less based on the equation 6.1 calcualtion. It is seems that EGDM prefer to diffuse and polymerized on the PCMs droplets inteface rather than in the bulk.

**Table 6.5** Thermal properties of RT21 microcapsules prepared with different mixture concentrations of cross-linking agents and emulsion circulating time

	Mixture A (Two hours irradiated time)		Mixture B (Two hours irradiated time)		Mixture B (One hour irradiated time)	
	Heating	Cooling	Heating	Cooling	Heating	Cooling
T <sub>onset</sub> (°C)	17.46	10.62	16.85	10.55	16.74	10.62
T <sub>peak</sub> (°C)	22.04	7.81	22.17	7.79	22.12	8.38
T <sub>endset</sub> (°C)	23.52	5.75	24.12	4.73	24.31	4.35
ΔH (kJ/kg)	94.6	94.6	80.5	80.7	90.3	90.5

Monomers mixture ‘A’: 35 wt. % PETRA, 15 wt. % EGDM and 50 wt. % MMA

Monomers mixture ‘B’: 15 wt. % PETRA, 35 wt. % EGDM and 50 wt. % MMA

No serious change in the surface morphology of the RT21 microcapsules have been observed when the irradiated time reduced from 2 hours to 1 hour when mixture ‘B’ was used as shown in Figure 6.15 b and c. In fact the heat storage capacity of the RT21 microcapsules increased from 80.5 to 90.3 J/g when the irradiated time decreased from 2 hours to 1 hour respectively (Table 6.5). This could be due to the less conversion of the monomers, thus produced a thinner shell capsules.

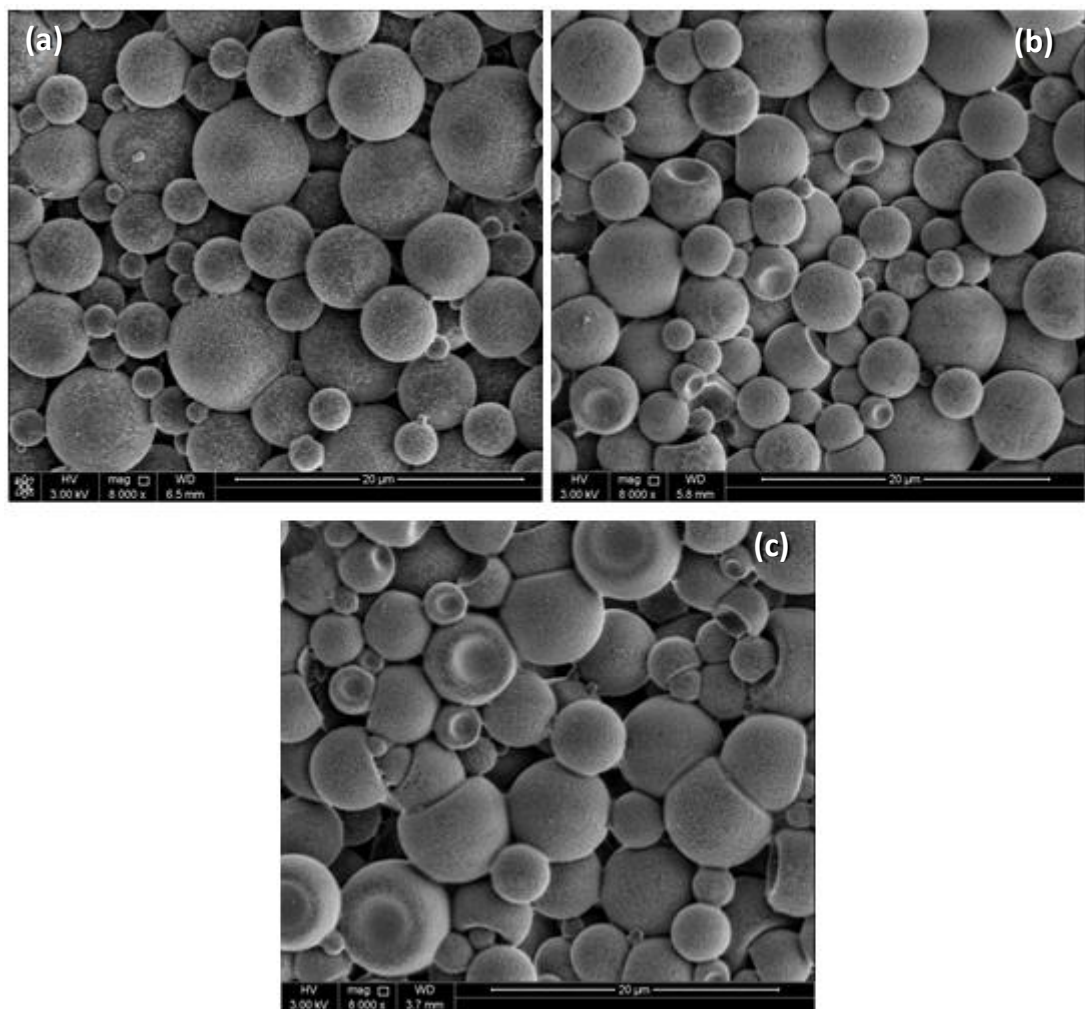


Figure 6.15 SEM photos of RT21 microcapsules prepared with different mixture concentrations of cross-linking agents and emulsion circulating time: (a) mixture A (two hours irradiated time) (b) mixture B (two hours irradiated time) and (c) mixture B (one hour irradiated time)

# Fabrication and Characterization of PCMs Microcapsules Coated with Silver

7

## Abstract

The heat storage capacity of phase change materials (PCMs), its efficient containment inside the microcapsule and the useful life of these microcapsules as well as the shell mechanical strength are considered to be key parameters in assessing quality of PCMs microcapsules. In practical applications, especially in the building field, the shell of PCMs microcapsules must have enough robustness to avoid the shell rupturing during the mixing process with building materials. PCMs microcapsules are also used in slurries to improve thermal performance of heat exchangers and these microcapsules need to sustain the high shear caused by pumping the suspension. In an attempt to improve the mechanical strength of the PCMs microcapsules shell, a novel double shell PCMs microcapsule with both polymer and metal coatings was fabricated. The developed PCMs microcapsules were coated with metal in two simple steps: (1) surface functionalization of PCMs microcapsules using polydopamine (PDA) and (2) electroless plating of silver (Ag) metal. The effect of PDA as chemi-sorption sites for silver ions to promote the silver deposition on the surface of the PCMs microcapsules was investigated. Furthermore, the mechanical strength of the developed microcapsules (double shell) in comparison to the PCMs microcapsules (single shell) was studied. SEM images did not show evidence of Ag metal on the surface of PCMs microcapsules which were not treated with PDA. However, PCMs microcapsules were completely covered with Ag metal when the PCMs microcapsules were functionalized with PDA prior the electroless plating of Ag. The nanocompression test of single microcapsules before and after metal coating was performed using a MTS XP Nanoindenter fixed with a 10 $\mu$ m radius conical tip and 40 x optical microscope lens. The loads vs. displacement curves show a significant increase in the mechanical strength of the PCMs microcapsules shell when is coated with Ag metal. The polymer rupturing load was increased from 0.45 to 6.6 mN. Metal coated microcapsules undergo two steps shell rupturing: (1) inner polymer shell rupturing and (2) outer metal shell rupturing. In addition, optical microscope images before and after nanocompression of a single microcapsules were taken and confirmed that the microcapsules had indeed ruptured. It is be noted that this approach could be expanded in future to cover metals, which are less expensive than silver.

## 7.1 Introduction

Coating PCMs with a metallic layer is used to enhance many properties required in many thermal energy storage applications [135]. Generally PCMs are coated with a hard polymeric shell to prevent liquid PCM from leaking out when producing commercial microcapsules [136]. With coating an additional metallic layer, the thermo-mechanical properties of the PCM is improved as discussed elsewhere [137]. Electrodeposition of copper over a template of spherical microcapsules of PCMs leads to an enhanced thermal conductivity of the fabricated micro porous metal matrix-PCM composite [138]. Furthermore, copper foam with copper volume fraction of 5% was fabricated to enhance the thermal conductivity of paraffin wax [139]. Experimental studies demonstrated 2.5 times more PCM utilization compared to the samples without the copper foam. Metal encapsulation of novel PCM was developed by Dow Automotive Systems, enabling long-term durability and high heat transfer rates [140].

Mechanical strength of PCMs microcapsules is an important property to be enhanced. In practical applications especially in building, the shell of PCMs microcapsules should have a high mechanical strength to avoid microcapsule rupture during mixing processes with building materials. PCMs microcapsules are also used in slurry to improve thermal performance of heat exchangers and these microcapsules need to sustain the high shear caused by pumping the suspension [141].

The mechanical strength of the PCMs microcapsules is determined by their chemical composition, structure, size and shell thickness. Single and double shell structures of PCM microcapsules with an average diameter of 5–10  $\mu\text{m}$  were successfully fabricated using melamine-formaldehyde resin [142]. The mechanical properties of single and double shell PCM microcapsules (both single and double shell PCM microcapsules made from polymers) were tested under compression and evaluated with a pressure sensor. Stress vs. strain curves showed that both single and double shell PCMs microcapsules have a conventional plastic behaviour when the applied pressure was beyond the yield strength of the shell. The reported results show a large variation in the mechanical strength of the tested single shell PCM microcapsules with yield point range from  $3 \times 10^4$  to  $4 \times 10^4$  Pa and burst point range from  $9 \times 10^4$  to  $12 \times 10^4$  Pa. These variations indicate that the shell formed is not structurally uniform. However, the double polymeric shell PCM microcapsules showed much more consistency in the results with yield point and burst point of  $5.5 \times 10^4$  and  $13.4 \times 10^4$  Pa respectively. The double shell PCM microcapsules were found to be structurally

homogeneous with a better mechanical stability than that of single shell PCM microcapsules [143].

Methanol-modified melamine-formaldehyde (MMF) shell was used in an attempt to enhance the mechanical properties of melamine-formaldehyde (MF) shell [64]. The rigidity of the MMF shell was tested by placing the microcapsules between two pieces of glass and compressing them. A pressure sensor under the bottom glass measured the pressure intensity and directly recorded it. The results show that the shell microcapsules undergo a plastic deformation when the applied pressure was beyond the yield point of the shell. The MMF shells show enhancement in the mechanical properties in comparison to the MF shells at the same core: shell mass ratio.

Controlling the size of the PCMs microcapsules is considered a realistic option for improving shell mechanical strength. The force required to rupture a single microcapsule of commercial product (Microtek MPCM-18D) with different sizes was investigated [115, 144]. The nanocompression test of a single microcapsule was performed using MTS XP Nanoindenter with 10 $\mu\text{m}$  radius 60° conical diamond tip and 40-X optical microscope lens. The results show that the MPCM-18D with size diameters between 18.75 and 28.3  $\mu\text{m}$  required a force of 0.67 and 0.29 mN to rupture respectively; thus smaller microcapsules required greater force to rupture. Unsaturated monomers such as methyl methacrylate can be tuned with cross-linking agents to produce polymers with high mechanical strength. Cross-linked polymethyl methacrylate (PMMA) microcapsules containing n-octadecane were successfully prepared using the suspension-like polymerization method. Four cross-linking agents with different numbers of cross-linking functional moieties were selected for comparison. The results show that the PCMs microcapsules prepared using a high number of cross-linking functional moieties exhibited a greater shell mechanical strength [79, 80].

Electroless plating uses a redox reaction in aqueous solution to deposit metal on a substrate without requiring passing an electric current. Electroless plating deposition of a metal on PCM microcapsules to improve the electrical and thermal conductivity has been disclosed in many patents [135, 145, 146]. The surface of the PCM microcapsules first needs to be sensitized and then activated with metal catalyst such as salts of palladium, nickel, platinum and rhodium. This metal catalyst is expensive; so in this work a simple and versatile strategy for surface modification of organic or inorganic surfaces using polydopamine is used as reported elsewhere [147]. The chemical structure of polydopamine (PDA) has catechol

compounds and amino groups, which have the ability to establish interactions with both organic and inorganic substrates. PDA was used as chemi-sorption sites for silver ions and promoted the silver deposition on the surface of the silica microspheres [148, 149]. The SEM results show that, when silica microspheres are treated with PDA prior to electroless plating of Ag, the silica becomes completely covered with silver.

The approaches mentioned earlier show slight improvements in the shell mechanical strength of the PCMs microcapsules. In this chapter PCMs microcapsules coated with silver metal using electroless plating technique were fabricated in an attempt to enhance the shell mechanical strength. Polydopamine (PDA) was prepared by oxidative self-polymerization of dopamine in buffer solution and was used as interface modifier between the polymer shell and metal prior to electroless plating of silver. The thermal properties and mechanical strength of PCMs microcapsules before and after metal coating were investigated. The morphology, surface chemical compositions, thermal and mechanical properties of the metal coated PCMs microcapsules were investigated using scanning electron microscope (Nova NanoSEM 450), energy dispersive X-ray spectroscopy (EDX), differential scanning calorimeter (Perkin Elmer DSC 7) and Nanoindentation (MTS XP) respectively.

## 7.2 Experimental

### 7.2.1 Materials

Commercial 24-D microcapsules coated with melamine-formaldehyde resin ( $T_{pm}= 23.7\text{ }^{\circ}\text{C}$  and  $\Delta H_m= 123\text{ J/g}$ , Microtek Laboratories, USA) and RT21MC-5wt. % RT58 microcapsules made in our lab (see chapter 5). Silver nitrate (ACS reagent,  $\geq 99.0\%$ ), dopamine hydrochloride, tris (hydroxymethyl) aminomethane (ACS reagent,  $\geq 99.0\%$ ), poly vinylpyrrolidone (PVP, MW 40,000 g/mol), glucose (99.5 %), ammonia hydroxide solution (ACS reagent, 28-30% NH<sub>3</sub> basis), absolute ethanol, sodium hydroxide and hydrochloric acid purchased from Sigma Aldrich were used without any purification.

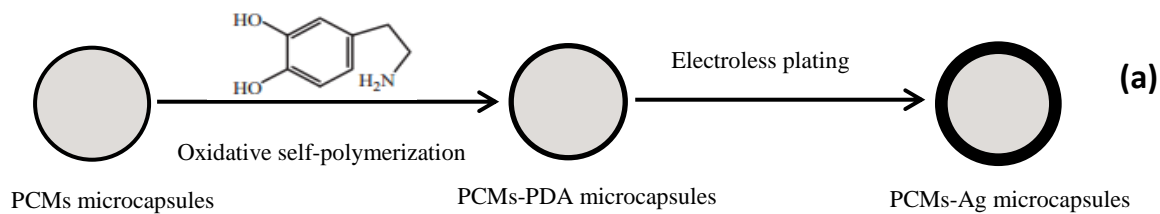
### 7.2.2 Synthesis of metal coated PCMs microcapsules

The synthesis of PCMs/Ag microcapsules consists of two steps as follow:

### 7.2.2.1 Surface functionalization of PCMs microcapsules

Poly (dopamine) was formed and deposited on the surface of PCMs microcapsules as an adherent coating by the oxidative self-polymerization of dopamine in tris solution. The PCMs-PDA microcapsules were prepared as follow [148]:

- (1) 100 g of dopamine solution was prepared by dissolving 0.2 g of dopamine into 100 g of tris (hydroxymethyl) aminomethane solution (10 mM).
- (2) The dopamine solution pH was adjusted to 8.5 by adding sodium hydroxide solution (1M) or hydrochloric acid solution (1M) in stepwise in order to control the pH of dopamine solution.
- (3) 5 g of PCMs microcapsules was suspended in the 100 g of dopamine solution under stirring for 24 hours at room conditions. The possible mechanism of dopamine oxidative self-polymerization reaction is shown in Figure 7.1 b as reported in the literature [147, 150].
- (4) The PCMs-DPA microcapsules was filtered and washed three times with deionized distilled water and then placed in an oven at 50 °C for 24 hours for drying before electroless plating of silver.



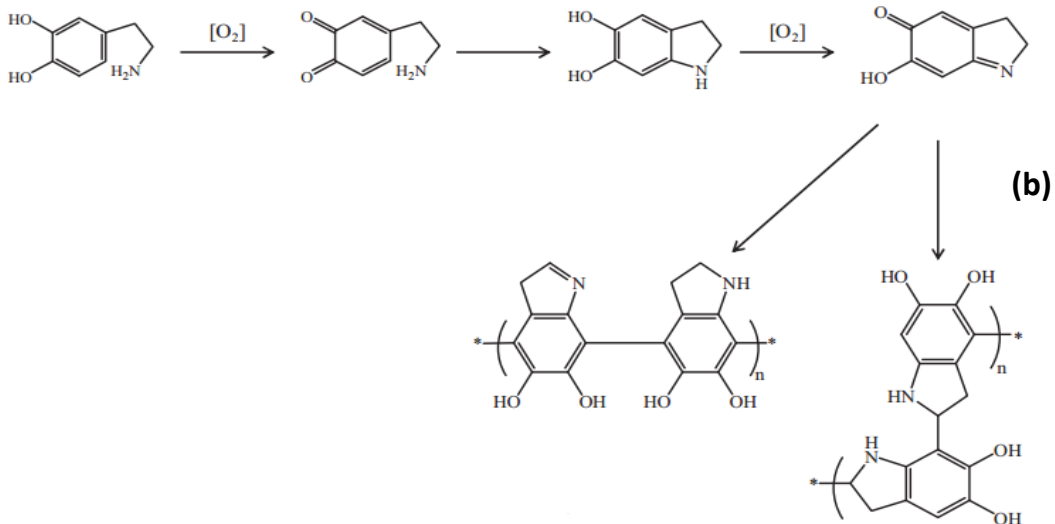


**Figure 7.1** (a) Schematic illustration of sequence steps for preparing PCMs-Ag microcapsules and (b) possible mechanism of dopamine oxidative self-polymerization [147, 150].

### 7.2.2.2 Electroless plating

Followed by surface functionalization of PCMs microcapsules, electroless plating of silver was carried out as follow [149]:

- (1) Silver nitrate solution was prepared by dissolving 1 g of silver nitrate ( $AgNO_3$ ) into 100 ml of deionized distilled water under magnetic stirring. Drops of ammonia were added stepwise into silver nitrate solution till the colour changed from darkness to transparency.
- (2) 3 g of PCMs-DPA microcapsules were added to the silver nitrate solution and maintained stirring for 15 minutes to give a chance of  $AgNO_3$  ions absorbed on the surface of PCMs-DPA microcapsules by the catechol and amino groups presents in the PDA.
- (3) Reducing agent solution was prepared separately by dissolving 0.5 g of glucose (reducing agent) into 100 ml of deionized distilled water. Beside glucose 0.04 g of ethanol and 0.04 g of poly vinylpyrrolidone (PVP) were added.
- (4) Reducing agent solution was added slowly to the PCMs-DPA microcapsules silver nitrate solution under stirring, and then the electroless bath solution kept stirring for 30 minutes. The PCMs-Ag microcapsules was separated and rinsed three times with

distilled water and then placed in an oven at 50 °C for 24 hours for drying prior testing.

### **7.2.3 PCMs/Ag microcapsules characterizations**

#### **7.2.3.1 Scanning electron microscope (SEM) and energy dispersive X-ray spectroscopy (EDX) integrated system**

The surface morphology and chemical compositions of the PCMs, PCMs-DPA and PCMs-Ag microcapsules were investigated using Nova NanoSEM 450 scanning electron microscope (SEM) integrated with energy X-ray spectroscopy (EDX). All samples were coated with a thin layer of gold prior testing.

#### **7.2.3.2 Differential scanning calorimeter (DSC)**

Phase change thermal properties of PCMs, PCMs-DPA and PCMs-Ag microcapsules were measured using a differential scanning calorimeter (DSC) (Perkin Elmer DSC 7). The measurements were performed by varying the temperature from -15 to 40 °C with heating and cooling rate of 3 °C/min.

#### **7.2.3.3 MTS XP Nanoindenter**

The nanocompression test of a single microcapsule was performed using a MTS XP nanoindenter fixed with 10µm radius conical tip (diamond cone 60°) and 40-X optical microscope lens. The details of this technique are described elsewhere [144]. Figure 7.2 shows the sequence steps of nanocompression of single microcapsule compressed until rupture. These steps are summarized as follow:

**Step A:** The conical tip approaches the surface of single microcapsule prior to commencing the test. The surface approach velocity and distance were set to 10 nm/sec and 1000 nm respectively.

**Step B:** The conical tip continues approaching the surface of the microcapsule until it makes physical contact, then the compression force is applied.

**Step C:** The compression force is increased until past the point of microcapsule rupture.

**Step D:** The test continues until the maximum set distance of 10000 nm is met, ensuring that the substrate has been penetrated by the tip for control measurements.

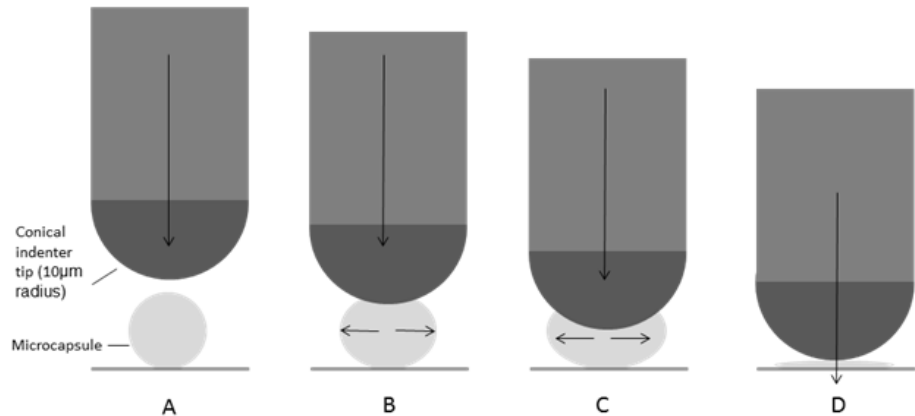


**Figure 7.2** Sequence steps of nanocompression of a single microcapsule [144]

### 7.3 Results and discussion

The sequence steps for preparing PCMs microcapsules coated with silver metal is shown in Figure 7.1a. The surface of PCM microcapsules was functionalized using polydopamine followed by electroless plating of silver. Polydopamine is synthesised easily by oxidative self-polymerization of dopamine in a tris solution under basic conditions. Dopamine was added to tris solution and the pH was adjusted to 8.5. The colour of the dopamine solution quickly changed from colourless to pink, indicating the catechol oxidized to benzoquinone. Eventually the pink solution turned to a deep dark [151].

Polydopamine has gained much attention recently as it has catechol and amino groups. These groups have the ability to coat several materials such as metals, ceramics, carbon nanotubes and polymers. PDA was successfully attached to the PCM microcapsules as can be seen by the dark distinctive layer and small fragments of PDA on the surface of RT21 microcapsules (Figure 7.3b). In order to investigate the effect of PDA on the promoted silver deposition, SEM photos of RT21/Ag microcapsules and RT21-PDA/Ag microcapsules were taken. SEM images showed distinctly, no appearance of Ag metal in the surface of PCMs microcapsules when the microcapsules have not treated with PDA (Figure 7.3c). However, PCMs microcapsules were completely covered with Ag metal when the PCMs microcapsules have functionalized with PDA prior to the electroless plating of Ag (Figure 7.3d). Higher magnifications images shown in Figure 7.3 e and f confirmed the deposition of Ag across the whole surface of RT21-PDA microcapsules.

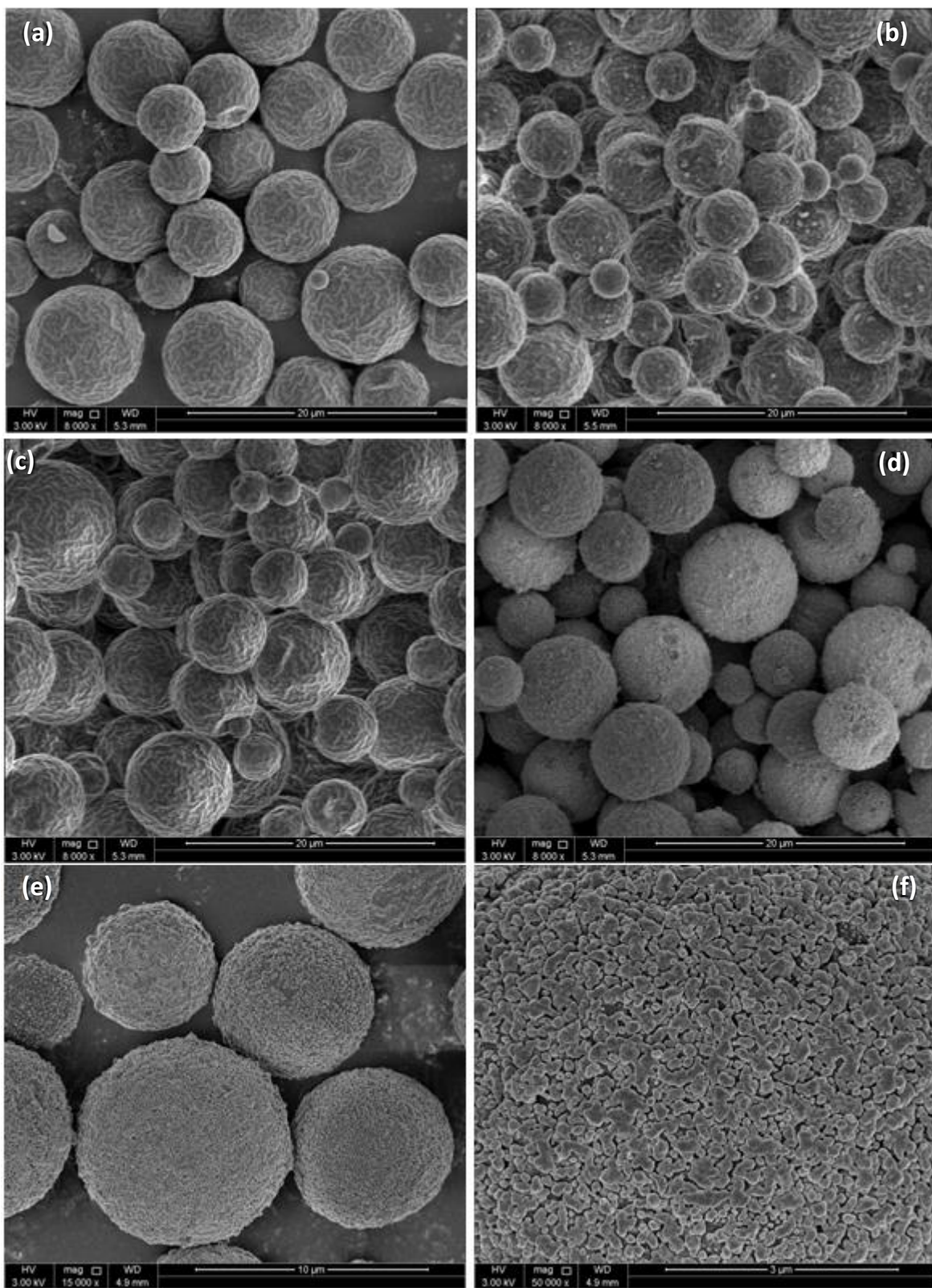


**Figure 7.3** SEM photos of (a) RT21 microcapsules, (b) RT21-PDA microcapsules, (c) RT21/Ag microcapsules, (d) RT21-PDA/Ag microcapsules-magnification 8000 x, (e) RT21-PDA/Ag microcapsules-magnification 15000x and (f) RT21-PDA/Ag microcapsules-magnification 50000x.

Energy dispersive X-ray spectroscopy (EDX) was used to determine the element compositions and concentrations on the surface of RT21 microcapsules before and after metal coating as shown in Figure 7.4. The resulting spectrum and tabulated results in Figure 7.4b reveal that C, O, and Ag are the elements present with Ag being the highest weight percent in RT21-PDA/Ag microcapsules surface as much as 70.45 wt. %. However, C and O peaks only detected as shown in Figure 7.4a with C being the most abundant in the RT21 microcapsules surface. These results are in agreement with what is observed in Figure 7.3.

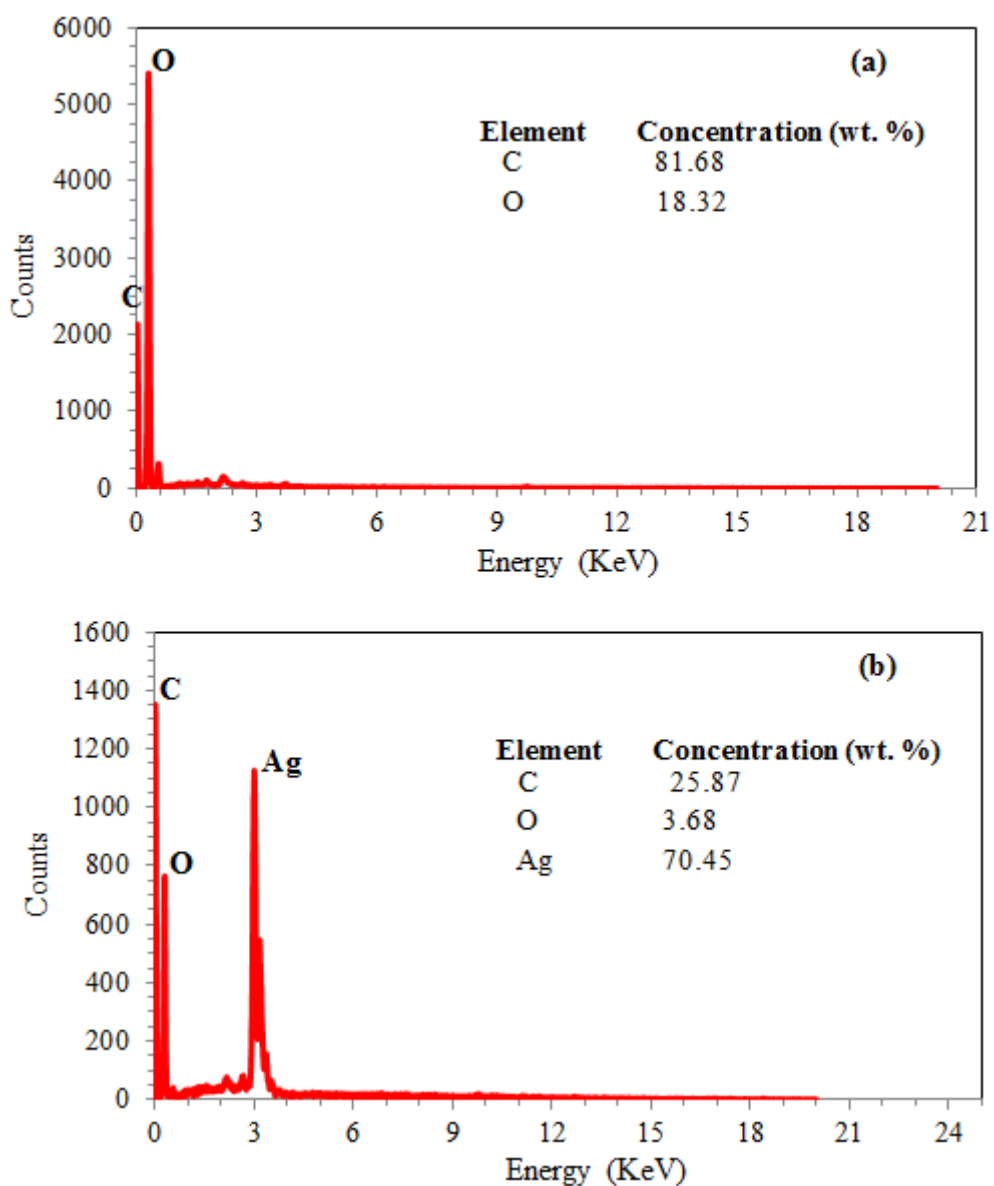


**Figure 7.4** EDX patterns of (a) RT21 microcapsules and (b) RT21-PDA/Ag microcapsules

Thermal properties of RT21 microcapsules and RT21-PDA/Ag microcapsules in terms of phase transition temperatures and heat storage capacities are shown in Figure 7.5. Insignificant changes in phase transition temperature were observed due to metal coating of

RT21 microcapsules. However, the latent heat of RT21 microcapsules dropped from 91.2 to 62.7 J/g when it is coated with Ag.

In practical applications especially in building application, the occupied volume of PCMs microcapsules is concerned rather than mass. Latent heat of fusion per unit volume for PCMs microcapsules and PCMs microcapsules metal coated was calculated and reported in Table 7.1. The latent heat of fusion of RT21 microcapsules decreased by 31% (based on the mass) and only 13.7 % (based on the volume) when it is coated with Ag.

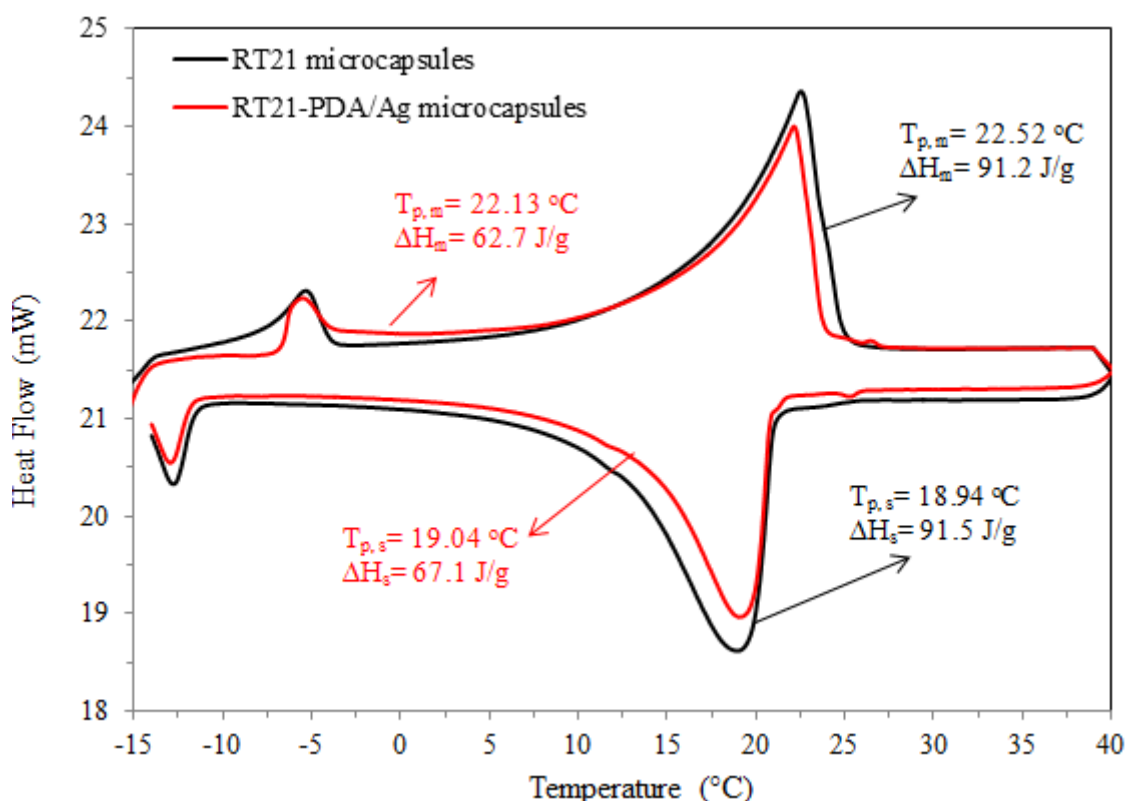


**Figure 7.5** DSC curves of RT21 microcapsules and RT21-PDA/Ag microcapsules

**Table 7.1** Thermal and physical properties of PCMs microcapsules

Product name	$\Delta H_m$ (J/g)	% dropped in $\Delta H_m$ (J/g)	Density (g/ml)	$\Delta H_m$ (J/ml)	% dropped in $\Delta H_m$ (J/ml)
RT21 microcapsules	91.2	31	0.4966	45.3	13.7
RT21-PDA/Ag microcapsules	62.9		0.6213	39.1	
24-D microcapsules	123.3	28.6	0.4576	56.4	9.2
24-D-PDA/Ag microcapsules	88		0.5814	51.2	

Currently there are several commercially available PCMs microcapsules on the market such as Microtek MPCM-24D, which are suitable for building applications due to their melting temperatures being within the range of human comfort temperatures (18-30 °C). The polymer shell of 24-D microcapsules is made from melamine-formaldehyde resin as mentioned in the MSDS sheet, so it is valuable to study the applicability of using the electroless plating technique to coat different types of polymer shells with Ag. Figure 7.6 shows the surface morphology of 24D microcapsules before and after silver coating. PDA as binding agent for metal coating was successfully attached to the surface of 24D microcapsules as can be seen by PDA fragments (Figure 7.6b). Continuous and compact silver shells were seen on the 24D microcapsules surface as shown in Figure 7.6 c, d and e. It seems that PDA assisted electroless plating could provide a successful coating technique to different kind of polymers. The shell and metal layer thickness of 24D-PDA/Ag microcapsules were measured as 450.6 and 175.9 nm respectively as shown in Figure 7.6 f.

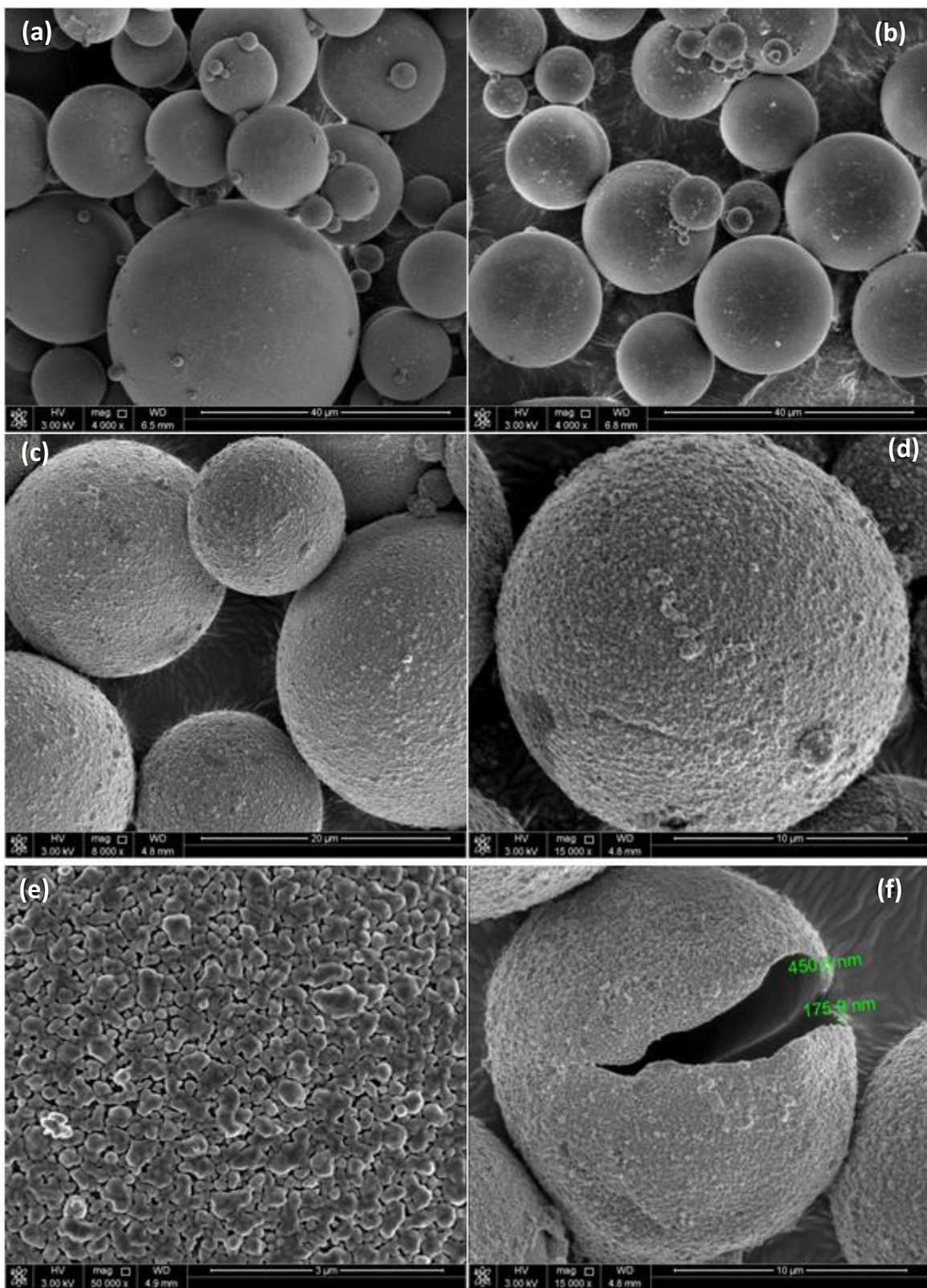


**Figure 7.6** SEM images of (a) 24D microcapsules, (b) 24D-PDA microcapsules, (c, d and e) 24D-PDA/Ag microcapsules with different magnifications and (f) broken 24D-PDA/Ag microcapsules with shell and Ag layer thickness of 450.6 and 175.9 nm respectively.

Studying the mechanical strength of metal coated PCM microcapsules is required in many applications such as in building, the shell of PCM microcapsules needs to have enough robustness to a void shell rupturing during mixing with building materials. Also, when PCM microcapsules are used in slurry to improve thermal performance of heat exchanger, these microcapsules need to sustain the high shear caused by pumping the suspension. Aforementioned in the literature, the mechanical strength of PCM microcapsules is determined by their chemical composition, structure, size and shell thickness [64]. In the present study, double shell polymer-metal coated PCM microcapsules were produced in an attempt to improve the shell mechanical strength. Nanocompression test were carried out to measure the force required to burst a single microcapsule. Single shell microcapsules (24D) and double shell microcapsules (24D/Ag) were placed and glued on the surface of epoxy stub separately and then nanocompression tests were performed on a single microcapsule. Figure 7.7 shows the Load vs. displacement curve of blank epoxy resin, which gives an indication of typical nanocompression curve. Blank substrate samples made from epoxy resin was also tested to determine when the microcapsule had been ruptured by knowing the fingerprint of the substrate curve.

In Figure 7.8 the lines from A to B and A to D refer to the compression load on the single and double shell microcapsule before shell deformation. Point B (0.45 mN, 524.6 nm) and D (6.6 mN, 2367.3 nm) are the starting points of the shell deformation of the single and double shell microcapsules respectively. The starting deformation force and the corresponding displacement of the inner polymer shell of the double shell microcapsules were increased dramatically in comparison to the single polymer shell microcapsule (Figure 6). The metal outer shell of the microcapsules protects the inner polymer shell from deformation in the early stage of applying load.

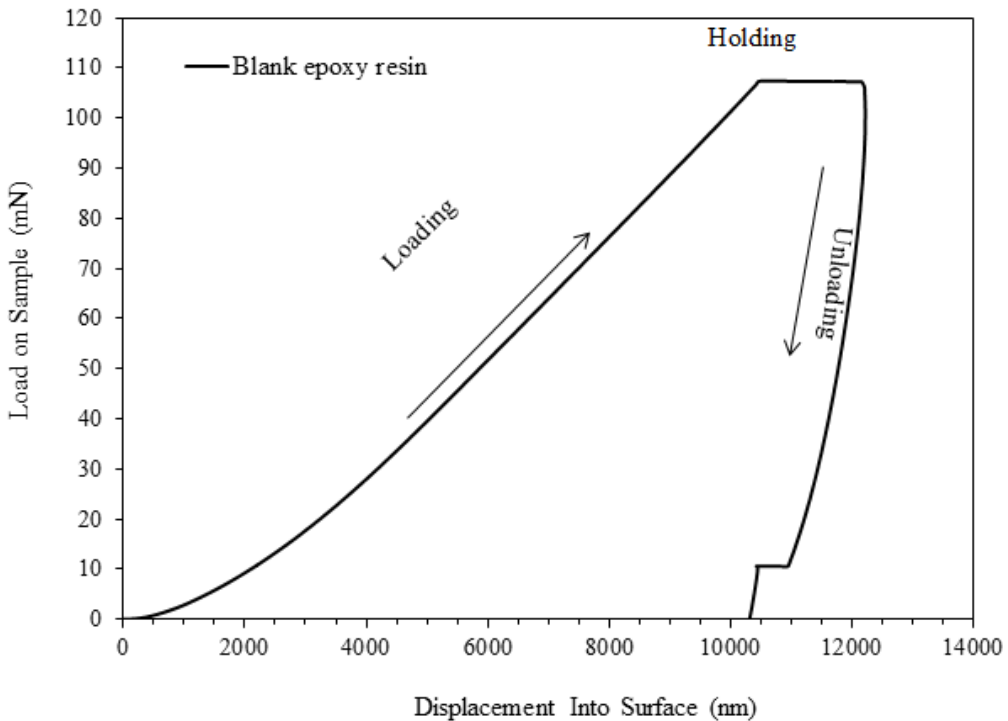


**Figure 7.7** Force vs. Displacement curve for the nanoindentation of blank epoxy resin, with a  $10\mu\text{m}$  radius Diamond conical tip.

When a viscoelastic material is subjected to constant load, it deforms with time with the rate of this deformation known as creep rate which gives an indication about the materials viscous response to force overtime. Stiffer samples tend to show lower creep rates than less stiff samples and by looking at the lines from B to C and D to E vs time the creep portion of both the single and double shell microcapsules can be estimated. The silver coated microcapsules show a much higher creep rate than the uncoated shells, indicating more energy is being absorbed and thus the silver coatings have a higher toughness value. The coated shells also indicate a two part failure mechanism with the rupture of the inner polymer shell occurring at 6.6 mN (indicating by point E on Figure 7.8) and final failure occurring at 20.55 mN (point F) which is 45 times higher than the uncoated shell which ruptured at the much lower force of 0.45 mN shown by point C on Figure 7.8. These results indicate that the addition of silver coating to the polymer coating provides significant mechanical enhancement and that the shell rupture occurs through a two stage process consisting of inner polymer shell failing first followed by the outer metal shell rupturing.

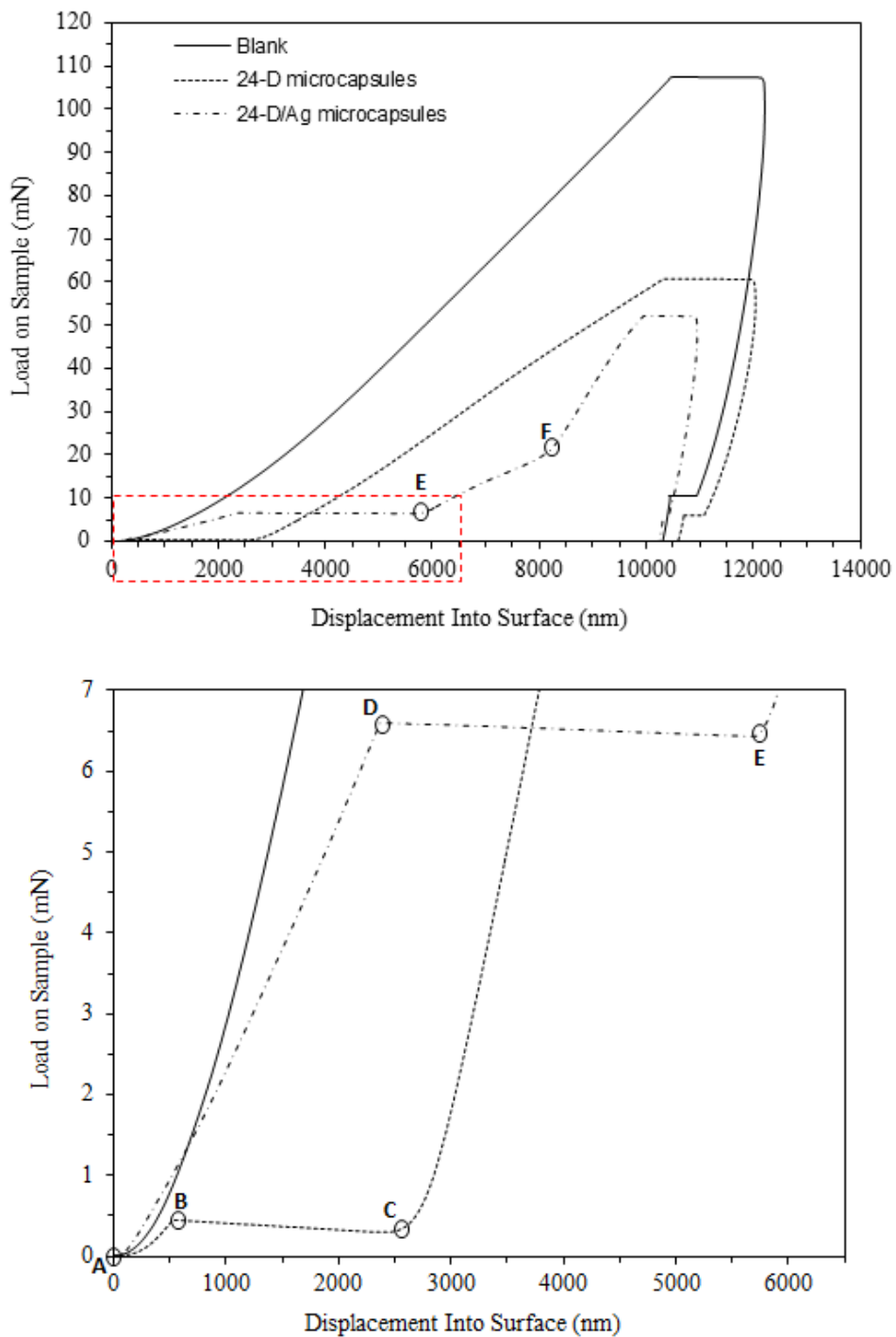


**Figure 7.8** Force vs. Displacement curve for the nanoindentation of blank epoxy resin, 24D and 24D/Ag microcapsules.

To confirm that the shifts on the load displacement curves correlated to shell rupture, optical microscope images were taken before indentation and immediately after. Figure 7.9 shows example of this using the single polymer shell (24D microcapsules). It is evident from image (a) in Figure 7.9 that the microcapsule is intact and spherical in shape, however after compression the dark shadow on the image indicates that the microcapsule has been ruptured

and lost its uniform shape as shown in Figure 7.9 (b). Figure 7.10 shows an increase in the diameter of the double shell microcapsule due to compression without any rupture unlike what could be seen in Figure 7.9. When these observations are correlated with the matching force vs. displacement curves (Figure 7.8) they indicate that the mechanical strength of the PCM microcapsules is enhanced significantly when coated with silver.

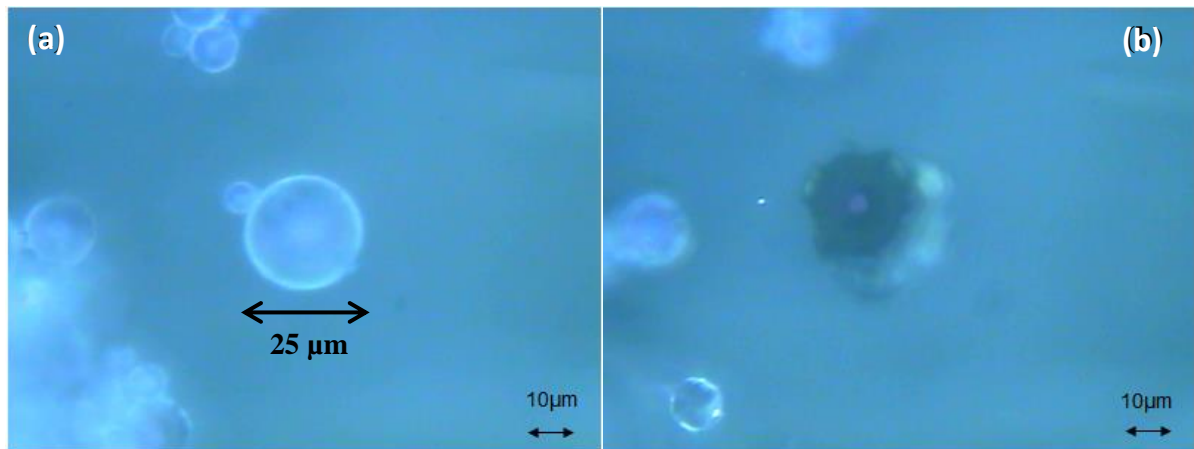


**Figure 7.9** Optical microscope images of 24D microcapsule (a) before compression and (b) after compression

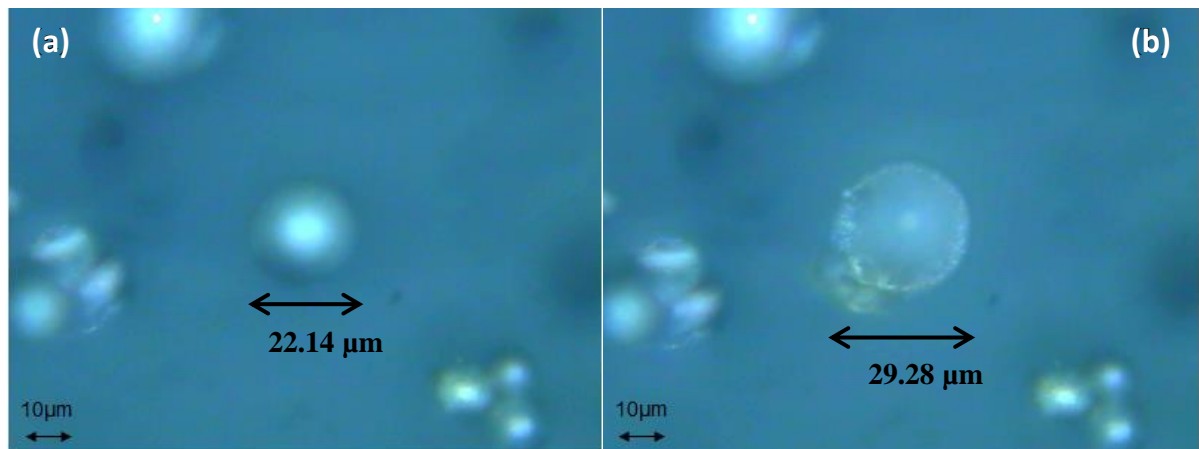


**Figure 7.10** Optical microscope images of 24-D/Ag microcapsule (a) before compression and (b) after compression

# **Microencapsulation of Fatty Acids, Fatty Acid Esters, Fatty Alcohols and Paraffin**

**8**

## **8.1 Field of the invention**

The present invention relates to a process for microencapsulating compounds selected from fatty acids, fatty acid esters (including triglycerides), fatty alcohols, and paraffins, which may be useful as phase change materials (PCMs). The microencapsulated PCMs produced by the process are useful for thermal energy storage, and many other applications.

## **8.2 Background of the invention**

Phase change materials (PCMs) are materials that melt and solidify at a nearly constant temperature, and are capable of storing and releasing large amounts of energy when they undergo phase change. Heat is absorbed or released when the material changes between the solid and liquid phases at a certain temperature, the phase change temperature, and vice versa.

PCMs have many applications. They are commonly used to improve thermal performance of buildings, for example by use in walls, ceilings or flooring. Other applications include thermal protection, cooling (such as food storage coolers), air-conditioning, and for solar heating systems. PCMs are also used to keep the temperature of electronic devices relatively constant.

PCMs can be classified into three different types: organic, inorganic and eutectic compounds. Paraffins and non-paraffin compounds, including fatty acid esters, are two major groups of the organic phase change materials.

A challenge with PCMs, especially with PCMs undergoing phase change at ambient temperature, such as those used in buildings, is in containing them in an appropriate matrix. This is because organic PCMs have a tendency to leak or exude to the surface of the matrices in which they are contained, during the phase change process. This leads to the surface becoming oily and stained, and to the thermal storage properties of the PCM gradually diminishing.

One solution to preventing leakage of melted PCM during the phase change process is microencapsulation. Microencapsulation is a process of coating individual particles or droplets with a continuous film of a polymer or inorganic shell. Several physical and chemical methods have been used for the production of microcapsules [152].

Physical methods of microencapsulation include pan coating, air-suspension coating, centrifugal extrusion, vibrational nozzle, spray drying and solvent evaporation. Physico-chemical methods include ionic gelation, coacervation and sol-gel.

The chemical technique most commonly used for microencapsulation of PCMs is in situ polymerisation, which includes interfacial polymerisation, suspension polymerisation and emulsion polymerisation. These methods generally involve carrying out the polymerisation in an aqueous emulsion or suspension. For example, in suspension polymerisation a water-immiscible reaction mixture is suspended as droplets in an aqueous continuous phase. The droplets are formed through vigorous agitation of the mixture and dissolution of stabilisers in the aqueous phase. Polymerisation is then initiated at the desired temperature until completion.

The above methods of in situ polymerisation have some disadvantages. In particular, they are generally quite complex, the processing time required for making the microencapsulated PCMs is rather long, and a washing process to recover un-encapsulated PCM, surfactant and unreacted monomers is required. The aqueous phase at the end of the encapsulation process will contain some of the unreacted monomer, PCM and probably other chemicals, which would require wastewater treatment before disposal. The cost of manufacturing PCM microcapsules using these methods is accordingly rather high, and is an impediment to industrial application of microencapsulated PCMs. It would therefore be desirable to have a simpler, faster, and consequently less expensive method of producing microencapsulated PCMs, which is still effective in producing microcapsules that are stable and withstand thermal cycling without degradation.

WO 2005/097935 [153] and WO 2007/040395 [154] describe processes where monomers are polymerised in the presence of salt hydrate PCMs, but they do not mention fatty acids, fatty acid esters, fatty alcohols, or paraffin based PCMs. Also the processes described in these references generally require many hours to complete the reaction.

It is an object of the present invention to go at least some way towards providing a process of microencapsulating the above-mentioned PCMs that overcomes the disadvantages mentioned above of prior art processes involving the use of aqueous suspensions or emulsions, or at least to offer the public a useful choice.

### **8.3 Summary of the invention**

In a first aspect, the present invention provides a process for preparing a product comprising a fatty acid, fatty acid ester (including a triglyceride), fatty alcohol or paraffin encapsulated by an acrylate polymer, wherein the process comprises:

- (a) forming a reaction mixture by combining the following reactants: (i) a first reactant selected from the group consisting of fatty acids, fatty acid esters (including triglycerides), fatty alcohols and paraffins, (ii) an acrylate monomer, (iii) an acrylate cross-linking agent, and (iv) a polymerisation initiator, and
- (b) mixing the reactants at a temperature at which polymerisation of the acrylate monomer occurs, and continuing mixing until the polymerisation is complete;

Wherein the reaction mixture does not contain an aqueous phase and the reaction is not carried out in an aqueous suspension or emulsion.

In certain embodiments, the polymerisation initiator is added to the other reactants after combining the other reactants and heating them to a temperature at which polymerisation will occur on addition of the initiator.

In other embodiments, all of the reactants, including the initiator, are combined before heating the reaction mixture to a temperature at which polymerisation will occur.

In certain embodiments, the first reactant comprises a fatty acid ester selected from the group consisting of: tallow, hydrogenated tallow, methyl, ethyl, propyl and butyl tallow esters, methyl, ethyl, propyl and butyl palm oil esters, methyl, ethyl, propyl and butyl coconut oil esters, methyl, ethyl, propyl and butyl sunflower oil esters (including hydrogenated forms of any of the foregoing esters), methyl stearate, ethyl stearate, propyl stearate, butyl stearate, methyl palmitate, ethyl palmitate, propyl palmitate and butyl palmitate, triglycerides, and mixtures of any two or more of these. In particular embodiments, the fatty acid ester comprises tallow propyl ester.

In other embodiments, the first reactant may be a fatty alcohol, fatty acid, or paraffin (such as n-nonadecane or n-pentadecane).

In certain embodiments, the acrylate monomer is selected from the group consisting of methyl methacrylate, methyl acrylate, ethyl acrylate, 2-chloroethyl vinyl ether, 2-ethylhexyl acrylate, hydroxyethyl methacrylate, butyl acrylate, and butyl methacrylate, and mixtures of any two or more of these. In particular embodiments, the acrylate monomer comprises methyl methacrylate.

In certain embodiments, the acrylate cross-linking agent may be an acrylate monomer selected from the group consisting of ethylene glycol dimethacrylate, trimethylolpropane triacrylate, trimethylol propane trimethacrylate and pentaerythritol tetraacrylate, and mixtures of any two or more of these. In other embodiments, the cross-linking agent may be selected from the group consisting of ethylene glycol diacrylate, di (ethylene glycol) diacrylate, tetra (ethylene glycol) diacrylate, di (ethylene glycol) dimethacrylate, and tri (ethylene glycol) dimethacrylate, and mixtures of any two or more of these. In particular embodiments, the acrylate cross-linking agent comprises ethylene glycol dimethacrylate.

In certain embodiments, the polymerisation initiator comprises a free radical initiator, and may be selected from the group consisting of organic peroxides and azo compounds. In particular embodiments, the initiator is selected from benzoyl peroxide and 2, 2'-Azobis-(2, 4-dimethylvaleronitrile (ADVN).

In certain embodiments, the temperature of the reaction mixture at which polymerisation is initiated is in the range of about 60°C to about 100°C, such as about 70°C to about 97°C. In certain embodiments, the initiator comprises an organic peroxide and the temperature at which polymerisation is initiated is in the range of about 80°C to about 95°C. In other embodiments, the initiator comprises an azo compound and the temperature at which polymerisation is initiated is in the range of about 70°C to about 80°C.

In certain embodiments, the cross-linking agent is present in the reaction mixture in an amount of at least about 10 wt.%, based on the total combined weight of the first reactant, acrylate monomer, cross-linking agent and initiator present initially in the reaction mixture. In certain embodiments, the cross-linking agent is present in an amount of from about 10 wt.

% to 20 wt. %, such as from about 11 wt. % to about 18 wt. %, such as from about 12 wt. % to about 16 wt. %.

In certain embodiments, the fatty acid ester is present in the reaction mixture in an amount of up to about 80 wt. %, such as from about 60 wt. % to about 80 wt. %, such as from about 60 wt. % to about 75 wt. %, such as from about 60 wt. % to about 70 wt. %, based on the total combined weight of the first reactant, acrylate monomer, cross-linking agent and initiator present initially in the reaction mixture.

In certain embodiments, the acrylate monomer is present in the reaction mixture in an amount of from about 10 wt. % to about 20 wt. %, such as from about 12 wt. % to about 18 wt. %, such as from about 14 wt. % to about 16 wt. %, based on the total combined weight of the first reactant, acrylate monomer, cross-linking agent and initiator present initially in the reaction mixture.

In certain embodiments, the polymerisation initiator is present in the reaction mixture in an amount of from about 0.5 wt. % to about 1.5 wt. % based on the total combined weight of the first reactant, acrylate monomer, cross-linking agent and initiator present initially in the reaction mixture.

In certain embodiments, the process includes adding one or more additional compounds to the reaction mixture before polymerisation occurs. In particular embodiments, the additional compounds may be selected from the group consisting of graphite, fire retardants, nucleating agents, thermal conductivity enhancement materials, and foaming agents. In such embodiments, the reaction mixture consists of the first reactant, the acrylate monomer, the acrylate cross-linking agent, the polymerisation initiator and the additional compounds.

In other embodiments, the reaction mixture consists solely of the first reactant, the acrylate monomer, the acrylate cross-linking agent, and the polymerisation initiator.

In a further aspect, the invention provides a product comprising a fatty acid, fatty acid ester (including a triglyceride), fatty alcohol or paraffin, encapsulated by an acrylate polymer, obtained by or obtainable by a process according to the first aspect of the invention.

In a further aspect, the invention provides a composition for storing or removal of thermal energy, the composition comprising a fatty acid, fatty acid ester (including a triglyceride), fatty alcohol or paraffin, encapsulated by an acrylate polymer, obtained by or obtainable by a process according to the first aspect of the invention.

In a further aspect, the present invention provides a method of increasing thermal energy storage in a building or building material, the method including the step of incorporating into the building or building material a composition comprising a fatty acid, fatty acid ester (including a triglyceride), fatty alcohol or paraffin, encapsulated by an acrylate polymer, obtained by or obtainable by a process according to the first aspect of the invention.

As used in this specification, the term "fatty acid ester" is to be construed in its broadest sense, and is intended to encompass any type of ester that can be formed from the reaction of a fatty acid with any alcohol. For example, as used, herein, "fatty acid ester" includes, without limitation, monoglycerides, diglycerides and triglycerides, including triglycerides from natural fats and oils.

For the purposes of construing this specification and claims, when a method is described including a plurality of steps, those steps are not necessarily intended to be carried out in the chronological order that they are shown in, unless logic dictates that they need to be.

The term "comprising" as used in this specification means "consisting at least in part of". When interpreting statements in this specification that include that term, the features prefaced by that term in each statement all need to be present but other features can also be present. Related terms such as "comprise" and "comprised" are to be interpreted in the same manner.

To those skilled in the art to which the invention relates, many changes in construction and widely differing embodiments and applications of the invention will suggest themselves without departing from the scope of the invention. The disclosures and descriptions herein are illustrative only and are not intended to be in any sense limiting.

## **8.4 Description of the invention**

### **8.4.1 General description of process of the invention**

As defined above, the present invention relates to a process for preparing encapsulated fatty acids, fatty acid esters (including triglycerides), fatty alcohols and paraffins, which may be used as phase change materials, and may also have other applications. The applicants have unexpectedly invented a relatively simple, quick and effective process of encapsulating such materials (herein also referred to as "PCMs.") The encapsulated PCMs produced by the process of the invention have been found, at least in certain preferred embodiments, to be of high quality. In particular, they have a smooth and compact surface, a relatively high PCM content and have been found to be thermally stable under heating and cooling cycling processes. In addition, the process of the invention, at least in certain preferred embodiments, gives a relatively high materials recovery rate, e.g. up to 90%, or higher.

In general terms, the process of the invention involves preparing a reaction mixture by combining (i) a first reactant selected from fatty acids, fatty acid esters (including triglycerides), fatty alcohols and paraffins (herein the first reactant is also referred to as "PCM reactant") , (ii) an acrylate monomer, (iii) an acrylate cross-linking agent, and (iv) a polymerisation initiator. The reactants are then mixed at a temperature at which polymerisation of the acrylate monomer occurs, with the mixing being continued until the polymerisation is complete. The reaction produces a product comprising microcapsules, generally in the form of a light coloured powder, in which the PCM is encapsulated by an acrylate polymer.

In the process of the invention, the reaction mixture does not contain an aqueous phase and the reaction is not carried out in an aqueous suspension or emulsion. Instead, the inventive process involves simple mixing of the reactants together and carrying out the reaction in the resulting organic phase, which is generally initially in the form of a solution once the reaction mixture is heated to a temperature at which the polymerisation reaction is initiated. At least in certain preferred embodiments, the reactants may be substantially completely converted into encapsulated PCM product. As a consequence, it is not generally necessary to carry out significant further processing to recover un-encapsulated PCM reactant, surfactant and unreacted monomer. In certain embodiments, the product may be washed, for example in hot water, to remove any unreacted materials.

In the process of the invention, the polymerisation initiator may be added to the other reactants after combining the other reactants and heating them to a temperature at which polymerisation will occur on addition of the initiator. Alternatively, all of the reactants, including the polymerisation initiator, may be combined before heating the reaction mixture to a temperature at which polymerisation will occur.

Generally, as soon as the polymerisation reaction starts, additional heating is not required. The reaction is exothermic, so it will generate heat and raise the temperature of the reaction mixture, for example by about 20°C in a few seconds, and the reaction will be completed, typically in a matter of a number of seconds.

## **8.4.2 Components of the reaction mixture**

### **8.4.2.1 PCMs**

The particular PCM reactant to be used in the process of the invention will depend on the end use to which the product is intended to be put. If the encapsulated PCM is to be used in a thermal energy storage application, the desired phase transition temperature or melting point of the PCM will vary, depending on whether it is to be used in a building application or some other application. By way of example, for a building application, a fatty acid ester, having a phase transition temperature of between about 18°C to about 25°C, may be used.

In certain embodiments of the invention, the PCM reactant comprises a fatty acid ester selected from any of the following, and blends of any two or more of them: tallow, hydrogenated tallow, methyl, ethyl, propyl and butyl tallow esters, methyl, ethyl, propyl and butyl palm oil esters, methyl, ethyl, propyl and butyl coconut oil esters, methyl, ethyl, propyl and butyl sunflower oil esters (including hydrogenated forms of any of the foregoing esters), methyl stearate, ethyl stearate, propyl stearate, butyl stearate, methyl palmitate, ethyl palmitate, propyl palmitate and butyl palmitate, and triglycerides.

In other embodiments, the PCM reactant may comprise a fatty acid, fatty alcohol or paraffin. It is generally preferred that the PCM reactant is present in the reaction mixture in an amount of up to about 80 wt.%, based on the total combined weight of the PCM reactant, acrylate monomer, cross-linking agent and initiator present initially in the reaction mixture.

In other embodiments, the PCM reactant may be selected from the PureTemp™ (PT) thermal energy storage materials available from PureTemp, Entropy Solutions, Inc., such as PT24, PT4, PT6 and others.

#### **8.4.2.2 Acrylate monomer**

In principle, any type of acrylate monomer can be used in the process of the present invention, to form an acrylate polymer encapsulating the PCM reactant. Examples of acrylate monomers that may be used are: methyl methacrylate, methyl acrylate, ethyl acrylate, 2-chloroethyl vinyl ether, 2-ethylhexyl acrylate, hydroxyethyl methacrylate, butyl acrylate, and butyl methacrylate, and mixtures of any two or more of these.

It is generally preferred that the acrylate monomer is present in the reaction mixture in an amount of from about 10 wt.% to about 20 wt.% based on the total combined weight of the PCM reactant, acrylate monomer, cross-linking agent and initiator present initially in the reaction mixture.

#### **8.4.2.3 Cross-linking agent**

The cross-linking agent used in the process of the invention may in principle be any cross-linking acrylate monomer. Examples of such acrylate monomers are ethylene glycol dimethacrylate, trimethylolpropane triacrylate, trimethylol propane trimethacrylate and pentaerythritol tetraacrylate, ethylene glycol diacrylate, di (ethylene glycol) diacrylate, tetra (ethylene glycol) diacrylate, di (ethylene glycol) dimethacrylate, and tri (ethylene glycol) dimethacrylate, and mixtures of any two or more of these.

It is generally preferred that the cross-linking agent is present in the reaction mixture in an amount of at least about 5 wt.%, based on the total combined weight of the PCM reactant, acrylate monomer, cross-linking agent and initiator present initially in the reaction mixture. In certain embodiments, the cross-linking agent is present in an amount of from about 5 wt. % to 20 wt. %, such as about 10 wt. % to about 20 wt. %.

#### **8.4.2.4 Polymerisation initiator**

The polymerisation initiator used in the process of the invention may be any suitable type of thermal free radical initiator. For example, the initiator may be an organic peroxide or an azo

compound. Specific examples of suitable initiators are benzoyl peroxide and 2, 2'-Azobis-(2, 4-dimethylvaleronitrile (ADVN).

It is generally preferred that the polymerisation initiator is added to the reaction mixture in an amount of from about 0.5 wt. % to about 1.5 wt.%, based on the total combined weight of the PCM reactant, acrylate monomer, cross-linking agent and initiator present initially in the reaction mixture.

#### **8.4.2.5 Other additives**

If desired, one or more additional compounds may be added to the reaction mixture before polymerisation occurs, to alter the properties of the resulting product. Examples of additional compounds that may be added include graphite, other thermal conductivity enhancement materials, fire retardants, nucleating agents and foaming agents. Adding graphite, nano tube or metal particles will increase the thermal conductivity of the product. It is preferred that if graphite is used, it is in the form of a fine powder, which may be soaked in the fatty acid ester before the polymerisation reaction. Higher melting ester or fatty acid may also be used in small quantities to reduce super cooling.

#### **8.4.3 Process conditions**

The process of the invention may be carried out in any suitable vessel or reactor, for example as a batch process in a batch reactor. Alternatively, it may be carried out as a continuous process, using a continuous reactor selected from those known in the art. The reactor should allow for appropriate heating to initiate polymerisation. The reactor should also be able to provide a degree of mixing that is effective to maintain the reaction mixture in a substantially homogenous state throughout the reaction, which in turn will allow the polymerisation reaction to proceed substantially through to completion. The reactor should also desirably provide means of removing the solid product formed as a powder.

The process of the invention is generally carried out at a relatively low temperature. It will be appreciated that the precise optimal temperature at which the reaction is carried out will depend on the decomposition temperature of the particular initiator used. However, in general, the temperature of the reaction mixture at which polymerisation is initiated may range from about 60°C to about 100°C, such as about 70°C to about 97°C. If the initiator comprises organic peroxide, then the temperature at which polymerisation is initiated may

range from about 80°C to about 95°C. Alternatively, if the initiator is an azo compound, then the temperature at which polymerisation is initiated may be lower.

The polymerisation reaction proceeds quite rapidly. The exact reaction time will depend on the volume of the reaction mixture and other variables. However, by way of example, it has been found that when carried out in a small beaker-sized vessel, the reaction time generally ranges from about 12-55 seconds following the process of heating. If sufficient mixing is provided, the expected reaction time in industrial reactors will be similar.

## **8.5 WHAT WE CLAIM IS:**

1. A process for preparing a product comprising a fatty acid, fatty acid ester, fatty alcohol or paraffin encapsulated by an acrylate polymer, wherein the process comprises:
  - (a) forming a reaction mixture by combining the following reactants: (i) a first reactant selected from the group consisting of fatty acids, fatty acid esters (including triglycerides), fatty alcohols and paraffins, (ii) an acrylate monomer, (iii) an acrylate cross-linking agent, and (iv) a polymerisation initiator, and
  - (b) mixing the reactants at a temperature at which polymerisation of the acrylate monomer occurs, and continuing mixing until the polymerisation is complete;

Wherein the reaction mixture does not contain an aqueous phase and the reaction is not carried out in an aqueous suspension or emulsion.

2. A process according to claim 1, wherein the polymerisation initiator is added to the other reactants after combining the other reactants and heating them to a temperature at which polymerisation will occur on addition of the initiator.
3. A process according to claim 1, wherein all of the reactants, including the initiator, are combined before heating the reaction mixture to a temperature at which polymerisation will occur.
4. A process according to any one of the preceding claims, wherein the first reactant comprises a fatty acid ester selected from the group consisting of: tallow, hydrogenated tallow, methyl, ethyl, propyl and butyl tallow esters, methyl, ethyl, propyl and butyl palm oil esters, methyl, ethyl, propyl and butyl coconut oil esters, methyl, ethyl, propyl and butyl sunflower oil esters (including hydrogenated forms of

any of the foregoing esters), methyl stearate, ethyl stearate, propyl stearate, butyl stearate, methyl palmitate, ethyl palmitate, propyl palmitate and butyl palmitate, triglycerides, and mixtures of any two or more of these.

5. A process according to any one of claims 1 to 3, wherein the first reactant comprises a fatty alcohol, fatty acid, or paraffin (such as n-nonadecane or n-pentadecane).
6. A process according to any one of the preceding claims, wherein the acrylate monomer is selected from the group consisting of methyl methacrylate, methyl acrylate, ethyl acrylate, 2-chloroethyl vinyl ether, 2-ethylhexyl acrylate, hydroxyethyl methacrylate, butyl acrylate, and butyl methacrylate, and mixtures of any two or more of these.
7. A process according to any one of the preceding claims, wherein the acrylate monomer comprises methyl methacrylate.
8. A process according to any one of the preceding claims, wherein the acrylate cross-linking agent comprises an acrylate monomer selected from the group consisting of ethylene glycol dimethacrylate, trimethylolpropane triacrylate, trimethylol propane trimethacrylate and pentaerythritol tetraacrylate, and mixtures of any two or more of these. In other embodiments, the cross-linking agent may be selected from the group consisting of ethylene glycol diacrylate, di (ethylene glycol) diacrylate, tetra (ethylene glycol) diacrylate, di (ethylene glycol) dimethacrylate, and tri (ethylene glycol) dimethacrylate, and mixtures of any two or more of these.
9. A process according to any one of the preceding claims, wherein the acrylate cross-linking agent comprises ethylene glycol dimethacrylate.
10. A process according to any one of the preceding claims, wherein the polymerisation initiator comprises a free radical initiator, and is selected from the group consisting of organic peroxides and azo compounds.
11. A process according to any one of the preceding claims, wherein the temperature of the reaction mixture at which polymerisation is initiated is in the range of about 60°C to about 100°C, such as about 70°C to about 97°C.

12. A process according to any one of the preceding claims, wherein the initiator comprises organic peroxide and the temperature at which polymerisation is initiated is in the range of about 80°C to about 95°C.
13. A process according to claim 12, wherein the initiator comprises benzoyl peroxide.
14. A process according to any one of claims 1 to 11, wherein the initiator comprises an azo compound and the temperature at which polymerisation is initiated is in the range of about 70°C to about 80°C.
15. A process according to claim 14, wherein the initiator comprises 2, 2'-Azobis-(2, 4-dimethylvaleronitrile (ADVN).
16. A process according to any one of the preceding claims, wherein the cross-linking agent is present in the reaction mixture in an amount of at least about 5 wt. %, based on the total combined weight of the first reactant, acrylate monomer, cross-linking agent and initiator present initially in the reaction mixture.
17. A process according to any one of the preceding claims, wherein the cross-linking agent is present in an amount of from about 5 wt. % to 20 wt. %.
18. A process according to any one of the preceding claims, wherein the first reactant is present in the reaction mixture in an amount of from about 60 wt. % to about 80 wt. %, based on the total combined weight of the first reactant, acrylate monomer, cross-linking agent and initiator present initially in the reaction mixture.
19. A process according to any one of the preceding claims, wherein the acrylate monomer is present in the reaction mixture in an amount of from about 10 wt. % to about 20 wt. %, based on the total combined weight of the first reactant, acrylate monomer, cross-linking agent and initiator present initially in the reaction mixture.
20. A process according to any one of the preceding claims, wherein the polymerisation initiator is present in the reaction mixture in an amount of from about 0.5 wt.% to about 1.5 wt.% based on the total combined weight of the first reactant, acrylate monomer, cross-linking agent and initiator present initially in the reaction mixture.

21. A process according to any one of the preceding claims, wherein the process includes adding one or more additional compounds to the reaction mixture before polymerisation occurs, wherein said additional compounds are selected from the group consisting of graphite, fire retardants, nucleating agents, thermal conductivity enhancement materials, and foaming agents.
22. A process according to any one of claims 1 to 20, wherein the reaction mixture consists solely of the first reactant, the acrylate monomer, the acrylate cross-linking agent, and the polymerisation initiator.
23. A product comprising a fatty acid, fatty acid ester (including a triglyceride), fatty alcohol or paraffin, encapsulated by an acrylate polymer, obtained by or obtainable by a process according to any one of the preceding claims.
24. A composition for storing or removal of thermal energy, the composition comprising a fatty acid, fatty acid ester (including a triglyceride), fatty alcohol or paraffin, encapsulated by an acrylate polymer, obtained by or obtainable by a process according to any one of claims 1 to 22.
25. A method of increasing thermal energy storage in a building or building material, the method including the step of incorporating into the building or building material a composition comprising a fatty acid, fatty acid ester (including a triglyceride), fatty alcohol or paraffin, encapsulated by an acrylate polymer, obtained by or obtainable by a process according to any one of claims 1 to 22.

## **8.6 Experimental**

### **8.6.1 Batch Reactions**

The batch reactions were carried out in a glass beaker that was heated by a hot plate. Known amounts of monomer (methyl methacrylate), cross-linker (ethylene glycol dimethacrylate) and PCM (tallow propyl ester) were combined in a beaker using a magnetic stirrer. The mixture was heated to around 85°C. The initiator (benzoyl peroxide) was added and the stirring was continued. The temperature at which the clear reacting mixture turned cloudy, the start temperature, was recorded and the stopwatch was started at the same time. The temperature and time at which all the PCM was encapsulated were recorded. The product was

then collected for testing. The experiment was then repeated by combining all of the reactants and PCM in the beaker before they were heated until the reaction occurred. The experiment was then repeated using different weight percentages of the reacting chemicals and PCM. Next the experiment was repeated several times using the other cross-linkers (trimethylolpropane triacrylate, trimethylolpropane trimethacrylate and pentaerythritol tetraacrylate) available, PT 24 (PT 24 is a PCM that is commercially available from PureTemp, Entropy Solutions, Inc. and is in the form of a clear liquid, waxy solid having a melting point of 24°C and a heat storage capacity of 185 J/g) and the low temperature initiator (ADVN). The reaction was then carried out with no mixing, the temperatures and time recorded and the product collected. A further experiment was conducted where the PCM and other reactants were heated separately before being combined for the reaction to occur.

## **8.6.2 Product testing**

### **8.6.2.1 Differential Scanning Calorimeter (DSC)**

Phase change properties of the fabricated PCM microcapsules were determined using a SHIMADZU DSC-60 differential scanning calorimetry. The measurements were performed by varying the temperature from -15 to 40 °C with heating and cooling rate of 3 °C/min.

### **8.6.2.2 Scanning Electron Microscopy (SEM)**

The product PCMs microcapsules morphology was examined using a scanning electron microscope (SEM) (Philips XL30S FEG, Netherland) operating under low vacuum pressure of 0.9 torr. All samples were coated with gold prior to the investigation.

### **8.6.2.3 Thermal Cycling**

Accelerated thermal cycling experiments of PCM microcapsules were performed in a controlled heating/cooling water bath at temperatures cycling between 10 and 40 °C (Figures 5.1 and 5.2)

## **8.7 Results and Discussion**

Table 8.1 and Figure 8.1 summarise the results obtained for the encapsulation of PT24. The results show that the average reaction starting temperature when using the benzoyl peroxide initiator is 96.5°C and the average reaction starting temperature when using the ADVN initiator is 71.5°C. Even though using the benzoyl peroxide requires more energy for the

reaction to start, it is still the preferred initiator because the ADVN initiator is more expensive and more difficult to source. It is clear that changing the chemical composition or the type of cross-linker and PCM used, has a minimal effect on the starting temperature of the reaction. Whether the initiator is added before heating the reacting mixture, is added after the mixture has been heated or the PCM and other reacting chemicals are heated separately before being mixed has little effect on the reaction time and reaction starting temperature. The reaction time is slightly longer if the initiator is added after heating the other reacting chemicals because the initiator powder has to be dissolved first. The reaction time ranges from 12 to 55 seconds. The reaction time when using the ADVN initiator is significantly less than when using the benzoyl peroxide initiator. Increasing the initiator concentration decreases the reaction finishing temperature and the reaction time. Increasing the PCM concentration increases the reaction time and increasing the cross-linker concentration generally decreases the reaction finishing temperature as well as decreasing the reaction time. The type of PCM used in the batch reactions has no significant effect on the reaction starting or finishing temperature or the reaction time. When the batch reaction is carried out using no mixing, it results in incomplete encapsulation. One gram of fine graphite powder was added to three of the batch reaction to increase the thermal conductivity of the powder. Using a finer graphite powder increases the thermal conductivity of the product produced. When using the ester soaked graphite in the batch reactions, it is difficult to determine the starting and finishing temperature as well as the reaction time because the reacting mixture is no longer clear and the start of the liquid clouding cannot be determined. During the batch reactions some of the chemicals, the cross-linker and monomer, are evaporated when the mixture is heated above 70°C causing the PCM content of the product to increase as reported in Table 8.1.

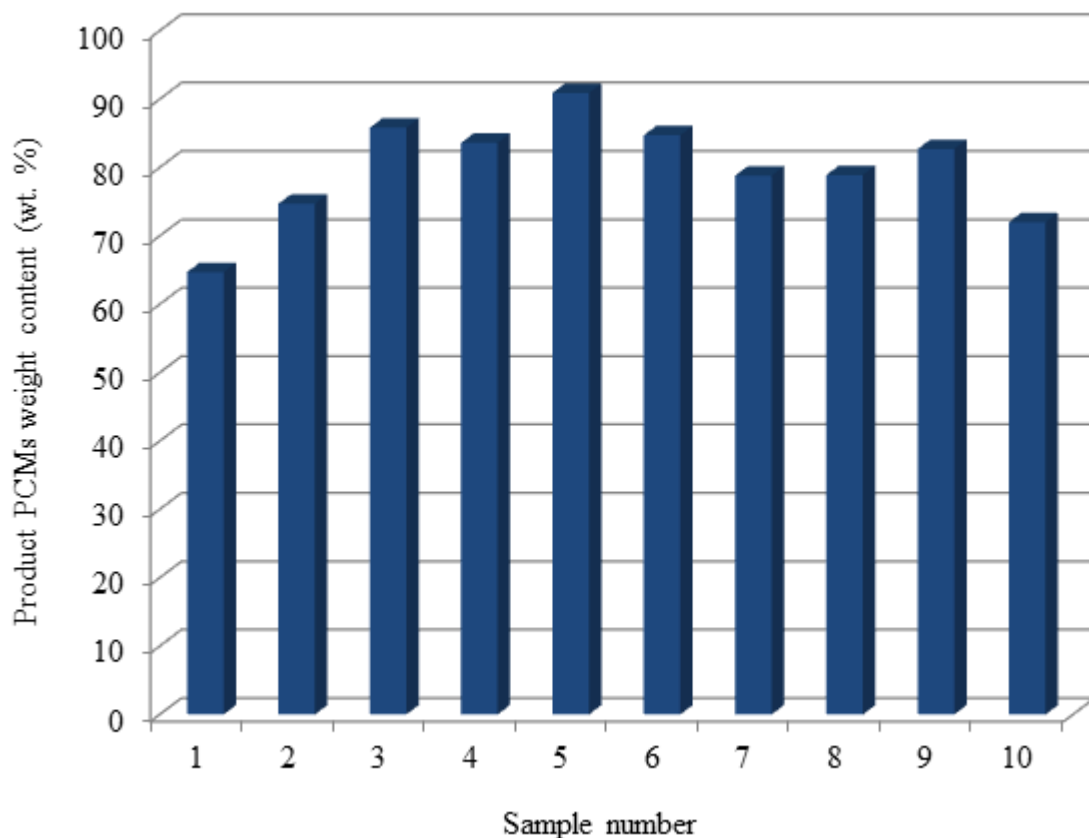


**Figure 8.1** Product PCMs weight content vs. sample number as reported in the Table 8.1

Several samples were tested using a differential scanning calorimeter in order to determine the effective latent heat of the samples as well as to get an estimate of the samples' PCM content after the batch reactions were completed. Figure 8.1 and Tables 8.1 summarise the results. The DSC graphs of the samples are included in the appendix 8.8. The estimated PCM content of the samples is the ratio of the sample's effective latent heat to that of the PCM on its own multiplied by a hundred. From Tables 8.1, it is clear that some of the samples' PCM content is significantly more than at the start of the batch reaction. This increase in PCM content is due to the fact that some of the cross-linker and monomer is evaporated during the reaction. After the encapsulation reaction, the samples produced still have a large effective latent heat suitable for thermal energy storage. According to the DSC results, the encapsulated products made range from a PCM content of 64.7 wt. % up to 90.9 wt. %. However, Table 8.1 shows that products with encapsulation more than 80 % may not be of good quality as they were found to be wet indicating that some of the PCM is not encapsulated.

**Table 8.1** Summarised results of PT24 microcapsules

Sample number	Monomer (MMA) (g)	Cross linking agent (EGDM) (g)	PCMs (PT24) (g)	Initiator (BPO) (g)	Latent heat of fusion (J/g)	Initial PCMs weight content (wt. %)	Product PCMs weight content (wt. %)	Product quality
1	3.3	3.3	15	0.4	98.9	68	64.7	dry/good
2	<b>10</b>	<b>10</b>	<b>45</b>	<b>1.2</b>	<b>114.2</b>	<b>68</b>	<b>74.7</b>	<b>dry/good</b>
3	10	10	50	1.2	131.1	70.2	85.8	wet
4	10	10	75	1.2	127.7	78	83.6	very wet
5	10	3	30	0.6	138.8	68.8	90.9	very wet
6	5	10	45	0.6	129.3	74.3	84.7	wet
7	10	8	45	1	120.3	70.3	78.8	wet
8	10	10	45	1	120.6	68.2	78.9	dry/good
9	3.3	3.3	15	0.3	126.4	68.2	82.7	dry/good
10	160	160	720	16	110	68.2	72	dry/good

$$\Delta H_m (\text{PT24}) = 152.8 \text{ J/g.}$$

$$\text{Initial PCMs weight content (wt. \%)} = \frac{\text{mass of PCMs}}{\text{total mass}} \times 100\% \quad (\text{Total mass} = \text{mass of MMA} + \text{mass of EGDM} + \text{mass of PCM} + \text{mass of BPO})$$

$$\text{Product PCMs weight content (wt. \%)} = \frac{\Delta H_{MPCM}}{\Delta H_{PCM}} \times 100\% \quad (\Delta H_{MPCM} \text{ is the latent heat of PCM microcapsules (J/g) and } \Delta H_{PCM} \text{ is the latent heat of PT24 (J/g)})$$

SEM photographs of cross-linked PMMA without PCM and encapsulated PCMs (sample 2) were taken and can be seen in the Figure 8.2. Figure 8.2 b and c shows a rough surface covered with small spherical particles. The particles are clumped together and appear to be porous. The surface of some of the samples before and after cycling appears similar indicating good stability over cycling as shown in Figure 8.3.

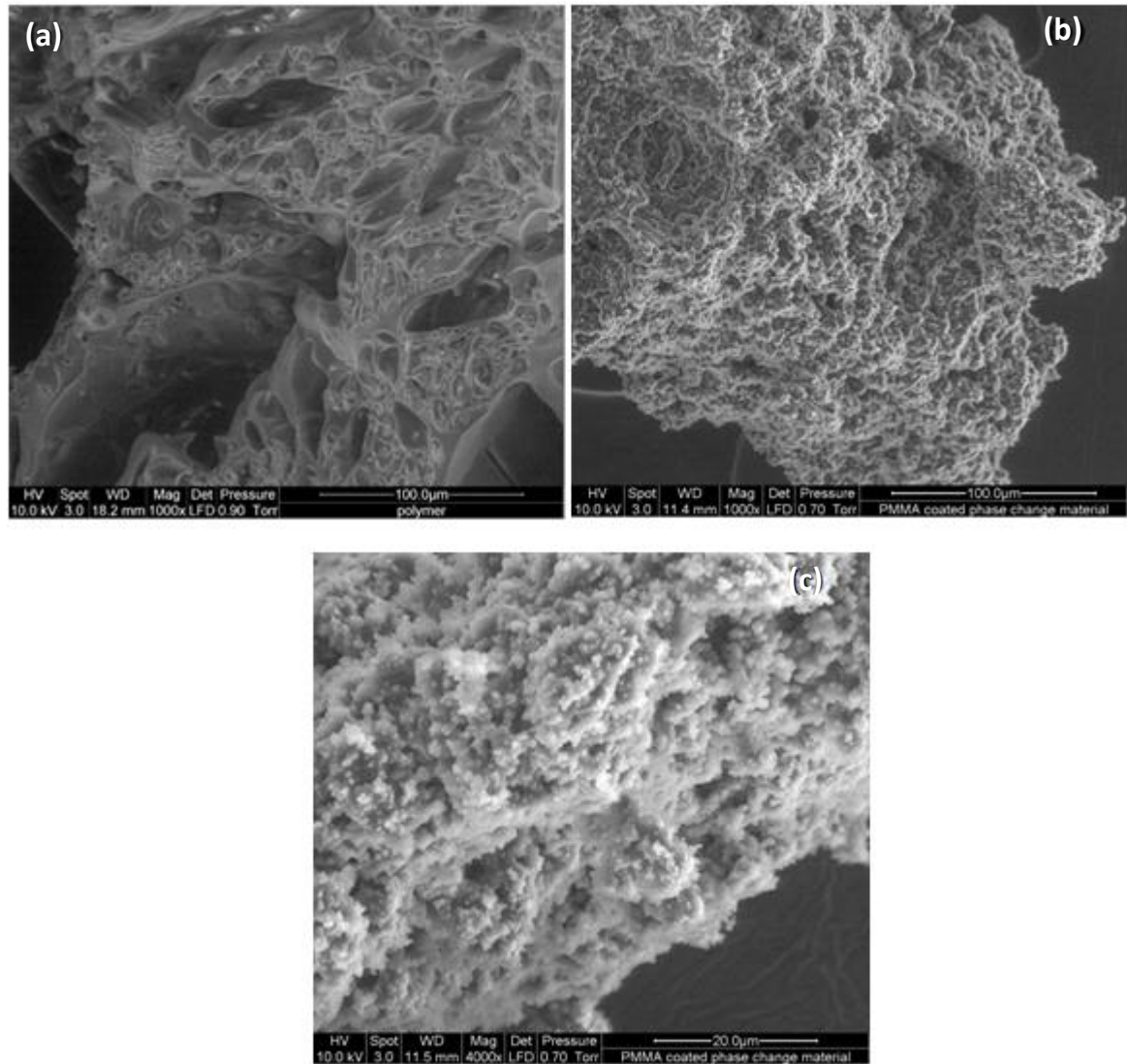


**Figure 8.2** SEM images of: (a) Cross-linked PMMA (without PCMs) and (b and c) PT24 capsules (sample 2) with different magnifications

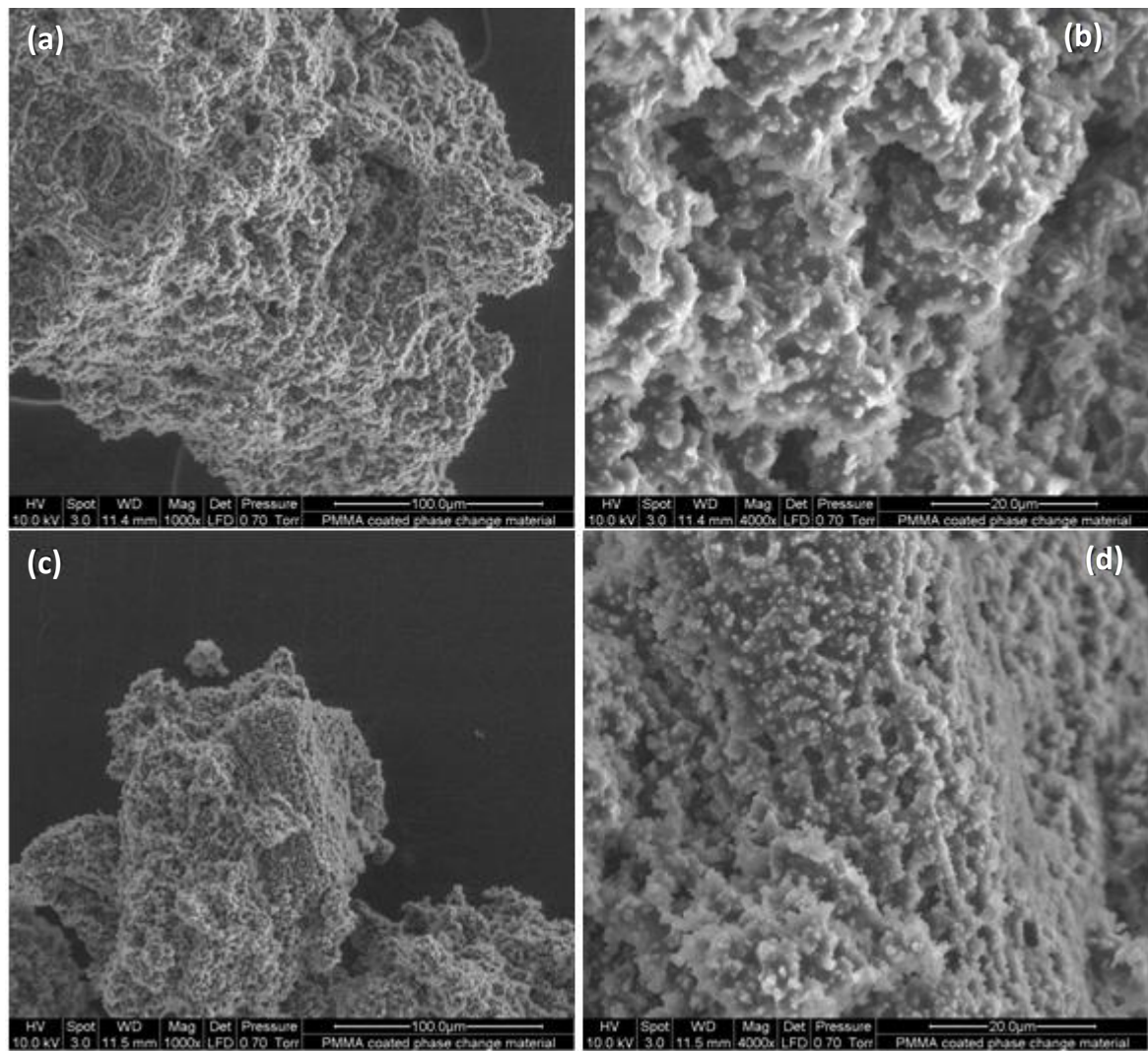


**Figure 8.3** SEM images of PT24 capsules (sample 2) at different positions after 50 thermal cycles (a and b) position 1 and (c and d) position 2

Samples were added to a controlled temperature water bath and were cycled between 10 and 40°C. The temperatures were recorded using an electronic data logger. Figure 8.4 is a graph illustrating the thermal cycling of PT24 microcapsules (sample 2). The figure shows that clear reduction in the temperature change of the sample near the transition temperatures of PT24 (20-24°C). It also shows that the encapsulated product is very stable over very large number of cycles (only a few were shown for clarity).

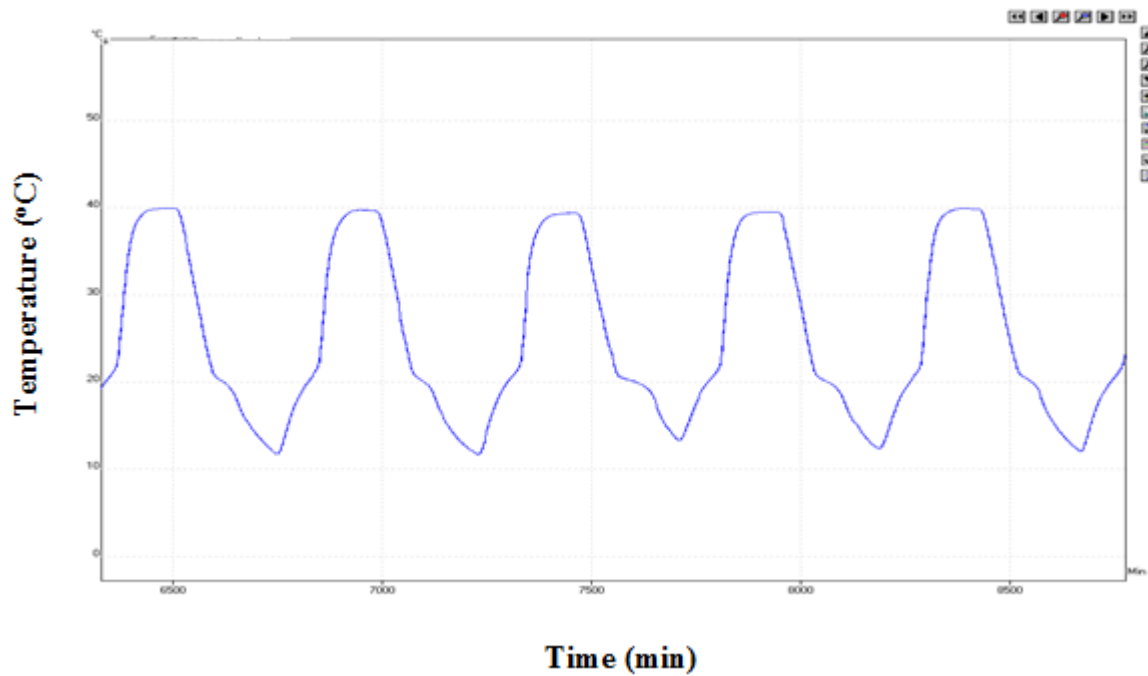


**Figure 8.4** Thermal cycling test of sample 2

## 8.8 Appendix (DSC curves of some selected samples)

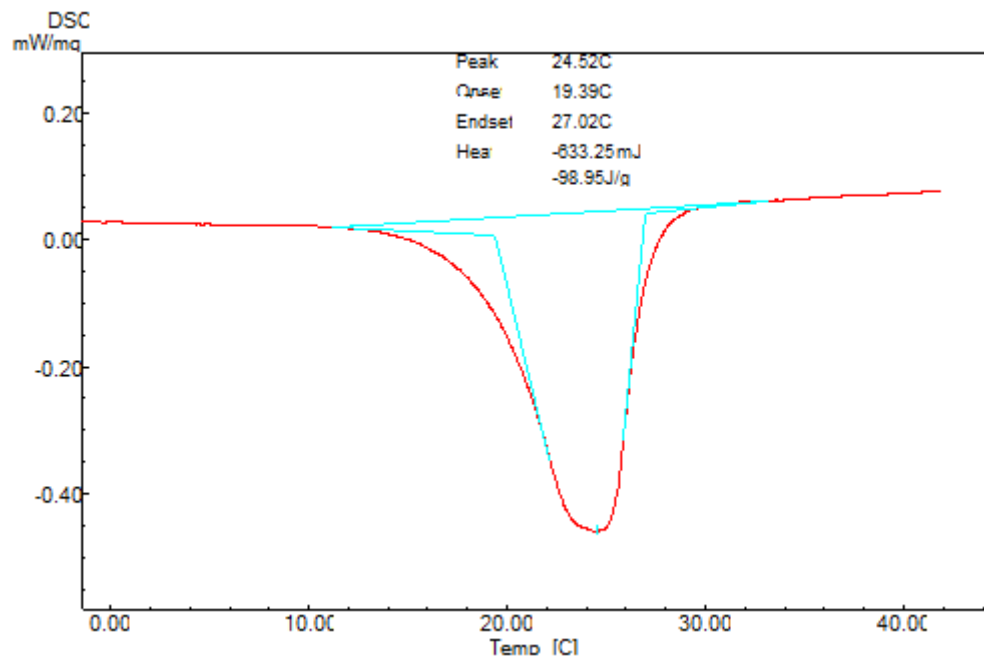


**Figure 8.5** DSC curve of sample 1

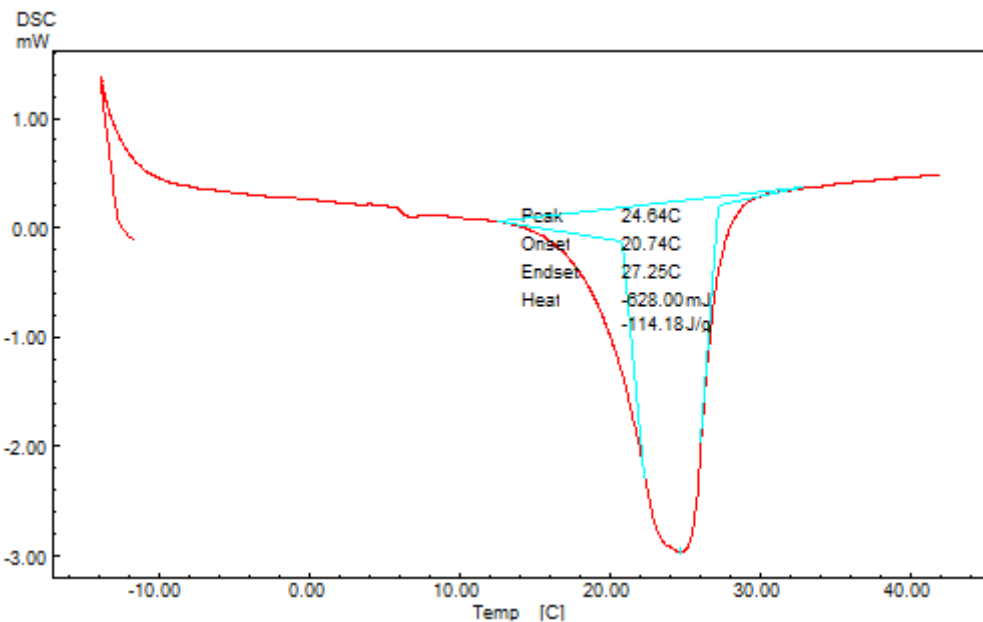


**Figure 8.6** DSC curve of sample 2

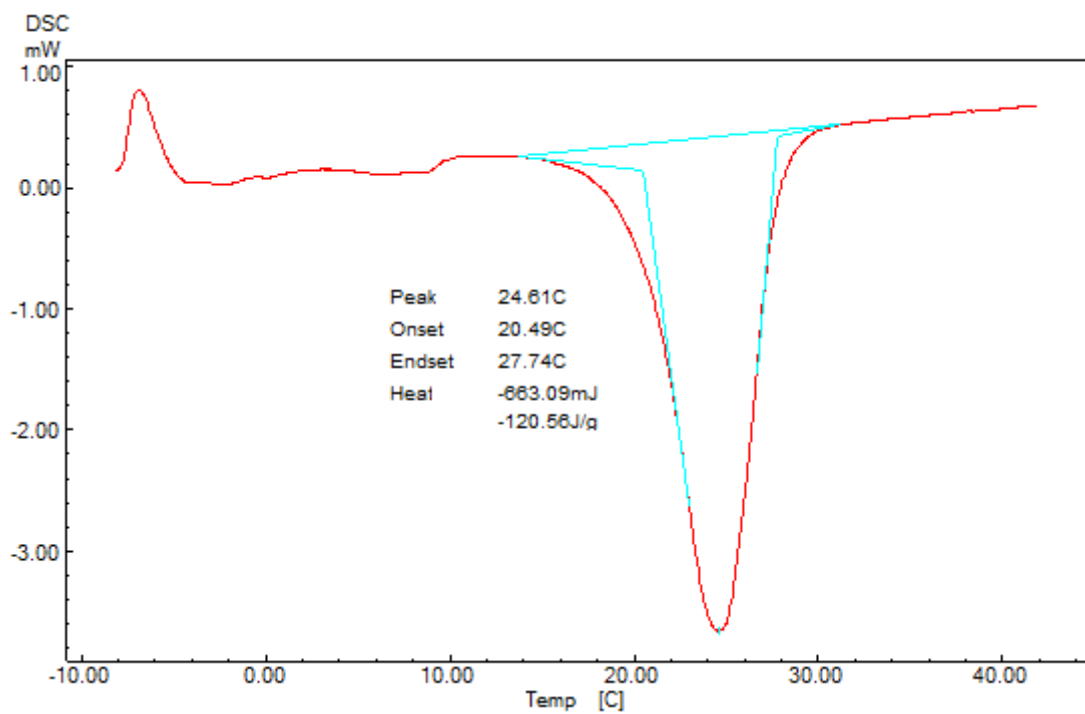


**Figure 8.7** DSC curve of sample 8

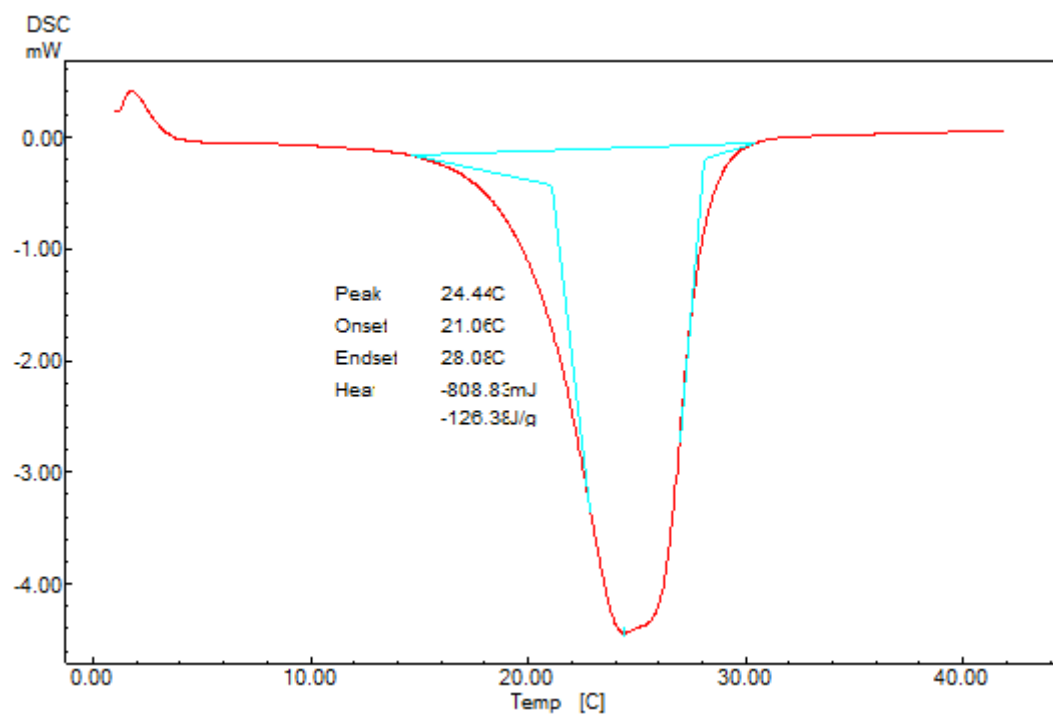


**Figure 8.8** DSC curve of sample 9

# Conclusions and Recommendations

9

## 9.1 Author's contributions/achievements

- (1) Developed PCMs microcapsules using suspension polymerization that have high content of PCMs, no supercooling and thermally stable under heating and cooling cycling processes.
- (2) Experimental study for producing PCMs microcapsules based on ultraviolet-initiated polymerization using thin film close loop UV reactor.
- (3) Experimental study for producing double shell PCMs microcapsules coating with metal using electroless plating technique.
- (4) Invented a simple, efficient, cheap and quick method of microencapsulation PCMs.

## 9.2 Conclusions

### 9.2.1 Conclusion from Chapter Four

PMMA microcapsules containing PCM were successfully prepared using suspension polymerization method. The used of mixed surfactants (PVP and SDS) improved the suspension stability of the emulsion. The use of mixed surfactants produced a monodisperse droplets size distribution with no significant shifting of droplets size over time. The use of mixed surfactants also reduced the buckles and microcapsule size significantly. Adding PETRA to the system improves the surface morphology and produces microcapsules with a much higher PCM content. The core/shell mass ratio of 2:1 produced microcapsules with regular spheres and smooth surface. PCM content of the microcapsules produced in this work was as high as 85.6 wt. %, which is high compared to most microcapsules reported in the literature.

### 9.2.2 Conclusion from Chapter Five

PCM microcapsules containing nucleating agents were successfully prepared by means of suspension polymerization method. The addition of 5 wt. % of Rubitherm®RT58 is found to be completely effective in preventing the supercooling of RT21 microcapsules by shifting the onset crystallization temperature from 10.9 to 19.8 °C. From calorimetric measurements (DSC), the latent heat of RT21 microcapsules in presence of 5 wt. % of Rubitherm®RT58 is

110.4 J/g, which corresponds to 83.6 % of RT21. No significant changes in the surface morphology of RT21 microcapsules have been observed with limited number of buckles and dimples appear on the surface of some of the capsules. The mass loss of RT21 microcapsules when placed in oven at 50 °C decreased to half when 5 wt. % of Rubitherm®RT58 was added to the RT21; indicating that the higher melting RT58 assist to seal the PCM better.

### **9.2.3 Conclusion from Chapter Six**

Cross-linked polymethylmethacrylate microcapsules containing commercial PCMs are successfully prepared using falling thin film closed loop UV reactor. PCMs microcapsules properties depend mainly on the method used for preparing the emulsion. Smooth, compact and dry spherical microcapsules with reasonable heat storage capacity were prepared when a mixture of monomers was used (method ‘2’). Particles are agglomerated to lumps and no microcapsules obtained when only MMA was used. However, the morphology of the PCMs microcapsules improved dramatically when cross linking agent (PETRA) was used. The morphology of the microcapsules was similar when the irradiated time reduced from 2 hours to 1 hour with an associated significant increase in thermal energy storage of the PCMs microcapsules.

### **9.2.4 Conclusion from Chapter Seven**

A simple method based on two steps (1) surface functionalization of PCMs microcapsules using polydopamine (PDA) and (2) electroless plating of silver (Ag) metal was used to coat the PCMs microcapsules with Ag metal. PDA was used as interface modifier between the polymer and metal to promote silver deposition on the surface of the PCMs microcapsules. SEM images show that the PDA was successfully attached to the PCMs microcapsules as shown by dark distinctive layer and small fragments of PDA on the surface of RT21 microcapsules. The inner polymer shell of the PCMs microcapsules was completely covered with Ag (outer metal shell). The mechanical strength of the double shell PCMs microcapsules was improved significantly in comparison to the single polymer shell.

### **9.2.5 Conclusion from Chapter Eight**

A simple, quick and effective process of encapsulating PCMs was invented. The encapsulated PCMs produced by the process of the invention have been found to be of high quality. In particular, they have a smooth and compact surface, a relatively high PCM content and were

found to be thermally stable under heating and cooling cycling processes. In addition, the process of the invention gives a relatively high materials recovery rate, e.g. up to 90%, or higher.

### **9.3 Recommendations for future work**

- (1) Investigate the feasibility of microencapsulation of other organic PCMs such as fatty acid, fatty acids ester and fatty acid alcohol using suspension polymerization method.
- (2) Investigate the applicability of producing PCMs nanocapsules by producing nano-emulsion using sonification emulsification process.
- (3) Incorporate fire retardant materials within the PCM microcapsules. A third compatible component may be required; thus the PCMs and fire retardant materials become soluble with each other.
- (4) Study the stability of PCMs microcapsules against different solvent washing and shear force such as that induced by pumping.
- (5) Improve the UV microencapsulation efficiency by selecting a narrow UV light spectra lamp that matching the photoinitiator excitation.
- (6) Reduce the monomers losses in the UV process by adding a compatible agent to the PCMs, thus attract the monomers to diffuse and set on the interface of PCMs droplets and polymerized rather than polymerized in the bulk and produce microspheres.
- (7) Use different types and concentrations of photoinitiators
- (8) The metal coated PCMs could be expended to cover metals, which are less expensive than silver.

# References

1. MED, New Zealand Energy Data File, Technical report, 2012: NZ Ministry of Economic Development.
2. Bp.com/statisticalreview, BP Statistical Review of World Energy, Technical report, 2014.
3. Isaacs, N., et al., Energy Use in New Zealand Households, Report in the Year 10 Analysis for the Household Energy End-use Project (HHEP) 2006.
4. Zhou, D., C.Y. Zhao, and Y. Tian, Review on thermal energy storage with phase change materials (PCMs) in building applications. *Applied Energy*, 2012. 92(0): p. 593-605.
5. Khudhair, A.M. and M.M. Farid, A review on energy conservation in building applications with thermal storage by latent heat using phase change materials. *Energy Conversion and Management*, 2004. 45(2): p. 263-275.
6. Cabeza, L.F., et al., Materials used as PCM in thermal energy storage in buildings: A review. *Renewable and Sustainable Energy Reviews*, 2011. 15(3): p. 1675-1695.
7. Jaworski, M., Thermal performance of building element containing phase change material (PCM) integrated with ventilation system – An experimental study. *Applied Thermal Engineering*, 2014. 70(1): p. 665-674.
8. Khudhair, A.M. and M.M. Farid, Use of Phase Change Materials for Thermal Comfort and Electrical Energy Peak Load Shifting: Experimental Investigations, in Proceedings of ISES World Congress 2007 (Vol. I – Vol. V), D.Y. Goswami and Y. Zhao, Editors. 2009, Springer Berlin Heidelberg. p. 283-288.
9. Zhang, H., et al., Preparation and thermal performance of gypsum boards incorporated with microencapsulated phase change materials for thermal regulation. *Solar Energy Materials and Solar Cells*, 2012. 102(0): p. 93-102.
10. Tyagi, V.V., et al., Development of phase change materials based microencapsulated technology for buildings: A review. *Renewable and Sustainable Energy Reviews*, 2011. 15(2): p. 1373-1391.
11. Toppi, T. and L. Mazzarella, Gypsum based composite materials with micro-encapsulated PCM: Experimental correlations for thermal properties estimation on the basis of the composition. *Energy and Buildings*, 2013. 57(0): p. 227-236.
12. Borreguero, A.M., et al., Development of smart gypsum composites by incorporating thermoregulating microcapsules. *Energy and Buildings*, 2014. 76(0): p. 631-639.
13. Borreguero, A.M., et al., Improvement of the thermal behaviour of gypsum blocks by the incorporation of microcapsules containing PCMS obtained by suspension

- polymerization with an optimal core/coating mass ratio. *Applied Thermal Engineering*, 2010. 30(10): p. 1164-1169.
14. Zalba, B., et al., Review on thermal energy storage with phase change: materials, heat transfer analysis and applications. *Applied Thermal Engineering*, 2003. 23(3): p. 251-283.
  15. Hasnain, S.M., Review on sustainable thermal energy storage technologies, Part I: heat storage materials and techniques. *Energy Conversion and Management*, 1998. 39(11): p. 1127-1138.
  16. Sharma, A., et al., Review on thermal energy storage with phase change materials and applications. *Renewable and Sustainable Energy Reviews*, 2009. 13(2): p. 318-345.
  17. Behzadi, S. and M.M. Farid, Long term thermal stability of organic PCMs. *Applied Energy*, 2014. 122(0): p. 11-16.
  18. Feldman, D., M.M. Shapiro, and D. Banu, Organic phase change materials for thermal energy storage. *Solar Energy Materials*, 1986. 13(1): p. 1-10.
  19. Mondal, S., Phase change materials – An overview. *Applied Thermal Engineering*, 2008. 28(11–12): p. 1536-1550.
  20. Mehling, H., Innovative PCM technology. 2004: p. Garching, Munich (Germany).
  21. Cabeza, L.F., et al., Experimentation with a water tank including a PCM module. *Solar Energy Materials and Solar Cells*, 2006. 90(9): p. 1273-1282.
  22. Nelson, G., Application of microencapsulation in textiles. *International journal of pharmaceutics*, 2002. 242(1-2): p. 55-62.
  23. Lv, Y., Y. Zou, and L. Yang, Feasibility study for thermal protection by microencapsulated phase change micro/nanoparticles during cryosurgery. *Chemical Engineering Science*, 2011. 66(17): p. 3941-3953.
  24. Tan, F.L. and C.P. Tso, Cooling of mobile electronic devices using phase change materials. *Applied Thermal Engineering*, 2004. 24(2–3): p. 159-169.
  25. Kim, K.-b., et al., Feasibility study on a novel cooling technique using a phase change material in an automotive engine. *Energy*, 2010. 35(1): p. 478-484.
  26. Yimer, B. and M. Adami, Parametric study of phase change thermal energy storage systems for space application. *Energy Conversion and Management*, 1997. 38(3): p. 253-262.
  27. Gin, B. and M.M. Farid, The use of PCM panels to improve storage condition of frozen food. *Journal of Food Engineering*, 2010. 100(2): p. 372-376.
  28. Scalat, S., et al., Full scale thermal testing of latent heat storage in wallboard. *Solar Energy Materials and Solar Cells*, 1996. 44(1): p. 49-61.

29. Feldman, D., D. Banu, and D.W. Hawes, Development and application of organic phase change mixtures in thermal storage gypsum wallboard. *Solar Energy Materials and Solar Cells*, 1995. 36(2): p. 147-157.
30. Tyagi, V.V. and D. Buddhi, PCM thermal energy storage in buildings: a state of art. *Renew. Sust. Energy Rev.*, 2007. 11: p. 1146-1166.
31. Mehling, H. and L.F. Cabeza, Heat and cold storage in PCM. An up to date introduction into basics and applications 2008: Springer.
32. Li, W., et al., Fabrication and morphological characterization of microencapsulated phase change materials (MicroPCMs) and macrocapsules containing MicroPCMs for thermal energy storage. *Energy*, 2012. 38(1): p. 249-254.
33. Pekarek, K.J., J.S. Jacob, and E. Mathiowitz, Double-walled polymer microspheres for controlled drug release. *Nature*, 1994. 367(6460): p. 258-260.
34. Champagne, C.P. and P. Fustier, Microencapsulation for the improved delivery of bioactive compounds into foods. *Current Opinion in Biotechnology*, 2007. 18(2): p. 184-190.
35. Miyazawa, K., et al., Preparation of a new soft capsule for cosmetics. *Journal of cosmetics science* 2000. 51: p. 239-252
36. Hawlader, M., M. Uddin, and H. Zhu, Preparation and evaluation of a novel solar storage material: Microencapsulated paraffin. *International Journal of Solar Energy* 2000. 20(4): p. 227-238.
37. Ghosh, S., Functional coatings by polymer microencapsulation. 2006, WILEY-VCH Verlag GmbH & Co. KGaA Weinheim
38. Smith, M., Microencapsulated phase change materials for thermal energy storage: Development, Evaluation and application, in *Chemical & Materials Engineering* 2009, The University of Auckland Auckland, New Zealand
39. Alexandridou, S. and C. Kiparissides, Production of oil-containing polyterephthalamide microcapsules by interfacial polymerization. An experimental investigation of the effect of process variables on the microcapsule size distribution. *J. MICROENCAPSULATION*, 1994. 11(6): p. 603-613.
40. Hsu, Y., Microencapsulated liquid crystal and a method and system for using same U. patent, Editor 2000.
41. Mahabadi, H. and H. Tan, Interfacial/free radical polymerization microencapsulation: kinetics of particle formation. *J. MICROENCAPSULATION*, 1996. 13(5): p. 559-573.
42. Yeo, Y., N. Baek, and K. Park, Microencapsulation Methods for Delivery of Protein Drugs. *Biotechnol. Bioprocess Eng*, 2001. 6: p. 213-230.

43. Pitaksuteepong, T., et al., Factors influencing the entrapment of hydrophilic compounds in nanocapsules prepared by interfacial polymerisation of water-in-oil microemulsions. *European Journal of Pharmaceutics and Biopharmaceutics*, 2002. 53(3): p. 335-342.
44. Cho, J.-S., A. Kwon, and C.-G. Cho, Microencapsulation of octadecane as a phase-change material by interfacial polymerization in an emulsion system. *Colloid and Polymer Science*, 2002. 280(3): p. 260-266.
45. Su, J.-F., L.-X. Wang, and L. Ren, Synthesis of polyurethane microPCMs containing n-octadecane by interfacial polycondensation: Influence of styrene-maleic anhydride as a surfactant. *Colloids and Surfaces A: Physicochemical and Engineering Aspects*, 2007. 299(1–3): p. 268-275.
46. Long, Z., et al., Microencapsulation of n-Hexadecane as a Phase Change Material in polyurea. *Acta Physico-Chimica Sinica*, 2004. 20(1): p. 90-93.
47. Zhang, H. and X. Wang, Synthesis and properties of microencapsulated n-octadecane with polyurea shells containing different soft segments for heat energy storage and thermal regulation. *Solar Energy Materials and Solar Cells*, 2009. 93(8): p. 1366-1376.
48. Lone, S., et al., Facile and highly efficient microencapsulation of a phase change material using tubular microfluidics. *Colloids and Surfaces A: Physicochemical and Engineering Aspects*, 2013. 422(0): p. 61-67.
49. Xing, J., et al., Method for encapsulating phase transitional paraffin compound that can undergo phase transition and microcapsule resulting therefrom, in US patent 2006: US.
50. Lu, S., et al., Preparation and characterization of polyurea/polyurethane double-shell microcapsules containing butyl stearate through interfacial polymerization. *Journal of Applied Polymer Science*, 2011. 121(6): p. 3377-3383.
51. Liang, C., et al., Microencapsulation of butyl stearate as a phase change material by interfacial polycondensation in a polyurea system. *Energy Conversion and Management*, 2009. 50(3): p. 723-729.
52. Yamagishi, Y., et al. An evaluation of microencapsulated PCM for use in cold energy transportation medium. in *Energy Conversion Engineering Conference, 1996. IECEC 96.*, Proceedings of the 31st Intersociety. 1996.
53. Choi, J.K., et al., Preparation of Microcapsules Containing Phase Change Materials as Heat Transfer Media by In-Situ Polymerization. *Journal of Industrial and Engineering Chemistry*, 2001. 7(6): p. 358-362.
54. Zhang, H. and X. Wang, Fabrication and performances of microencapsulated phase change materials based on n-octadecane core and resorcinol-modified melamine-

- formaldehyde shell. *Colloids and Surfaces A: Physicochemical and Engineering Aspects*, 2009. 332(2-3): p. 129-138.
55. Zhang, X.-x., et al., Structure and thermal stability of microencapsulated phase-change materials. *Colloid and Polymer Science*, 2004. 282(4): p. 330-336.
56. Zhang, X.X., et al., Expansion space and thermal stability of microencapsulated n-octadecane. *Journal of Applied Polymer Science*, 2005. 97(1): p. 390-396.
57. Zhang, X.X., et al., Fabrication and properties of microcapsules and nanocapsules containing n-octadecane. *Materials Chemistry and Physics*, 2004. 88(2-3): p. 300-307.
58. Fan, Y.F., et al., Thermal stability and permeability of microencapsulated n-octadecane and cyclohexane. *Thermochimica Acta*, 2005. 429(1): p. 25-29.
59. Song, Q., et al., Thermal stability of composite phase change material microcapsules incorporated with silver nano-particles. *Polymer*, 2007. 48(11): p. 3317-3323.
60. Li, W., et al., Preparation and characterization of microencapsulated phase change material with low remnant formaldehyde content. *Materials Chemistry and Physics*, 2007. 106(2-3): p. 437-442.
61. Sumiga, B., et al., Production of Melamine-Formaldehyde PCM Microcapsules with Ammonia Scavenger used for Residual Formaldehyde Reduction. *Acta Chimica Slovenica*, 2011. 58: p. 14-25.
62. Su, J.-F., et al., Interface stability behaviors of methanol-melamine-formaldehyde shell microPCMs/epoxy matrix composites. *Polymer Composites*, 2011. 32(5): p. 810-820.
63. Su, J.-F., et al., Fabrication and interfacial morphologies of methanol-melamine-formaldehyde (MMF) shell microPCMs/epoxy composites. *Colloid and Polymer Science*, 2011. 289(2): p. 169-177.
64. Su, J.-F., et al., Physicochemical properties and mechanical characters of methanol-modified melamine-formaldehyde (MMF) shell microPCMs containing paraffin. *Colloid and Polymer Science*, 2011. 289(2): p. 111-119.
65. Yeum, J.-H. and Y. Deng, Synthesis of high molecular weight poly(methyl methacrylate) microspheres by suspension polymerization in the presence of silver nanoparticles. *Colloid and Polymer Science*, 2005. 283(11): p. 1172-1179.
66. Ma, G.H., et al., Microencapsulation of oil with poly(styrene-N,N-dimethylaminoethyl methacrylate) by SPG emulsification technique: Effects of conversion and composition of oil phase. *Journal of Colloid and Interface Science*, 2003. 266(2): p. 282-294.
67. Sánchez, L., et al., Microencapsulation of PCMs with a polystyrene shell. *Colloid and Polymer Science*, 2007. 285(12): p. 1377-1385.

68. Supatimusro, D., et al., Poly(divinylbenzene) Microencapsulated Octadecane for Use as a Heat Storage Material: Influences of Microcapsule Size and Monomer/Octadecane Ratio. *Polymer-Plastics Technology and Engineering*, 2012. 51: p. 1167-1172.
69. Chaiyasat, P., et al., Thermal properties of hexadecane encapsulated in poly(divinylbenzene) particles. *Journal of Applied Polymer Science*, 2009. 112(6): p. 3257-3266.
70. Chaiyasat, P., et al., Preparation and Characterization of Poly(divinylbenzene) Microcapsules Containing Octadecane. *Materials Sciences and Application*, 2011. 2: p. 1007-1013.
71. Sari, A., et al., Microencapsulated n-octacosane as phase change material for thermal energy storage. *Solar Energy*, 2009. 83(10): p. 1757-1763.
72. Sari, A., C. Alkan, and A. Karaipekli, Preparation, characterization and thermal properties of PMMA/n-heptadecane microcapsules as novel solid–liquid microPCM for thermal energy storage. *Applied Energy*, 2010. 87(5): p. 1529-1534.
73. Alkan, C., et al., Preparation, characterization, and thermal properties of microencapsulated phase change material for thermal energy storage. *Solar Energy Materials and Solar Cells*, 2009. 93(1): p. 143-147.
74. Alkan, C., A. Sari, and A. Karaipekli, Preparation, thermal properties and thermal reliability of microencapsulated n-eicosane as novel phase change material for thermal energy storage. *Energy Conversion and Management*, 2011. 52(1): p. 687-692.
75. Wang, Y., et al., Fabrication and performances of microencapsulated paraffin composites with polymethylmethacrylate shell based on ultraviolet irradiation-initiated. *Materials Chemistry and Physics*, 2012. 135(1): p. 181-187.
76. Ma, S., et al., UV irradiation-initiated MMA polymerization to prepare microcapsules containing phase change paraffin. *Solar Energy Materials and Solar Cells*, 2010. 94(10): p. 1643-1647.
77. Sánchez-Silva, L., et al., Microencapsulation of PCMs with a styrene-methyl methacrylate copolymer shell by suspension-like polymerisation. *Chemical Engineering Journal*, 2010. 157(1): p. 216-222.
78. Sánchez-Silva, L., et al., Synthesis and Characterization of Paraffin Wax Microcapsules with Acrylic-Based Polymer Shells. *Industrial & Engineering Chemistry Research*, 2010. 49(23): p. 12204-12211.
79. Qiu, X., et al., Microencapsulated n-octadecane with different methylmethacrylate-based copolymer shells as phase change materials for thermal energy storage. *Energy*, 2012. 46(1): p. 188-199.

80. Qiu, X., et al., Fabrication and characterization of microencapsulated n-octadecane with different crosslinked methylmethacrylate-based polymer shells. *Solar Energy Materials and Solar Cells*, 2012. 98(0): p. 283-293.
81. Qiu, X., et al., Microencapsulated n-alkane with p(n-butyl methacrylate-co-methacrylic acid) shell as phase change materials for thermal energy storage. *Solar Energy*, 2013. 91(0): p. 212-220.
82. Qiu, X., et al., Preparation, thermal properties and thermal reliabilities of microencapsulated n-octadecane with acrylic-based polymer shells for thermal energy storage. *Thermochimica Acta*, 2013. 551(0): p. 136-144.
83. Hawlader, M., M. Uddin, and M. Khin, Microencapsulated PCM thermal-energy storage system. *Applied Energy*, 2003. 74(1–2): p. 195-202.
84. Bayés-García, L., et al., Phase Change Materials (PCM) microcapsules with different shell compositions: Preparation, characterization and thermal stability. *Solar Energy Materials and Solar Cells*, 2010. 94(7): p. 1235-1240.
85. Shu, B., et al., Study on microencapsulation of lycopene by spray-drying. *Journal of Food Engineering*, 2006. 76(4): p. 664-669.
86. Wan, L., P. Heng, and C. Chia, SPRAY DRYING AS A PROCESS FOR MICROENCAPSULATION AND THE EFFECT OF DIFFERENT COATING POLYMERS. *DRUG DEVELOPMENT AND INDUSTRIAL PHARMACY*, 1992. 18(9): p. 997-1011.
87. Borreguero, A.M., et al., Synthesis and characterization of microcapsules containing Rubitherm®RT27 obtained by spray drying. *Chemical Engineering Journal*, 2011. 166(1): p. 384-390.
88. Gravalos, M., et al., Procedure for microencapsulation of phase change materials by spray drying,, in Patent EP2119498 (A1)2009.
89. Zhang, T., et al., Fabrication and performances of new kind microencapsulated phase change material based on stearic acid core and polycarbonate shell. *Energy Conversion and Management*, 2012. 64(0): p. 1-7.
90. Yang, R., et al., Preparation of n-tetradecane-containing microcapsules with different shell materials by phase separation method. *Solar Energy Materials and Solar Cells*, 2009. 93(10): p. 1817-1822.
91. Chang, C.C., et al., Preparation of phase change materials microcapsules by using PMMA network-silica hybrid shell via sol-gel process. *Journal of Applied Polymer Science*, 2009. 112(3): p. 1850-1857.
92. Fortuniak, W., et al., Synthesis of a paraffin phase change material microencapsulated in a siloxane polymer. *Colloid and Polymer Science*, 2013. 291(3): p. 725-733.

93. Schossig, P., et al., Micro-encapsulated phase-change materials integrated into construction materials. *Solar Energy Materials and Solar Cells*, 2005. 89(2–3): p. 297-306.
94. Miyazawa, K., et al., Preparation of a new soft capsule for cosmetics. *Journal of cosmetics science*, 2000. 5: p. 239-252.
95. Nelson, G., Application of microencapsulation in textiles. *International Journal of Pharmaceutics*, 2002. 242(1–2): p. 55-62.
96. Junfeng, S., L. Wang, and L. Ren, Fabrication and thermal properties of microPCMs: Used melamine-formaldehyde resin as shell material. *Journal of Applied Polymer Science*, 2006. 101(3): p. 1522-1528.
97. Sánchez-Silva, L., J.F. Rodríguez, and P. Sánchez, Influence of different suspension stabilizers on the preparation of Rubitherm RT31 microcapsules. *Colloids and Surfaces A: Physicochemical and Engineering Aspects*, 2011. 390(1–3): p. 62-66.
98. Li, W., et al., Morphology, structure and thermal stability of microencapsulated phase change material with copolymer shell. *Energy*, 2011. 36(2): p. 785-791.
99. Chaiyasat, A., et al., Preparation of polydivinyl benzene/natural rubber capsule encapsulating octadecane: Influence of natural rubber molecular weight and content *Express Polymer Letters*, 2012. 6: p. 70-77.
100. Alay, S., C. Alkan, and F. Göde, Synthesis and characterization of poly(methyl methacrylate)/n-hexadecane microcapsules using different cross-linkers and their application to some fabrics. *Thermochimica Acta*, 2011. 518(1–2): p. 1-8.
101. Pichot, R., Stability and Characterisation of Emulsions in the presence of Colloidal Particles and Surfactants, 2010, PhD thesis-The University of Birmingham.
102. Zhang, X.-x., et al., Crystallization and prevention of supercooling of microencapsulated n-alkanes. *Journal of Colloid and Interface Science*, 2005. 281(2): p. 299-306.
103. Chaiyasat, P., et al., Influence of water domain formed in hexadecane core inside cross-linked capsule particle on thermal properties for heat storage application. *Colloid and Polymer Science*, 2008. 286(6-7): p. 753-759.
104. Huang, J., et al., Preparation, characterization, and thermal properties of the microencapsulation of a hydrated salt as phase change energy storage materials. *Thermochimica Acta*, 2013. 557(0): p. 1-6.
105. Lane, G.A., Phase change materials for energy storage nucleation to prevent supercooling. *Solar Energy Materials and Solar Cells*, 1992. 27(2): p. 135-160.
106. Farid, M.M., et al., A review on phase change energy storage: materials and applications. *Energy Conversion and Management*, 2004. 45(9–10): p. 1597-1615.

107. Chaiyasat, P., M.Z. Islam, and A. Chaiyasat, Preparation of poly(divinylbenzene) microencapsulated octadecane by microsuspension polymerization: oil droplets generated by phase inversion emulsification. *RSC Advances*, 2013. 3(26): p. 10202-10207.
108. You, M., et al., Microencapsulated n-Octadecane with styrene-divinylbenzene co-polymer shells. *Journal of Polymer Research*, 2011. 18(1): p. 49-58.
109. Chaiyasat, P., et al., Preparation of divinylbenzene copolymer particles with encapsulated hexadecane for heat storage application. *Colloid and Polymer Science*, 2008. 286(2): p. 217-223.
110. Song, Q., et al., Supercooling of Silver Nano Composite PCM Microcapsules *Journal of Fiber Bioengineering and Informatics*, 2008. 1: p. 239-248.
111. Fan, Y.F., et al., Super-cooling prevention of microencapsulated phase change material. *Thermochimica Acta*, 2004. 413(1–2): p. 1-6.
112. Cao, F. and B. Yang, Supercooling suppression of microencapsulated phase change materials by optimizing shell composition and structure. *Applied Energy*, 2014. 113(0): p. 1512-1518.
113. El Rhafiki, T., et al., Crystallization of PCMs inside an emulsion: Supercooling phenomenon. *Solar Energy Materials and Solar Cells*, 2011. 95(9): p. 2588-2597.
114. Sun, G. and Z. Zhang, Mechanical properties of melamine-formaldehyde microcapsules. *Journal of Microencapsulation*, 2001. 18: p. 593-602.
115. Rahman, A., M. Dickinson, and M. Farid, Microencapsulation of a PCM through membrane emulsification and nanocompression-based determination of microcapsule strength. *Materials for Renewable and Sustainable Energy*, 2012. 1(1): p. 1-10.
116. Hu, J., H.-Q. Chen, and Z. Zhang, Mechanical properties of melamine formaldehyde microcapsules for self-healing materials. *Materials Chemistry and Physics*, 2009. 118(1): p. 63-70.
117. Alvarado, J., et al., Characterization of supercooling suppression of microencapsulated phase change material by using DSC. *Journal of thermal analysis and calorimetry*, 2006. 86: p. 505-509.
118. ZHU Kong-ying, W.S., QI Heng-zhi, LI Hui, ZHAO Yun-hui, YUAN Xiao-yan, Supercooling Suppression of Microencapsulated n-Alkanes by Introducing an Organic Gelator. *CHEMICAL RESEARCH IN CHINESE UNIVERSITIES*, 2012. 28(3): p. 539-541.
119. Montenegro, R., et al., Crystallization in Miniemulsion Droplets. *The Journal of Physical Chemistry B*, 2003. 107(21): p. 5088-5094.
120. Mehling, H. and L. Cabeza, Solid-liquid phase change materials, in Heat and cold storage with PCM. 2008, Springer Berlin Heidelberg. p. 11-55.

121. Chen, J., et al., Photoinitiated dispersion polymerization of methyl methacrylate: A quick approach to prepare polymer microspheres with narrow size distribution. *Journal of Polymer Science Part A: Polymer Chemistry*, 2008. 46(4): p. 1329-1338.
122. Wright, A., Photopolymerized film, coating and product, and method of forming, 1970: US patent 3522076 A.
123. Noguchi, H., Ink, ink-jet recording method using the same, and photopolymerization initiator, 2002: US patent 6428862 B1.
124. Altin, A., et al., Synthesis, photopolymerization, and adhesive properties of hydrolytically stable phosphonic acid-containing (meth)acrylamides. *Journal of Polymer Science Part A: Polymer Chemistry*, 2014. 52(4): p. 511-522.
125. Kurokawa, T., et al., Fiber optic sheet formation by selective photopolymerization. *Applied Optics*, 1978. 17(4): p. 646-650.
126. Stansbury, J.W., Curing Dental Resins and Composites by Photopolymerization. *Journal of Esthetic and Restorative Dentistry*, 2000. 12(6): p. 300-308.
127. Crivello, J.V., 4.37 - Photopolymerization, in *Polymer Science: A Comprehensive Reference*, K. Matyjaszewski and M. Möller, Editors. 2012, Elsevier: Amsterdam. p. 919-955.
128. Cai, Y. and J.L.P. Jessop, Photopolymerization, Free Radical, in *Encyclopedia of Polymer Science and Technology*. 2002, John Wiley & Sons, Inc.
129. Crivello, J.V., K. Dietliker, and G. Bradley, Photoinitiators for free radical cationic & anionic photopolymerisation. 1998, New York: J. Wiley in association with SITA Technology.
130. Sigma, A., Applications: Free Radical Initiators [http://www.sigmaaldrich.com/aldrich/brochure/al\\_pp\\_applications.pdf](http://www.sigmaaldrich.com/aldrich/brochure/al_pp_applications.pdf).
131. Chai, X.S., F.J. Schork, and E.M. Oliver, ATR-UV monitoring of methyl methacrylate miniemulsion polymerization for determination of monomer conversion. *Journal of Applied Polymer Science*, 2006. 99(4): p. 1471-1475.
132. Miller Chris, W., et al., N-Vinylamides and Reduction of Oxygen Inhibition in Photopolymerization of Simple Acrylate Formulations, in *Photoinitiated Polymerization*. 2003, American Chemical Society. p. 2-14.
133. Tran, M.T.T. and M. Farid, Ultraviolet treatment of orange juice. *Innovative Food Science & Emerging Technologies*, 2004. 5(4): p. 495-502.
134. Jiao, L., et al., Synthesis and Properties of Polyacrylate Emulsion Modified by Pentaerythritol Tetraacrylate. *Advanced Materials Research*, 2013. 781-784: p. 550-553.

135. Bellemare, J., Thermally reflective encapsulated phase change pigment, US Patent: 20070031652 A1 (2007).
136. Microtek, L. Standard MicroPCM Products: <http://www.microteklabs.com/>.
137. Malfliet, A., et al., Synthesis and Characterization of Composite Coatings for Thermal Actuation. *Journal of The Electrochemical Society*, 2007. 154(1): p. D50-D56.
138. Lingamneni, S., M. Asheghi, and K.E. Oodson, A Parametric Study of Microporous Metal Matrix-Phase Change Material Composite Heat Spreaders for Transient Thermal Applications, in *IEEE Intersociety Conference on Thermal and Thermomechanical Phenomena in Electronic Systems (ITHERM)2014*: Orlando, FL, USA.
139. Vadwala, P.H., Thermal Energy Storage in Copper Foams filled with Paraffin Wax, 2011, Thesis, University of Toronto: Canada.
140. Dow, A.S. Thermal Energy Storage System Based on Novel Phase Change Material. [http://msdssearch.dow.com/PublishedLiteratureDOWCOM/dh\\_054b/0901b8038054b9b1.pdf?filepath=automotive/pdfs/noreg/299-51805.pdf&fromPage=GetDoc](http://msdssearch.dow.com/PublishedLiteratureDOWCOM/dh_054b/0901b8038054b9b1.pdf?filepath=automotive/pdfs/noreg/299-51805.pdf&fromPage=GetDoc).
141. Farid, M. and S. Al-Hallaj, Microchannel heat exchanger with micro-encapsulated phase change material for high flux cooling, 2006, US 20060231233 A1.
142. Su, J.-F., L.-X. Wang, and L. Ren, Preparation and characterization of double-MF shell microPCMs used in building materials. *Journal of Applied Polymer Science*, 2005. 97(5): p. 1755-1762.
143. Jun-Feng, S., et al., Mechanical properties and thermal stability of double-shell thermal-energy-storage microcapsules. *J Appl Polym Sci*, 2006. 103(2): p. 1295-1302.
144. Rahman, A., Microencapsulation of Phase Change Materials with Membrane Emulsification, and Development of a Nanocompression Technique to Test Microcapsule Strength, 2010, Master thesis, The University of Auckland New Zealand
145. Satish C. M, et al., Phase change materials encapsulated with metal shell; high thermal conductivity, Patent: US 7919184 B2.
146. Fransaer, J., Composite materail, Patent: WO 2006053405 A1 (2006).
147. Lee, H., et al., Mussel-Inspired Surface Chemistry for Multifunctional Coatings. *Science* 2007. 318: p. 426.
148. Wang, W., et al., Fabrication of silver-coated silica microspheres through mussel-inspired surface functionalization. *Journal of Colloid and Interface Science*, 2011. 358(2): p. 567-574.

149. Wang, W., et al., Preparation and characterization of polystyrene/Ag core–shell microspheres – A bio-inspired poly(dopamine) approach. *Journal of Colloid and Interface Science*, 2012. 368(1): p. 241-249.
150. Herlinger, E., R.F. Jameson, and W. Linert, Spontaneous autoxidation of dopamine. *Journal of the Chemical Society, Perkin Transactions 2*, 1995(2): p. 259-263.
151. Liebscher, J., et al., Structure of Polydopamine: A Never-Ending Story? *Langmuir*, 2013. 29(33): p. 10539-10548.
152. Jamekhorshid, A., S.M. Sadrameli, and M. Farid, A review of microencapsulation methods of phase change materials (PCMs) as a thermal energy storage (TES) medium. *Renewable and Sustainable Energy Reviews*, 2014. 31(0): p. 531-542.
153. Reezigt, H., et al., Polymer composition containing a heat accumulating phase change material, a process for producing such a composition and product which includes such a composition Patent : WO 2005/097935 (2005).
154. Reezigt, H., et al., polymer Ccmposition containing a heat accumulating phase change material, a process for producing such a composition and a product in which such a composition is included ", , Patent : WO 2007/0400395 (2007).